REGULATION OF NON-ALCOHOLIC STEATOHEPATITIS AND HEPATIC FIBROSIS DEVELOPMENT BY THE BILE ACID-FXR-FGF19 PATHWAY

By

JUSTIN DOUGLAS SCHUMACHER

A dissertation submitted to

The School of Graduate Studies

Rutgers, The State University of New Jersey

In partial fulfillment of the requirements

For the degree of

Doctor of Philosophy

Graduate Program in Toxicology

Written under the direction of

Dr. Grace L. Guo

And approved by

_____

_____

_____

_____

_____

New Brunswick, New Jersey

OCTOBER, 2018

ABSTRACT OF THE DISSERTATION

REGULATION OF NON-ALCOHOLIC STEATOHEPATITIS AND HEPATIC FIBROSIS DEVELOPMENT BY THE BILE ACID-FXR-FGF19 PATHWAY

By: JUSTIN DOUGLAS SCHUMACHER, PharmD, MS

Dissertation Director: Grace L. Guo, MBBS, PhD

Introduction: Activation of the nuclear receptor farnesoid X receptor (FXR) by bile acids (BAs) in the intestine leads to the induction of fibroblast growth factor 19 (FGF19; ortholog of mouse FGF15). In the liver, FGF19 activates fibroblast growth factor receptor 4 (FGFR4) and the obligate co-receptor β-KLOTHO to negatively regulate BA synthesis. Many additional roles of FGF15 and FGF19 aside from regulation of BA homeostasis are now emerging: increasing insulin sensitivity, reducing total body weight, reducing serum lipid levels, decreasing gluconeogenesis while increasing glycogenesis, and enhancing liver regeneration. For this reason, the development of FXR agonists and FGF19 mimetics is currently a hotbed of research within the pharmaceutical industry for the treatment of non-alcoholic steatohepatitis (NASH) and other liver diseases. We therefore sought to determine the mechanisms by which FGF15 and FGF19 affect the development of NASH and hepatic fibrosis.

Methods: To identify the effects of FGF15 and FGF19 on NASH and hepatic fibrosis, three aims were developed. In Aim 1, wild type and FGF15 deficient mice were fed a high fat diet (HFD) for 6 months to induce NASH. In Aim 2, we treated the human hepatic stellate cell (HSC) line LX-2 with recombinant FGF19 to determine if FGF19 can function as a directly acting profibrogenic factor to HSCs. Lastly, in Aim 3, FGF15

deficient and overexpressing mice were fed a diet containing either cholestyramine or cholic acid and treated with chronic carbon tetrachloride (CCl_4). The combination of genotypes and diets would lead to the dissociation of BA levels from *Fgf15* expression and enable the determination of the BA dependent and independent effects of FGF15 on hepatic fibrosis.

Hypothesis: FGF15 overexpressing transgenic mice were previously shown to have reduced hepatic steatosis and improved insulin sensitivity. Therefore, in Aim 1, we hypthothesized that FGF15 deficiency would worsen all characteristics of NASH; steatosis, inflammation, fibrosis, and metabolic syndrome. FGFR activation by FGFs other than FGF15 and FGF19 has been shown to lead to HSC activation and proliferation. Thus, in Aim 2, we hypothesized that treatment of LX-2 cells with FGF19 would lead to HSC activation and proliferation. FXR activation in HSCs by BAs has been shown to be protective against the development of hepatic fibrosis. Therefore, in Aim 3, we hypothesized that FGF15 would affect CCl_4 induced hepatic fibrosis indirectly by regulating total BA pool size and subsequently altering FXR activity in HSCs.

Results: In agreement with our hypothesis, in Aim 1, FGF15 deficiency worsened HFD-induced metabolic syndrome, altered expression of lipid homeostatic genes, and led to a trend for worsened hepatic inflammation. Opposite of our hypothesis, FGF15 deficient mice were protected against the development of fibrosis. In Aim 2, we found that FGF19 can activate FGFR in LX-2 cells. However, contrary to our hypothesis, FGFR activation in LX-2 cells by FGF19 did not affect activation or proliferation. In Aim 3, the combinations of genotype and diet effectively led to multiple combinations of total BA pool sizes and *Fgf15* expression. Through these combinations, we were able to determine that FGF15 can affect hepatic inflammation and fibrosis development indirectly via regulation of BA homeostasis and subsequently FXR activity in the liver.

Conclusion: The findings from the three independent but integrated research aims indicate that FGF15 deficiency is protective against the development of hepatic fibrosis. FGF15 and FGF19 do not appear to directly induce HSC activation or proliferation as LX-2 cells were not activated by FGF19 treatment nor did FGF15 overexpression worsen hepatic fibrosis. The mechanism underlying the protective effect of FGF15 deficiency on hepatic fibrosis appears to be dependent upon FGF15 regulation of BA homeostasis and hepatic FXR activity.

DEDICATION

To my dearest Abby Jeanne and my family

for their unwavering love and support.

ACKNOWLEDGMENTS

To my mentor Dr. Grace Guo: Thank you for all your guidance, teachings, encouragement, and opportunities you have provided me over these past years. It is very obvious how much you care about the well-being and development of your students. I am extremely grateful for all the time and effort you have put into my development as a scientific researcher. The atmosphere in the laboratory, which is non-judgmental, encourages questioning, and facilitates learning, stems directly from your influence and leadership. Thank you.

To my committee members, Dr. Debra Laskin, Dr. Lauren Aleksunes, Dr. Kenneth Reuhl, and Dr. Renee Bergeron: Each of you is a strong advocate for the students of the JGPT. The effort you put into the development of your students is what makes this program excellent. Thank you for your input into my studies and scientific development. Dr. Aleksunes, thank you for your advice regarding earning a dual PharmD/PhD and for recruiting me to Rutgers. Dr. Bergeron, thank you for your insights into the pharmaceutical industry and for being, and continuing to be, a most appreciated professional mentor.

To the faculty of the JGPT: Thank you for your teachings, guidance, and aiding in my development as a scientist. The strength of the JGPT truly lies in the people who comprise it.

To the EOHSI staff, Liz, Eva, Linda, Sandi, Wilson, Sam, and so many others: Thank you for facilitating my progress through the JGPT and making EOHSI a pleasurable place at which to learn and work.

To my lab mates past and present: Thank you for creating an amazing learning and working environment. You were not only lab mates but also great friends. Bo, thank you for all your instructions, guidance, and patience. You were an amazing

teacher of laboratory techniques and always made me feel welcome to ask questions or for help. Laura, thank you for being an amazing partner with which to attend so many conferences. Dan, I could not have asked for a better person to share an office with and to serve as a sounding board for so many of my ideas and frustrations. Jason, you were an amazingly motivated student and it was a privilege to be your mentor. Julia, thank you for your patience and instruction during my early years in the lab.

To my dear friends and RATS: Thank you for all the board game nights, conversations over drinks, and softball games that helped me navigate the highs and lows of graduate school.

To my family: Your love and support has made me into the person I am today. I will always be grateful for all the time, effort, and sacrifice you have put in these past thirty years to raise me. Thank you for always encouraging me throughout my education and for not asking too often when I would be done.

To Abby Jeanne: Thank you for encouraging and supporting my decision to continue on to graduate school and for following me to New Jersey when I decided upon attending Rutgers. If willingly relocating to New Jersey is not love then I do not know what is. Coming home to you every day made the worst days in the lab feel like no trouble at all and the good days feel even better. Thank you for always being my anchor. I love you.

ACKNOWLEDGEMENT OF PUBLICATIONS

CHAPTER 1

Schumacher JD, Guo GL. Pharmacologic modulation of the bile acid-FXR-FGF19 pathway for the treatment of non-alcoholic steatohepatitis. Textbook chapter under review for the Spring Nature textbook titled “Bile acids and their receptors.”

Schumacher JD, Guo GL. Mechanistic review of drug-induced steatohepatitis. Toxicol Appl Pharmacol. 2015; 289(1):40-7.

Schumacher JD, Guo GL. Regulation of Hepatic Stellate Cells and Fibrogenesis by Fibroblast Growth Factors. BioMed Res Int. 2016; 8323747.

CHAPTER 2

Schumacher JD, Kong B, Yang P, Zhan L, Sun R, Aa J, Richardson JR, Chen A, Laskin D, Guo GL. The effect of fibroblast growth factor 15 deficiency on the development of high fat diet induced non-alcoholic steatohepatitis. Toxicol Appl Pharmacol. 2017 Sep 1; 330:1-8.

CHAPTERS 3 AND 4

Schumacher JD, Kong B, Wu J, Rizzolo D, Armstrong LE, Chow MD, Goedken M, Lee YH, Guo GL. Alterations in bile acid pool size mediate hepatic fibrogenesis in FGF15 deficient mice. *Manuscript in preparation for submission to Hepatology.*

NON-DISSERTATIONAL WORK

Huang M, Kong B, Zhang M, **Schumacher JD**, Rizzolo R, Armstrong LA, Chow M, Lee Y, Guo GL. Enterocyte specific FXR deficiency impairs the intestinal barrier and deteriorates alcohol induced liver injury in mice. *Manuscript in preparation for Dig Liver Dis.*

Kong B, Zhang M, Huang M, Rizzolo D, Armstrong LE, **Schumacher JD**, Chow M, Lee Y, Guo GL. FXR deficiency exacerbates chronic alcohol induced liver injury and bile acid metabolism. *Submitted manuscript to Toxicol Appl Pharmacol.*

Cheng K, Metry M, Felton J, Shang AC, Drachenberg CB, Xu S, Zhan M, **Schumacher JD**, Guo GL, Polli JE, Raufman JP. Diminished gallbladder filling, increased fecal bile acids, and promotion of colon epithelial cell proliferation and neoplasia in fibroblast growth factor 15-deficient mice. Oncotarget 2018 May 22, 9(39):25572-25585.

Zhang M, Kong B, Huang M, Wan R, Armstrong LE, **Schumacher JD**, Rizzolo D, Chow M, Lee Y, Guo GL. FXR deletion in hepatocytes does not affect the severity of alcoholic liver disease in mice. Dig Liver Dis. 2018 Apr 23. pii: S1590-8658(18)30706-0.

Sun R, Yang N, Kong B, Cao B, Feng D, Yu X, Ge C, Shen J, Wang P, Feng S, Jingqiu Huang FF, Guo J, He J, Aa N, Chen Q, Pan Y, **Schumacher JD**, Yang C, Guo GL, Aa J, Wang G. Orally administered berberine modulates lipid metabolism by targeting bile acid turnover and the intestinal FXR signaling pathway. Mol Pharmacol. 2017 Feb;91(2):110-122.

TABLE OF CONTENTS

LIST OF FIGURES

LIST OF TABLES

ABBREVIATIONS

ABHD5	Abhydrolase domain containing 5
ACSS2	Acyl-CoA synthetase short chain family member 2
AGRP	Agouti-related peptide
ALP	Alkaline phosphatase
ALT	Alanine aminotransaminase
ASBT	Apical sodium-dependent BA transporter
αSMA	Alpha smooth muscle actin
ATGL	Adipose triglyceride lipase
BA	Bile acids
BAX	BCL2-associated X protein
BBB	Blood brain barrier
BCL2	B-cell leukemia/lymphoma 2
bFKB1	Bi-specific activating antibody targeting FGFR1-βKL
βKL	Beta-Klotho
BrdU	Bromodeoxyuridine
BSEP	Bile salt export pump
BSH	Bile salt hydrolase
CA	Cholic acid
CAPE	Caffeic acid phenethyl ester
CCl_4	Carbon tetrachloride
CDCA	Chenodeoxycholic acid
CD36	Cluster of differentiation 36
CEBPα	CCAAT enhancer binding protein alpha
COL1α1	Collagen type I alpha 1 chain
CREB	cAMP response element binding protein

CRP	C-reactive protein
CTGF	Connective tissue growth factor
CYP27A1	Cytochrome P450 family 27 subfamily A member 1
CYP7A1	Cytochrome P450 family 7 subfamily A member 1
CYP7B1	Cytochrome P450 family 7 subfamily B member 1
CYP8B1	Cytochrome P450 family 8 subfamily B member 1
DDAH2	Dimethylarginine dimethylaminohydrolase 2
DEN	Diethylnitrosamine
ECM	Extra-cellular matrix
EETs	Epoxyeicosatrienoic acids
eNOS	Endothelial nitric oxide synthase
ERK	Extracellular signal-regulated kinase
ET-1	Endothelin-1
FABP1- Fgf15	*Fgf15* overexpressing mice
FAS	Fatty acid synthase
FGF	Fibroblast growth factor
FGFR	Fibroblast growth factor receptor
$Fgf15^{-/-}$	*Fgf15* knockout mice
FXR	Farnesoid X receptor
FXRRE	Farnesoid X receptor response element
GGT	Gamma-glutamyl-transferase
GLP1	Glucagon-like peptide-1
Gly-MCA	Glycine conjugated MCA
G6Pase	Glucose 6-phosphatase
HBV	Hepatitis B virus
HCC	Hepatocellular carcinoma
HCV	Hepatitis C virus
HDL	High density lipoprotein
HFD	High fat diet

HOMA-IR	Homeostatic model assessment of β cell function and insulin resistance
HSC	Hepatic stellate cell
H&E	Hematoxylin and eosin
IBABP	Ileal bile acid-binding protein
ICAM1	Intercellular Adhesion Molecule 1
ICV	Intracerebral ventricular injection
IHC	Immunohistochemistry
IκBα	NFκB inhibitor alpha
IKK	IκBα kinase
IL1β	Interleukin 1 beta
IL6	Interleukin 6
IL8	Interleukin 8
IP	Intraperitoneal
JNK	c-Jun NH2-terminal kinase
KO	Knockout mice
LDLR	Low density lipoprotein receptor
LPS	Lipopolysaccharide
MAPK	Mitogen-activated protein kinase
MCDD	Methionine and choline deficient diet
MFLC	Myofibroblast like cell
MMP2	Matrix metalloprotease 2
MTP	Microsomal triglyceride transfer protein
NAFLD	Non-alcoholic fatty liver disease
NAS	NAFLD activity score
NASH	Non-alcoholic steatohepatitis
NFκB	Nuclear factor kappa-light-chain-enhancer of activated B cells
NKT	Natural killer T-cell
NPY	Neuropeptide Y

NTCP	Sodium-taurocholate co-transporting polypeptide
OCA	Obeticholic acid
PBC	Primary biliary cirrhosis
PDC	Pyruvate dehydrogenase complex
PDGF	Platelet-derived growth factor
PDK	Pyruvate dehydrogenase kinase 4
PEPCK	Phosphoenolpyruvate carboxykinase
pERK	Phosphorylated ERK
PGC1α	Peroxisome proliferative activated receptor gamma coactivator 1
pIκBα	Phosphorylated IκBα
pJNK	Phosphorylated JNK
PNPLA3	Patatin like phospholipase domain containing 2
PPARα	Peroxisome proliferator-activated receptor alpha
PPARγ	Peroxisome proliferator activated receptor gamma
pSTAT3	Phosphorylated STAT3
PVDF	Polyvinylidene difluoride
RT-qPCR	Real time quantitative polymerase chain reaction
SAA3	Serum amyloid A3
SAF	Steatosis activity fibrosis
SAP	Serum amyloid P component
SD	Standard deviation
SHP	Small heterodimer partner
SHP	Small heterodimer partner
SREBP1c	Sterol regulatory element-binding protein 1c

STAT3	Signal transducer and activator of transcription 3
UCP1	Uncoupling protein 1
TBAP	Total bile acid pool
TβMCA	Taurocholate conjugated beta MCA
TG	*Fgf15* overexpressing transgenic mice
TGFβ	Transforming growth factor beta
TGR5	Takeda G-protein receptor 5
TIMP1	Tissue inhibitor of metalloproteases 1
TNFα	Tumor necrosis factor alpha
WT	Wild type

CHAPTER 1:

GENERAL INTRODUCTION

1.1 BA-FXR-FGF15/19 PATHWAY

Bile acids (BAs) are amphipathic detergents produced in the liver via the hydroxylation of cholesterol.[1, 2] The two predominant pathways responsible for the conversion of cholesterol to BAs are the classical (neutral) and alternative (acidic) pathways. In the classical pathway, cholesterol is sequentially oxidized by Cytochrome p450 7A1 (CYP7A1) and CYP8B1 to produce cholic acid (CA). The classical pathway accounts for the synthesis of roughly 75% of the total BA pool and the 7-alpha hydroxylation of cholesterol by CYP7A1 is the rate limiting step in BA synthesis. The alternative or acidic pathway produces chenodeoxycholic acid (CDCA) by the metabolism of cholesterol by CYP27A1 and CYP7B1. CA and CDCA can be conjugated to glycine or taurine by the enzyme BA-CoA amino acid N-acyltransferase. CA, CDCA, and their conjugates are considered primary BAs. In the intestine, certain microbial species express the enzyme bile salt hydrolase (BSH) which mediates the deconjugation of BAs. Gut microbes can further metabolize CA and CDCA to the secondary BAs, deoxycholic acid and lithocholic acid or ursodeoxycholic acid, respectively. Upon reabsorption and re-entry to the liver, secondary BAs can be conjugated.[1, 2] The total BA pool therefore consists of numerous species of BAs with unconjugated and conjugated primary and secondary BAs.

BAs undergo significant enterohepatic recirculation with roughly 95% of BAs reabsorbed from the small intestine transported back to the liver. The majority of BAs are reabsorbed in the ileum into enterocytes by an uptake transporter, apical sodium-dependent BA transporter (ASBT).[1] Once inside enterocytes, BAs can activate nuclear receptor farnesoid X receptor (FXR), and within the nucleus, FXR dimerizes with retinoid X receptor to interact with DNA at FXR response elements (FXRRE) to alter gene transcription.[3-5] Activation of FXR in enterocytes leads to the up-regulation of fibroblast growth factor 19 (FGF19) in humans and orthologous FGF15 in mice.[6] Though

orthologs, FGF15 and FGF19 share only 50% sequence homology.[7, 8] Both FGF15 and FGF19 are considered endocrine FGFs as they do not bind heparin sulfate and thus can escape extra-cellular matrix (ECM), unlike other subfamilies of FGF proteins.[9] The structural differences of endocrine FGFs that allow for their systemic circulation also reduce their affinity for fibroblast growth factor receptors (FGFR). Therefore, binding of FGF15 and FGF19 to their predominant receptors FGFR4, and to a lesser extent, FGFR1, requires the obligate co-receptor β-KLOTHO (βKL).[9] Upon induction in the intestine, FGF15/19 travels through portal circulation and activates FGFR4-βKL on hepatocytes.[6, 10, 11] This leads to activation of the extracellular signal-regulated kinase (ERK) and c-Jun N-terminal kinase (JNK) signal pathways and subsequently reduces BA synthesis by down-regulating the expression of *CYP7A1/Cyp7a1* and *CYP8B1/Cyp8b1* that encode enzymes, CYP7A1 and CYP8B1.[10, 12, 13] FGF15 and FGF19 thereby function as a negative feedback loop shutting down BA synthesis when BA levels are high in the intestine. BAs reabsorbed in the intestine activate FXR, transiently increase FGFR4 and βKL levels, and prime the liver for subsequent FGF15/19 signaling.[14] In humans, FGF19 is also expressed at low levels in the liver and is up-regulated during cholestasis.[15, 16] FXR activation in hepatocytes also suppresses *CYP7A1/Cyp7a1* and *CYP8B1/Cyp8b1* expression by inducing small heterodimer partner (SHP).[4, 17, 18] In hepatocytes, activation of FXR is primarily responsible for promoting BA biliary excretion, and does not suppress BA synthesis as strongly as FGF15/19 signaling.[19]

1.2 FIBROBLAST GROWTH FACTORS AND THEIR RECEPTORS

There are seven subfamilies of FGFs. These consist of the FGF1 subfamily (FGF1, FGF2), FGF4 subfamily (FGF4, FGF5, FGF6), FGF10 subfamily (FGF3, FGF7, FGF10, FGF22), FGF 8 subfamily (FGF8, FGF17, FGF18), FGF9 subfamily (FGF9, FGF16, FGF20), FGF11 subfamily (FGF11, FGF12, FGF13, FGF14), and FGF19 subfamily (FGF15, FGF19, FGF21, FGF23).[20] These subfamilies of FGFs have tissue

specific expression, varying binding affinity for each FGFR, and require different co-factors for receptor binding. A large degree of promiscuity has been identified in FGF activation of FGFRs allowing for redundancy in several biological systems.[20] All but one subfamily of FGFs are heparin binding proteins, which limits their functions to autocrine and paracrine signaling.[21] The FGF19 subfamily of FGFs has reduced affinity for heparin, allowing their members to circulate systemically, and bind FGFRs in distant organs, thereby acting as endocrine factors.[22] Heparin is also the binding co-factor required for activation of FGFRs, except for the FGF19 subfamily.[21] The co-factors required for FGFs of the FGF19 subfamily to activate FGFRs are the klotho proteins. There are two forms of klothos, αKL and βKL. The tissue specific expression of these klotho proteins controls the tissue specific effects of the endocrine FGFs.[20, 22]

There are four isoforms of FGFRs: FGFR1, FGFR2, FGFR3, and FGFR4. The general structure of FGFRs consists of 3 extracellular Ig-like domains, an acid box between the first two Ig-like domains, a transmembrane domain, and two intracellular tyrosine kinase domains (Figure 1.1).[20] The first Ig loop in FGFRs is not necessary for ligand binding and actually suppresses FGF and heparin sulfate binding affinity to the ligand binding domain located in the second and third Ig loops.[23, 24] Two forms of FGFRs are synthesized; an α form possessing the first Ig-like domain and a β form that lacks the first Ig-like domain. There are also variant forms of FGFRs that lack the acid box. FGFRs with the acid box present are designated with an AB (example: FGFR1βIIIcAB). The third Ig-like domain, Ig-III, in FGFR1, FGFR2, and FGFR3 can undergo alternative splicing resulting in two variant Ig-III loops, IIIb and IIIc.[25, 26] The third Ig-like domain in FGFR4 does not undergo alternative splicing.[27] The IIIb and IIIc FGFR splice variants display tissue specific expression. During organogenesis, IIIb FGFRs are expressed by the developing epithelium, whereas IIIc receptors are

expressed by the underlying mesenchymal layer. FGF factors produced by the epithelium activate the IIIc isoforms present in mesenchyme while the FGFs produced by the mesenchyme activate the IIIb FGFRs on the epithelium.[28-30] This acts as a paracrine axis controlling organogenesis. As described later in section 1.3.3, this axis is similar to the paracrine axis observed during liver injury in which there is coordinated regulation of FGFR activation on hepatic stellate cells (HSCs) and hepatocytes by subsequent FGFs; FGFs produced by HSCs activate FGFRs on hepatocytes and hepatocyte-derived FGFs activate FGFRs on HSCs.

1.3 NON-ALCOHOLIC STEATOHEPATITIS

1.3.1 *Disease characteristics, etiology, and risk factors:*

Non-alcoholic steatohepatitis (NASH) is the inflammatory stage of non-alcoholic fatty liver disease (NAFLD) characterized by steatosis, hepatocyte ballooning, inflammation, and fibrosis. [31, 32] NAFLD is a progressive disease beginning as simple steatosis but can develop into NASH that is characterized by inflammation and other cellular degenerations. Eventually, NASH can progress to fibrosis, cirrhosis, and even hepatocellular carcinoma (HCC).[31-33] Metabolic syndrome often accompanies the development of NASH. Metabolic syndrome is defined as having 3 of 5 clinical presentations: 1) serum triglycerides greater than 150 mg/dL; 2) serum high density lipoprotein (HDL) less than 40 or 50 mg/dL in men and women, respectively; 3) increase in waist circumference; 4) serum glucose levels greater than 100 mg/dL; and 5) systolic or diastolic blood pressures greater than 130 and 85 mmHg, respectively.[34]

The mechanisms regulating NAFLD to NASH progression remain unclear. A "two-hit" model was proposed in 1998.[35] This model speculates that NASH develops as the result of two sequential liver injuries. The "first hit" in the model is the accumulation of lipids in the liver leading to the development of simple steatosis. The "second hit" is a

subsequent insult that induces inflammation. Though this model has been well cited for two decades, it has come under recent scrutiny as it is likely a drastic oversimplification of the processes that lead to NASH. For instance, progression to fibrosis can occur in NAFLD without the development of NASH.[36] Patients can also present with cryptogenic fibrosis and have numerous risk factors for NAFLD and NASH but have minimal histological features of NASH.[37] Additionally, NASH patients can progress to HCC without the development of cirrhosis.[38] These findings indicate that more than just the "two-hit" model underlies NASH pathogenesis.

Although the etiologies and mechanisms of NASH are not well understood, many risk factors have been identified. The most common health condition associated with NASH is obesity, followed by type 2 diabetes mellitus, dyslipidemia, metabolic syndrome, polycystic ovary syndrome, while less common conditions include hypothyroidism, hypopituitarism, hypogonadism, pancreatoduodenal resection, psoriasis, and sleep apnea.[39] Age, sex, female reproductive status, and ethnicity are also associated with NASH development.[31] Lastly, genetic polymorphisms have been identified which correlate to NASH; the most notable being variation in the patatin-like phospholipase domain-containing protein (*PNPLA3*) gene.[40, 41] The prevalence of *PNPLA3* polymorphisms amongst different ethnic groups may explain ethnic differences in NAFLD and NASH prevalence.[41]

1.3.2 *Disease prevalence, diagnosis, and current treatment:*

With the rise of the obesity epidemic, the prevalence of NASH has greatly increased over the past two decades. Current estimates place the North American prevalence of NAFLD at 24.13% and of those patients with NAFLD 21% may have NASH.[42, 43] Further, of NASH patients worldwide, 40.76% will likely progress to fibrosis. The U.S. census data in 2017 placed the population at 325,719,178 people.[44] Based on

the census and the estimates of NASH and fibrosis prevalence, we estimate that over 7 million individuals in the United States alone have or will develop NASH with fibrosis. The high prevalence of NAFLD and NASH is not limited to North America with the global prevalence of NAFLD estimated at 25.24%.[42] Due to the increasing prevalence of NASH and recent breakthroughs in treatment of hepatitis C virus (HCV), NASH will surpass HCV as the primary indication for which patients are added to the liver transplant waiting list. From 2008 to 2014, the number of patients added to the United States transplant waiting list for treatment of HCV was stable at roughly 3000 patients per year.[45] In 2017, this number was decreased to 1705. Conversely, the number of patients who were added to the liver waiting list for the treatment of NASH increased from 643 in 2008 to 2100 in 2017.[45] Based on these numbers, it has appeared that NASH has already surpassed HCV to become the number one indication for patients to receive liver transplant or will do so in the very near future.

The gold standard for diagnosing NASH is histolopathologic evaluation of liver biopsy. The diagnosis of definitive NASH requires the presence of all histologic criteria including steatosis, hepatocellular ballooning, and lobular inflammation. The diagnosis of borderline NASH is given when a patient presents with steatosis and most but not all histologic features of NASH.[39] Several scoring systems have been developed to assess NASH histologic severity, including the NASH Clinic Research Network's NAFLD activity score (NAS), the steatosis, activity, and fibrosis (SAF), and Brunt staging.[46-48] Less invasive methods to assess NASH severity are currently under investigation with some being incorporated into clinical trials. Examples include magnetic resonance imaging (spectroscopy and proton density fat fraction), transient elastography, and serum fibrosis biomarkers.[49]

Despite the rising prevalence and burden NASH places on society and the medical system, there is currently no approved therapeutic agent to treat NASH. The current guideline for the management of NASH recommends changes in lifestyle; weight loss, diet, and exercise.[39] Vitamin E and thiazolidinediones may provide benefit to NASH patients but risks of thiazolidinedione therapy have to be weighed against the potential benefits. Guidelines recommended against using ursodeoxycholic acid, metformin, and omega-3 fatty acids for the treatment of NASH, however, these medications can be used to manage concomitant disease states. The guidelines also recommend against the off-label use of obeticholic acid (OCA) until clinical trial data regarding its use for the treatment of NASH become available. The only treatment for patients with advanced fibrotic NASH is liver transplant.[39] With the limited number of organs available for transplant, it is a paramount medical necessity to identify the molecular mechanisms underlying NASH pathogenesis and to develop novel therapies to prevent, mitigate, or reverse NASH progression.

1.4 HEPATIC STELLATE CELLS

1.4.1 *HSCs and hepatic fibrosis*

Hepatic fibrosis is the result of chronic injury leading to the accumulation of connective tissue that is primarily produced by the HSCs. Chronic injuries caused by viral hepatitis, alcoholic liver disease, NASH, or obstructive biliary diseases, trigger a persistent activation of HSCs causing the continual production of ECM and inhibition of the enzymes which degrade the matrix. In severe cases, hepatic fibrosis may advance to cirrhosis, a later stage of irreversible scarring that can cause potentially fatal sequelae; portal hypertension, variceal bleeding, and ascites to name a few.

The primary contributors to excessive ECM production during hepatic fibrosis development are HSCs.[50] HSCs account for up to 15% of the total resident liver cell

population.[51, 52] HSCs are mesenchymal pericytes located within the space of Disse between parenchymal hepatocytes and sinusoidal endothelial cells.[7] Their cell structure contains numerous processes which encircle sinusoids and also make contact with the hepatocyte parenchyma.[53] These processes serve as sensors to the hepatic microenvironment. HSCs are also located next to nerve cells.[54] The ability to sense and interact with many cell types in the liver makes quiescent HSCs regulators of many physiological functions including vasoregulation, immune modulation, maintenance of ECM, and metabolism.[50] Quiescent HSCs also act as the primary depot for vitamin A in the body.[55] Upon liver injury, quiescent HSCs differentiate into activated myofibroblasts and release their vitamin A stores. The activated HSCs express α-smooth muscle actin (αSMA), migrate to the area of injury via chemotaxis, release growth factors to stimulate hepatocyte regeneration and angiogenesis, produce ECM, and modulate immune responses.[56] These actions enhance the ability of the liver to repair after acute injury. Upon resolution of the injury, activated HSCs should revert back to a quasi-quiescent state.[57, 58] However, chronic liver injury leads to a perpetuated activation of HSCs and continuous accumulation of ECM leading to the eventual development of hepatic fibrosis.

1.4.2 *FXR signaling in HSCs*

HSCs express FXR in the liver albeit primary isolated rat HSCs express low levels of FXR compared to liver tissue homogenate.[59] The rat HSC cell line HSC-T6 and human HSC cell line LX-2 also express FXR.[60] Activation of FXR in HSCs affects numerous signaling pathways, which together, function to reduce hepatic fibrosis. The expression of SHP is induced in HSCs by activation of FXR.[61, 62] In HSCs, SHP binds to SMAD3 and JunD.[61, 62] By binding to SMAD3, SHP prevents SMAD3 from interacting with the transforming growth factor beta (*TGFβ*) promoter and reduces HSC

responsiveness to TGFβ.[62] Induction of *collagen 1α1* (*Col1α1*) by TGFβ in HSC-T6 cells was reduced by CDCA.[61] In LX-2 cells, OCA treatment reduced TGFβ inductions of *COL1α1*, *αSMA*, *matrix metalloprotease 2* (*MMP2*), *transforming growth factor beta receptor 2*, *TGFβ*, and *endothelin-1* (*ET-1*).[62] Through binding to JunD, SHP reduced the binding of activator protein-1 to DNA, thereby preventing HSC activation induced by thrombin.[61] OCA treatment of primary rat HSCs and HSC-T6 cells attenuated the induction of *tissue inhibitor of metalloproteases 1* (*Timp1*) by thrombin and increased MMP2 activity in a SHP dependent manner.[60]

FXR activation also induces the expression of peroxisome proliferator-activated receptor gamma (PPARγ) in HSCs.[63] The promoter of PPARγ has been shown to contain a functional FXRRE by luciferase assay.[64] By inducing PPARγ, FXR activation in HSCs reduced the expression of inflammatory cytokines.[64] PPARγ is also a negative regulator of collagen expression. During HSC transdifferentiation to an activated phenotype, PPARγ expression is drastically reduced and expression of collagen increases. Treatment of primary rat HSCs with OCA mitigated the down-regulation of *PPARγ* by random transdifferentiation in culture and reduced collagen expression.[63] Primary HSCs were isolated from OCA treated rats that underwent either the porcine serum, bile duct ligation, or carbon tetrachloride (CCl_4) liver fibrosis models. HSCs from the OCA treated animals had higher expression of PPARγ.[63] FXR also affects ECM production by regulating the expression of miRNA-29a in HSCs.[65] A FXRRE was identified in the miRNA-29a promoter. The expression of ECM proteins, collagen, elastin, fibrillin, was reduced by miRNA-29a.[65]

HSC contractility is regulated by FXR. The expression of dimethylarginine dimethylaminohydrolase 2 (DDAH2) is up-regulated in HSCs by FXR activation.[66] This leads to increased activity of enthothelial nitric oxide synthase (eNOS) as DDAH2

degrades asymmetric dimethylarginine and monomethyl-L-arginine, inhibitors of NOS.[66, 67] FXR also decreases HSC contractility by decreasing the expression of ET-1.[68, 69] Reductions in ET-1 reduces Rho-associated protein kinase pathway activation and reduces the phosphorylation of myosin light chain. FXR activation also reduces phosphorylation of myosin light chain by reducing myosin light chain kinase levels.[68] In summary, FXR activation in HSCs reduces ECM production while increasing ECM degradation, reduces HSC responsiveness to profibrotic mediators, reduces inflammatory mediator expression, and reduces HSC contractility.

1.4.3 *FGF signaling in HSCs*

A systematic survey of FGFR expression was performed in freshly isolated primary rat HSCs.[70] Primers were developed for real time quantitative polymerase chain reaction (RT-qPCR) that could detect the various splice variants of each FGFR isoform. As may be expected for a mesenchymal cell, HSCs were not found to express FGFR1IIIb, FGFR2IIIb, or FGFR3IIIb. However, HSCs did express the IIIc alternatively spliced isoforms of FGFR1, FGFR2, FGFR3, and FGFR4. Three variants of FGFR1IIIc were expressed; FGFR1βIIIcAB, FGFR1αIIIc, and FGFR1αIIIcAB. The predominant variant was FGFR1βIIIcAB. Three variants of FGFR2IIIc were present including FGFR2βIIIc, FGFR2βIIIcAB, FGFR2αIIIcAB with the primary form expressed being FGFR2βIIIc. Only 1 variant of FGFR3, FGFR3αIIIcAB was present. This study only looked at expression of FGFRs in freshly isolated rat HSCs or HSCs cultured only for three days and not in activated HSCs. This is important as FGFR expression may alter upon activation. A separate study determined that FGFR4 expression is up-regulated 2.47-fold in LX-2, a human HSC cell line, upon hypoxia induced transdifferentiation.[71] It is important to note that the above survey of FGFR expression in HSC was only performed in rats, and to our best knowledge, no similar studies have been performed to extensively characterize FGFR variant expression in HSCs of other species. FGFR1,

and to a much lesser extent FGFR4, have been shown to be expressed in isolated mouse HSCs.[72]

Several studies have shown that liver injury and *in vitro* transdifferentiation stimulate HSC production of FGFs including FGF2,[26, 30, 70, 72, 73] FGF7,[74-76] and FGF9.[26] FGF2 and FGF9 are also expressed by hepatocytes. The localized production of FGFs allows for potentially both autocrine and paracrine stimulation of FGFRs at the foci of liver damage. In addition to autocrine and paracrine FGFs, the effects of endocrine FGFs (FGF15/19 and FGF21) on hepatic fibrosis are now emerging. Several clinical studies have now been performed identifying the correlation of serum and liver concentrations of endocrine FGFs to various forms of hepatic fibrosis. A few animal studies have also now been published identifying the mechanisms by which FGF15/19 and FGF21 mediate the development of hepatic fibrosis. The findings from these studies regarding autocrine, paracrine, and endocrine FGF signaling on HSCs are described in the follow sections. In brief summary, FGF signaling during liver damage enhances liver regeneration but chronic production can also lead to the development of fibrosis (See Table 1.1).

1.4.3.1. *FGF1 subfamily:*

The members of the FGF1 subfamily, FGF1 and FGF2, have been investigated for their effects on hepatic fibrosis and HSC activation and proliferation. Though all studies have found that FGF1 or FGF2 regulates HSC function or proliferation, there are several conflicting reports. For example, some of the studies described below state that FGF2 does not affect αSMA expression or HSC proliferation whereas other studies state that FGF2 up-regulates αSMA and induces proliferation. Below are summaries of the key investigations into the effects of FGF1 and FGF2 on HSC function.

Lin et al. determined that primary rat HSCs spontaneously activated over 16 days of culturing produce FGF2. [73] This study also demonstrated that FGF2 induces the production of COL1α1 and αSMA *in vitro*. FGF2 treatment of HSCs led to increased proliferation indicated by increased incorporation of bromodeoxyuridine (BrdU). The effects on proliferation were determined to be induced by the activation of the ERK signaling pathway and altered expression of cyclin D and p21. The effects on HSC proliferation and gene expression by FGF2 were reversible by treatment with NP603, an inhibitor of FGFR1. This study also demonstrated that *in vivo* NP603 was found to ameliorate the up-regulation of *Col1α1* and *αSma* in rats treated with CCl_4.[73]

Corresponding to the FGF2 induced proliferation of primary rat HSCs in Lin et al., FGF2 was also shown to act as a mitogen for LX-2 cells.[77] The induction of LX-2 proliferation by FGF2 was inhibited by co-treatment with brivanib, an ATP-competitive inhibitor of FGFR, vascular endothelial growth factor receptor, and platelet derived growth factor receptor. [78] TGFβ induction of αSMA in LX-2 cells was not inhibited by brivinib indicating that FGF signaling does not affect TGFβ activation of HSCs. The effects of brivinib on hepatic fibrosis were tested in three animal models (CCl_4, bile-duct ligation, and thioacetamide fibrosis models) with results showing that brivinib decreased *αSma* and *Col1α1* expression. Unfortunately, isolating the role of FGF signaling in these animal studies is confounded by the lack of target specificity of brivnib.[77]

Juxtaposed to the previous studies, a study using mice deficient in FGF1 ($FGF1^{-/-}$), FGF2 ($FGF2^{-/-}$) or both ($FGF1^{-/-}FGF2^{-/-}$) found that FGF1 and FGF2 regulated the expression of *Col1α1*, but does not affect HSC migration or proliferation.[79] In this study, groups of 8-week old male $FGF1^{-/-}$, $FGF2^{-/-}$, and $FGF1^{-/-}FGF2^{-/-}$ mice were treated with CCl_4 acutely with one dose or chronically for 3 weeks. In both the acute and chronic studies, it was found that the $FGF1^{-/-}$, $FGF2^{-/-}$, and $FGF1^{-/-}FGF2^{-/-}$ mice had attenuated

expression of *Col1α1* but no effects on *αSma* expression were seen. The extent and time course of TGFβ expression upon injury was not altered in the $FGF1^{-/-}FGF2^{-/-}$, indicating that the mechanism by which these FGFs regulate the development of fibrosis is not through mitigation of TGFβ expression. Desmin expression, a surrogate estimator for the number of HSCs present in the liver, was similar between wild type (WT) and $FGF1^{-/-}FGF2^{-/-}$ mice. Therefore, the authors concluded that FGF1 and FGF2 do not regulate HSC proliferation. This finding is in congruence with an *in vitro* study using both primary rat HSCs and LX-2 cells.[70] During this study, HSCs were treated with FGF2 and cell proliferation was measured by ^{3}H-thymidine DNA incorporation. Though FGF2 was found to lead to the phosphorylation of ERK1, ERK2, JNK1, and JNK2/3, FGF2 did not alter HSC proliferation.

The studies described above all investigated the interaction between FGF2 and TGFβ signaling. This interaction was also studied *in vitro* using cultured human myofibroblastic liver cells (MFLCs).[80] TGFβ was found to increase the expression of FGF2 and FGFR1 by MFLCs. Treatment of MFLCs with anti-FGF2 antibodies inhibited the proliferative effects of TGFβ but not the expression of fibronectin. This study concluded that FGF2 acts as an autocrine factor mediating the proliferative response, but not the profibrotic response, of MFLCs to TGFβ. This is consistent with the finding that FGFR inhibition by brivinib did not modulate αSMA expression induced by TGFβ.[77]

In summary, FGF2 derived from HSCs and hepatocytes functions as an autocrine and paracrine signaling molecule regulating HSC function during liver injury. Correspondingly, autocrine stimulation of fibroblasts by FGF2 has also already been implicated as a key mediator of the development of bone marrow[81] and lung fibrosis.[74] In addition to its autocrine effects, HSC-derived FGF2 also functions in a paracrine manner to induce hepatocyte growth and regeneration during injury. It has been well

studied that FGF2 is a strong proliferative signal for hepatocytes.[75, 76, 82] After partial hepatectomy, injection with FGF2 increased uptake of ^{3}H-thymidine in the liver.[76] FGF2 is also required for the proper organization of cells within the liver, as FGF2 deficient mice that underwent partial hepatectomy had altered liver structures after regeneration.[82]

1.4.3.2. *FGF7 subfamily:*

The production of FGF7 by HSCs during liver injury has also been investigated. In two human studies, livers were collected from patients with cirrhosis, viral hepatitis, autoimmune hepatitis, and alcohol induced liver damage.[83, 84] Both studies found that FGF7 was expressed in fibrotic livers but not in healthy control liver samples. Steiling et al. noted that the fibrosis staging in HCV patients was positively correlated with FGF7 mRNA levels and immunohistochemistry (IHC) of the liver showed that FGF7 expression co-localized with αSMA.[83] Otte et al. also included an animal study parallel to their clinical investigation.[84] Male Wistar rats were exposed to phenobarbitone and CCl_4 for up to 70 days. Consistent with the human clinical data, IHC of liver sections from the treated rats revealed that FGF7 was exclusively expressed in myofibroblasts in fibrotic foci with isolated protein and mRNA levels of FGF7 positively correlated to fibrosis severity.[84] The function of HSC-derived FGF7 has been explored in a mouse partial hepatectomy model.[85] HSCs from hepatectomized mice had a 3.3 fold increase in FGF7 expression compared to HSCs from sham mice. Expression of FGFR2b, the receptor for FGF7, was found to increase 3 fold after partial hepatectomy, with IHC revealing strongest staining in hepatocytes. To perform a gain-of-function study, a group of mice was given a hydrodynamic tail vein injection of plasmid encoding a HA-tagged FGF7. Overexpression of FGF7 led to an accelerated incorporation of BrdU and expression of proliferating cell nuclear antigen in hepatocytes after partial hepatectomy. These data indicate that the up-regulation of FGF7 in HSCs and up-regulation of FGFR2b on

hepatocytes act as a paracrine axis driving hepatocyte regeneration after liver injury. No studies could be identified which investigated the direct effect of FGF7 on HSC activation or proliferation. However, it has been shown that HSCs in rats do not express FGFR2b, but instead, express FGFR2c that is not activated by FGF7.[70] Thus it is unlikely that FGF7 will affect HSCs directly.

1.4.3.3. *FGF9 subfamily:*

FGF9 is also expressed by HSCs.[70] Liver slices were cultured with or without CCl_4 treatment. IHC of the untreated cultured liver slices indicates that FGF9 is basally expressed in hepatocytes and a few HSCs. Upon treatment with CCl_4, the number of FGF9-positive HSCs was greatly increased. FGF9 expression was measured in isolated primary rat HSCs before and after activation. Upon transdifferentiation into an activated phenotype, HSCs up-regulate FGF9 expression 5 to 10 fold. Expression of FGF16 and FGF20, the two other members of the FGF9 subfamily, was not detected in HSCs by RT-qPCR. The authors noted that although HSCs express the receptors activated by FGF9, FGF9 failed to induce HSC proliferation as measured by ^{3}H-thymidine incorporation. However, FGF9 did act as a mitogen for hepatocytes.[70] Hence, similar to FGF2 and FGF7, FGF9 produced by HSCs functions to increase hepatocyte proliferation and regeneration upon injury.

1.4.3.4 *FGF19 subfamily:*

The effect of FGF15 on CCl_4 induced liver fibrosis has recently been investigated.[72] Mice were given an intraperitoneal (i.p.) injection of the carcinogen diethylnitrosamine at the age of 15 days and were subsequently given biweekly i.p. injections of CCl_4. After 27 weeks, FGF15 deficient mice were found to have decreased hepatic fibrosis compared to WT. In agreement with histologic findings, FGF15 deficient

mice were found to have down-regulated *Col1α1*, *Timp1*, *αSma*, and *connective tissue growth factor* (*Ctgf)* compared to WT mice. The induction of *Ctgf* observed in WT mice treated with CCl_4 was not observed in knockout mice. Overexpression of FGF15 using an adenovirus vector led to roughly 3 fold elevations of both hepatic *Tgfβ* and *Ctgf* expression. Using *in vitro* experiments, this study proposed that FGF15 affected HSCs indirectly; specifically, FGF15 signaling increases CTGF release from hepatocytes leading to the paracrine activation of HSCs. Treatment of isolated mouse HSCs with FGF19 showed no changes in cyclin D or αSMA expression.[72] Though no effects were seen during this study, a direct effect of FGF15/19 on HSCs should not be ruled out. As FGFR4 is up-regulated over 2 fold in HSCs upon activation,[71] FGF15/19 signaling may be enhanced in activated HSCs. Additionally, this study treated mouse HSCs with human FGF19 which may have failed to activate the mouse receptor efficiently.

Recently, many clinical studies have found correlations between serum FGF19 levels and severity of hepatic fibrosis of multiple etiologies.[15, 86] However, whether FGF19 serum levels were positively or negatively correlated to fibrosis score depended upon the etiology of disease. This may be attributed to the fact that FGF19 may affect disease pathogenesis via regulation of BA levels or through regulation of activation of HSCs. For this reason, understanding of disease progression is extremely important when considering the reasons underlying FGF19 and fibrosis correlations.

Severity of lobular and portal fibrosis in patients with pediatric onset intestinal failure was found to be negatively correlated to FGF19 levels.[86] Serum concentrations of the inflammatory markers and portal inflammation severity were also negatively correlated to FGF19 serum concentrations. Of the 42 patients screened, 57% were found to have serum bile levels out of range. As FGF19 is a negative feedback factor for BA synthesis, the observed hepatic fibrosis and inflammation in patients with low serum

concentrations of FGF19 may have been the result of dysregulated BA production and BA toxicity. The pattern of portal fibrosis and inflammation observed in these patients is in agreement with this hypothesis. Similar results have been found in an experimental model of short bowel syndrome. Bowel resection in piglets led to an altered microbiome, altered TBAP composition, altered FXR activation, and failure of hepatic SHP to down-regulate BA synthesis.[87] The authors proposed that the accumulation of hepatic BAs led to the observed liver damage.

A recent study also examined the use of serum and liver FGF19 levels as a biomarker for severity of primary biliary cirrhosis (PBC).[15] This study found that serum FGF19 levels were positively correlated to Mayo Risk Score for PBC. This paper reported that FGF19 is expressed 9 fold greater in the liver of non-cirrhotic PBC patients and 69 fold greater in the liver of cirrhotic PBC patients compared to healthy individuals. In patients with fibrosis, higher hepatic *FGF19* mRNA levels were associated with worsened fibrosis severity. Hepatocytes with up-regulated *FGF19* were also found to induce *FGFR4* expression. Therefore, the authors proposed that the production of FGF19 during PBC is a compensatory mechanism to decrease bile production in an autocrine fashion.[15]

The role of FGF21 in the regulation of HSC activation, apoptosis, and development of fibrosis has been reported in both gain-of-function and loss-of-function studies. In the gain-of-function study, male ICR mice were given 10 mg/kg dimethylnitrosamine for the first three consecutive days of each week for 4 weeks.[88] FGF21 was given to the mice every 12 hours after dimethylnitrosamine treatment. Animals receiving exogenous FGF21 treatment had reduced fibrosis and attenuated induction of COL1α1, αSMA, and TGFβ protein and mRNA levels. TGFβ signaling was also altered with FGF21-treated mice having decreased pSmad2/3: Smad2/3 ratio.

FGF21 seems to be protective against the development of hepatic inflammation as protein and mRNA levels of inflammatory molecules, tumor necrosis factor alpha (TNFα), interleukin 6 (IL6), and interleukin 1β (IL1β), were reduced as were the pIκB/IκB and p65/lamin b1 ratios. *In vitro* treatment of T6 cells, a rat HSC cell line, with FGF21 was performed in the presence of ethanol or platelet-derived growth factor (PDGF). FGF21 decreased COL1α1, αSMA, and TGFβ expression induced by both ethanol and PDGF. FGF21 was also found to be proapoptotic by reducing B-cell leukemia/lymphoma 2:BCL2-associated X protein (BCL2:BAX) ratios.

The effect of FGF21 on fibrosis was also studied in a loss-of-function study model. WT and FGF21 deficient mice were fed a methionine and choline deficient diet for 8 to 16 weeks.[89] The FGF21 deficient mice were found to have worsened steatosis, inflammation, and fibrosis. *Col1α1*, *αSma*, and *Tgfβ* mRNA levels were elevated in the knockout mice in addition to the expression of genes involved in inflammation and fatty acid transport: *monocyte chemoattractant protein 1*, *macrophage inflammatory protein 1α*, *Il1β*, and *cluster of differentiation 36* (*Cd36)*. The altered expression of all of the previously mentioned genes was reversible by continuous subcutaneous infusion of FGF21 to the FGF21 deficient mice.

Despite the protective nature of FGF21 in animal models, many clinical studies have reported a positive correlation between steatosis and fibrosis severity and serum FGF21 levels in humans.[90-94] Due to the correlations found in these studies, it has been proposed that serum FGF21 levels can be used as a biomarker for NAFLD, NASH, and other liver pathologies. As FGF21 is predominantly produced in the liver it is probable that the increased FGF21 serum levels observed in these studies is due to a compensatory increase in hepatic FGF21 production to attempt to mitigate liver injury. FGF21 may serve as a biomarker to reflect hepatic stress.

1.5 CURRENT STATE OF FXR AGONIST AND FGF19 ANALOG DEVELOPMENT FOR THE TREATMENT OF NASH

Many molecular targets are currently under investigation for their ability to halt or reverse NASH progression. Two promising targets that have been identified are the nuclear receptor FXR and FGF19. The mechanisms by which tissue specific FXR and FGF15/19 regulate NASH development in animal models will be discussed in detail. Several FXR agonists and an FGF19 analog protein have reached later phase clinical trials for treatment of NASH. The progress of these compounds and summary of released data will be provided. Lastly, the safety liabilities specific to the development of FXR agonists will be discussed.

1.5.1 FXR and FGF19 in animal models of NASH

1.5.1.1 Systemic FXR:

FXR is expressed in many tissues and cell types in the body. Manipulation of body-wide FXR activity either through pharmacologic or genetic means affects the development of each characteristic of NASH; steatosis, inflammation, fibrosis, and metabolic syndrome. This section will broadly describe the effects of systemic FXR activation or deficiency on NASH development. The roles of tissue specific FXR and the mechanisms by which they influence NASH development will be described in depth in following sections. FXR agonists used in the animal studies described below include WAY-362450, GW4064, OCA, and fexaramine. Briefly, WAY-362450 and GW4064 are non-steroidal, systemically acting, FXR agonists whereas OCA is a BA, systemically acting, FXR agonist. Fexaramine is a non-steroidal FXR agonist with extremely poor bioavailability when given orally and therefore serves as an intestinal specific FXR agonist.

Systemic activation of FXR is protective against the development of hepatic steatosis, inflammation, and fibrosis. In mice fed a high fat diet (HFD), treatment with OCA and GW4064 reduced the accumulation of hepatic triglycerides and free fatty acids and subsequently reduced steatosis severity.[95, 96] Similarly, in low density lipoprotein receptor (*LDLR*) knockout mice fed a Western Diet, WAY-362450 reduced hepatic triglyceride and cholesterol levels and attenuated steatosis.[97] Hepatic inflammation is also reduced by treatment with FXR agonists. In both HFD and methionine & choline deficient diet (MCDD) models, GW4064 and WAY-362450 reduced hepatic inflammation.[96, 98] Correspondingly, FXR deficient mice had worsened inflammation induced by MCDD.[99] Activation of whole body FXR ameliorates hepatic fibrogenesis. OCA, WAY-362450, and BAR704 decreased the severity of fibrosis in mouse HFD, MCDD, and CCl_4 models, respectively.[95, 96, 98] Deficiency of FXR worsened fibrosis induced by MCDD or knockout of *LDLR*.[99, 100]

Body wide activation of FXR has many beneficial effects on metabolic endpoints. In mice fed a HFD, GW4064 reduced body weights and fat mass. GW4064 also lowered fasting glucose concentrations and improved glucose tolerance. Hepatic gluconeogenesis was also reduced.[96] Serum lipids are also altered by modulation of whole body activity of FXR. Activation of FXR by GW4064 and WAY-362450 reduced triglyceride and cholesterol levels in HFD and *LDLR* knockout, Western diet murine models, respectively.[96, 97] However, in addition to lowering VLDL and LDL, WAY-362450 also decreased HDL.[97] In agreement with the gain-of-function studies, *FXR* knockout mice had increased serum triglyceride, cholesterol, and free fatty acid levels.[101]

1.5.1.2 Hepatic FXR:

Multiple cell types in the liver express FXR, including hepatocytes, hepatic stellate cells, endothelial cells, kupffer cells, and cholangiocytes.[61, 102, 103] The role of

FXR in inflammatory cells and in regulating inflammatory signaling pathways will be discussed in this section. The activation of FXR locally in the liver affects the development of each characteristic of NASH; steatosis, inflammation, fibrosis, and metabolic syndrome. The effects on each of these characteristics will be described below. For a summary of the effects of FXR activation in specific cell types, please see Figure 1.2.

Hepatic FXR activation has been shown to be protective against the development of hepatic steatosis. In a high cholesterol diet model, hepatic FXR deficiency, but not intestinal FXR deficiency, exacerbated hepatic steatosis.[104] Hepatic FXR activation mitigates hepatic lipid content by decreasing lipogenesis and increasing fatty acid oxidation.[105, 106] By inducing SHP, FXR activation decreased sterol regulatory element-binding protein 1c (SREBP1c) expression and consequently decreased the expression of genes involved in lipogenesis.[106] In human hepatocytes, FXR up-regulated peroxisome proliferator-activated receptor alpha (PPARα), which subsequently increased fatty acid oxidation.[105] It is important to note that the murine PPARα promoter does not have a functional FXRRE, therefore, in mice PPARα is not an FXR response gene.[105] Hepatic FXR also affects lipid homeostasis in the body by enhancing reverse cholesterol transport.[107] FXR deficient mice had reduced expression of scavenger receptor class B type 1, hepatic lipase, cholesterol ester hydrolase, sterol carrier protein, and lecithin-cholesterol acyltransferase and increased expression of apolipoproteins (ApoA-IV, ApoE, and ApoC-III).[107] Hepatic FXR deficient mice, but not intestinal deficient FXR mice, had increased serum cholesterol compared to wild type mice when fed a high cholesterol diet.[104]

In addition to regulating hepatic lipid levels, FXR affects hepatic glucose metabolism. FXR activation decreased gluconeogenesis and glycolysis while increasing

glycogenesis. CA induced FXR activation in mice reduced the hepatic protein levels of enzymes responsible for gluconeogenesis, peroxisome proliferator-activated receptor gamma coactivator 1-alpha (PGC1α), phosphoenolpyruvate carboxykinase (PEPCK), and glucose 6-phosphatase (G6Pase). The down-regulation of these proteins by CA did not occur in FXR or SHP deficient mice indicating that FXR regulates gluconeogenesis in the liver via a SHP-dependent pathway.[101] Glycogen levels in the liver are increased by FXR activation. In db/db mice, treatment with GW4064 for 5 days increased hepatic glycogen levels by increasing glycogenesis.[108] Nonphosphorylated glycogen kinase 3 reduced glycogen synthase activity, however this effect was reduced by phosphorylation.[109] Levels of phosphorylated glycogen kinase 3 were increased in the GW4064 treated mice. GW4064 treatment also increased the phosphorylation of insulin receptors 1 and 2. Therefore, FXR may also increase hepatic glycogen levels by enhancing insulin sensitivity.[108] In agreement with the previous gain-of-function study, FXR deficient mice had reduced levels of hepatic glycogen.[110] FXR activity can also increase hepatic glycogen levels by suppressing glycolysis. Pyruvate dehydrogenase complex (PDC) is an important metabolic switch that regulates the oxidation of glucose for fatty acid synthesis. Pyruvate dehydrogenase kinase 4 (PDK4) inhibits PDC and reduces glycolysis.[111] *In vitro* treatment of human hepatocytes and *in vivo* treatment of mice with FXR agonist GW4064 increased expression of PDK4 thus decreased glycolysis.[112]

The metabolic effects of FXR in the liver may also be mediated by fibroblast growth factor 21 (FGF21). The promotor of *FGF21* has a functional FXRRE and the expression of *FGF21* in the liver has been shown to be regulated by FXR. However, FGF21 is predominantly regulated by PPARα.[113, 114] *In vivo* treatment of mice and *in vitro* treatment of human hepatocytes with CDCA increases FGF21 expression and

secretion.[114] Numerous studies have demonstrated the effects of FGF21 on NASH and metabolic endpoints, which has been the subject of many review articles.[115-120] In brief, FGF21 increases browning of adipose tissue, energy expenditure, insulin production, glucose uptake by white adipose tissue, gluconeogenesis, ketogenesis, and lipolysis. In NASH models, FGF21 is protective against hepatic steatosis, inflammation, fibrosis and metabolic syndrome.[89, 121, 122] To our knowledge, in studies using FXR agonists, the extent to which the FXR-FGF21 axis affects NASH or metabolic disease development has not been shown.

FXR activation is anti-inflammatory and affects both innate and adaptive immune responses. Innate immune responses shown to be affected by FXR include the acute phase response and natural killer T-cell (NKT) activation. The acute phase response is a systemic reaction to local or systemic acute infection, illness, or injury.[123] During the acute phase response, the expression of acute phase proteins, which are predominantly produced in hepatocytes, is markedly altered; normally increased. In humans, the major acute phase protein is C-reactive protein (CRP) whereas in mice the major acute phase proteins are serum amyloid P component (SAP) and serum amyloid A3 (SAA3).[123] FXR activation has been shown to reduce the expression of CRP, SAP, and SAA3. In Hep3B cells, FXR agonism with GW4064 and WAY-362450 mitigated the induction of CRP by interleukin-6.[124] Treatment of mice with WAY-362450 reduced LPS stimulated induction of SAP and SAA3 whereas knockout of FXR increased the induction of SAP and SAA3.[124] In contrast, FXR activation, at least in mice, has been shown to induce the expression of a cohort of genes involved in acute phase response.[125, 126] The exact role of FXR in regulating acute phase response needs further investigation. FXR may also affect the innate immune system by regulating the activation of liver NKT cells. NKT cells have been shown to express both FXR and SHP. In NKT cells, activation of FXR

induces SHP, which prevents the binding of c-Jun to the osteopontin promoter.[127] Osteopontin has many effects on immune cells including chemotaxis, cellular adhesion, and cell survival.[128] In the Con A model of acute hepatitis, OCA treatment reduced the number of FasL positive NKT cells indicating the FXR may mediate NKT cell activation.[127]

The adaptive immune system is regulated by FXR by several mechanisms; directly altering inflammatory mediator expression, antagonism of the nuclear factor kappa-light-chain-enhancer of activated B cells (NFκB) pathway, and enhancing glucocorticoid signaling. Monocyte chemoattractant protein 1 (MCP-1) is a chemokine that regulates monocyte and macrophage migration and infiltration.[129] An FXRRE is present in the promoter of MCP-1. Activation of FXR by CDCA in macrophage cell lines, ANA-1 and RAW264.7, reduced both mRNA and protein levels of MCP-1.[130] In primary isolated kupffer cells, OCA mitigated the up-regulation of MCP-1 by both lipopolysaccharide (LPS) and TNFα.[102] In the MCDD model of NASH, treatment of mice with FXR agonist WAY-362450 decreased MCP-1 expression in the liver and reduced inflammatory infiltrate.[98]

Another mechanism by which FXR is anti-inflammatory is through the inhibition of the NFκB signaling pathway. Post-translational modification of FXR can occur at residue K277. This lysine can either be acetylated or SUMOylated. When SUMOylated, FXR can tether to NFκB subunit p65 and prevent the recruitment of p65 to the promoter of its inflammatory response genes. FXR activation increased the amount of SUMOylated FXR and consequently reduced NFκB signaling.[131] Treatment of mice with FXR agonists reduced the induction of inflammatory mediators by LPS challenge.[132] Similarly, preventing FXR activity or SUMOylation increases inflammatory mediator expression. When challenged with LPS, FXR deficient mice have higher induction of

NFκB response genes.[132] FXR may also reduce NFκB activation by increasing levels of NFκB inhibitor alpha (IκBα), the chaperone protein which prevents the translocation of p65 to the nucleus. In the thioacetamide model of cirrhosis, mice treated with OCA had increased hepatic protein levels of IκBα.[102] Lastly, FXR has recently been shown to decrease NFκB pathway activation by increasing the production of anti-inflammatory arachidonic acid derived epoxyeicosatrienoic acids (EETs) and reducing production of inflammatory leukotrienes. During NASH development in humans, the cytochrome p450s which produce EETs are reduced and expression levels inversely correlated to NAS score.[133] EETs have been previously shown to reduce NFκB activation.[134] In mice fed free fatty acids, OCA increased the expression of cytochrome p450s that synthesize EETs and reduced hepatic inflammation.[133]

In addition to modulating the activity of the NFκB pathway, FXR regulates glucocorticoid signaling. An FXRRE was identified in the distal portion of the murine and human glucocorticoid receptor promoter.[135, 136] As evidenced by chromatin immunoprecipitation and luciferase assay, FXR was recruited to this FXRRE but did not directly alter gene transcription. Instead, the FXRRE functions as an enhancer element and FXR recruitment to this FXRRE mediates chromatin head-to-tail looping, thereby increasing transcriptional efficiency.[135] Primary monocytes from wild type and FXR deficient mice were treated with LPS and dexamethasone. Monocytes from FXR deficient mice were less responsive to the anti-inflammatory effects of dexamethasone and had elevated inductions of *Il-1β*, *Tnfα*, and *interferon-γ*.[135]

In the liver, another cell type that expresses FXR is HSCs. The effects of FXR signaling in HSCs were described previously in section 1.4.2.

1.5.1.3 Intestinal FXR:

The role of intestinal FXR during NASH and metabolic disease development is currently unclear. Both inhibition and activation of FXR in the intestine has been shown to have beneficial effects in animal models. In this section we will review the data from studies using both intestinal specific FXR antagonists and agonists.

The beneficial effects of intestinal FXR antagonism on NASH and metabolic diseases are mediated through a microbiome-intestine-liver ceramide axis.[137-139] In the intestine, FXR has been shown to upregulate the genes involved in ceramide synthesis.[137, 138] Ceramide synthesized in the intestine entered circulation, increased SREBP1c activity in the liver, and subsequently increased lipogenic gene expression.[137] Mice fed a HFD were treated with the BA-based FXR antagonist, glycine conjugated MCA (Gly-MCA).[138] Gly-MCA reduced hepatic triglyceride accumulation. Gly-MCA also reduced total body weight and fasting insulin levels, improved insulin sensitivity, and led to the browning of adipose tissue. The beneficial effects of Gly-MCA were prevented by co-treatment with ceramide and the FXR agonist GW4064.[138] Additionally, treatment of mice with tempol or antibiotics modified the microbiome and increased levels of taurocholate conjugated beta MCA (TβMCA), a FXR antagonist. By increasing TβMCA and inhibiting intestinal FXR, tempol and antibiotic treatment reduced HFD induced hepatic steatosis.[137] In a similar study, mice fed a HFD were treated with caffeic acid phenethyl ester (CAPE), a BSH inhibitor.[139] CAPE treatment increased ileal levels of TβMCA thereby reducing intestinal FXR activity and ceramide synthesis. CAPE treated mice had reduced body weights, reduced fasting glucose and insulin levels, and improved glucose tolerance. By reducing ceramide levels, CAPE treatment also reduced hepatic endoplasmic reticulum stress and hepatic gluconeogenesis.[139] Intestine specific knockout of FXR reduced HFD induced hepatic triglyceride accumulation and steatosis development.[140]

Reports have also been published demonstrating the benefits of intestinal FXR agonism in animal models. Due to poor systemic bioavailability, fexaramine is an intestinal specific FXR agonist when administered orally.[141] In HFD models, mice treated with fexaramine had reduced body weight and body fat mass, increased browning of adipose tissue, and increased energy expenditure.[141, 142] Fexaramine treatment reduced expression of genes involved in lipogenesis, triglyceride levels, and steatosis in the liver.[141, 142] Glycemic endpoints were also improved by fexaramine; reduced fasting serum insulin and leptin levels, increased serum glucagon-like peptide-1 (GLP1) levels, improved insulin sensitivity, and reduced hepatic gluconeogensis.[142] Fexararmine increased intestinal barrier function and decreased circulating levels of inflammatory mediators.[141]

The effects of intestinal FXR activation described above are mediated through multiple pathways; FXR-Takeda G-protein receptor 5 (TGR5) crosstalk and induction of FGF15/19. *TGR5* has been shown to be an FXR response gene. The promoter of *TGR5* has a functional FXRRE and FXR activation increases TGR5 mRNA transcript and protein levels.[142, 143] Not only does intestinal FXR activation increase TGR5 levels but also increases TGR5 ligands. Fexaramine shifts the BA pool composition to contain markedly higher levels of TLCA and LCA, both strong agonists of TGR5.[144, 145] TGR5 activation in the intestine increases serum GLP1 levels. Therefore, the increases in GLP1 levels in fexaramine treated mice are the consequence of enhance TGR5 signaling. Knockout of either *Fxr* or *Tgr5* prevented fexaramine from inducing serum GLP1 concentration and browning of adipose tissue.[142] The effects of fexaramine can also be resultant of induction of FGF15. In the intestine, *Fgf15* is an FXR target gene. Fexaramine treatment increased intestinal *Fgf15* expression and circulating FGF15 protein levels.[141, 142] FGF15 and FGF19 have many beneficial effects on NASH and metabolic diseases, which will be described in depth in the following section.

1.5.1.4 FGF19:

Many of the effects stimulated by activation of intestinal FXR are mediated through the regulation of FGF19. As previously described, FXR activation in the intestine leads to the up-regulation of FGF19.[6] Unlike most FGFs, FGF19 does not bind heparin sulfate and therefore can circulate systemically.[9] The tissue specific activities of FGF19 are determined by the distribution of FGFR1, FGFR4, and co-receptor βKL throughout the body.[11] FGF19 has been shown to regulate the functions of numerous organs paramount to the development of NASH and metabolic diseases including liver, adipose, muscle, and brain. The effects of FGF19 on each of these organs and subsequent effects on NASH and metabolic diseases will be discussed below. For a summary of the effects of FGF19 signaling in specific cell types, please see Figure 1.3.

In the liver, FGF15 and FGF19 prevent the development of the major characteristics of NASH; steatosis, inflammation, fibrosis, and metabolic syndrome. FGF19 gain-of-function studies, either from transgenic overexpression or treatment with recombinant or modified FGF19 protein, have shown that FGF19 is protective against triglyceride and cholesterol accumulation in the liver and thereby decreases steatosis.[146-148] In agreement, a loss-of-function study found that *Fgf15* knockout mice fed a HFD have worsened steatosis.[148] A second study which fed a HFD diet to *Fgf15* knockout mice did not find worsened steatosis severity but did find altered expression of lipid homeostatic genes.[149] FGF15 and FGF19 reduce steatosis by negatively regulating genes involved in lipid synthesis (*Fas*, *Acly*, *Fatp4*, *Elovl6*, *Scd1*, *Mogat1*, *Dgat2*, *Scd1*) and lipid uptake (*Cd36*).[146-149] FGF19 has also been shown to reduce steatosis development through altering the composition of the BA pool to contain increased TβMCA. The increased TβMCA levels antagonize intestinal FXR activity and decreased intestinal ceramide synthesis. As previously described, reduced intestinal ceramide

production decreases SREBP1c activation in the liver and subsequently mitigates steatosis.[147] In addition to reducing lipid accumulation, FGF19 protects hepatocytes against lipoapoptosis and reduces endoplasmic reticulum stress.[147, 148] By altering the BA pool, FGF19 also reduces enterocyte cholesterol absorption, increases transintestinal cholesterol efflux, and increases fecal sterol content.[150]

FGF15 and FGF19 reduce the development of hepatic inflammation. In a high fat, high fructose, high cholesterol diet mouse model, overexpression of FGF19 or modified FGF19 protein (M70,NGM282) reduced hepatic inflammation severity observed histologically and reduced expression of inflammatory mediators.[147] Though not significant, FGF15 deficient mice fed a HFD had trends for worsened inflammation. One mechanism by which FGF19 may mitigate hepatic inflammation is via altering NFκB activity. FGFR4 activation by FGF19 has been shown to reduce NFκB signaling. Activated FGFR4 interacted with inhibitor of nuclear factor kappa-B kinase subunit beta (IKKβ) and decreased IKKβ mediated phosphorylation of IκBα.[151]

The effect of FGF15 and FGF19 on the development of hepatic fibrosis is currently unclear. In the aforementioned high fat, high fructose, high cholesterol mouse model, FGF19 and M70 overexpression markedly reduced the development of hepatic fibrosis.[147] However, in both HFD induced NASH model and CCl_4 hepatic fibrosis model, FGF15 deficiency was protective against hepatic fibrosis.[72, 149] In a study using the CCl_4 model, *CTGF* was shown to be a FGF19 target gene in human hepatocytes. Knockout of *Fgf15* reduced hepatocyte derived CTGF and ameliorated CCl_4 induced fibrosis. *Fgf15* knockout also increases total BA pool size and therefore may increase FXR activity in HSCs, which as described previously reduces HSC activation, responsiveness to TGFβ, extracellular matrix production, and contractility. In the FGF19 gain-of-function

study, it is possible the reduced fibrosis was resultant of mitigated hepatic steatosis and inflammation, thus reducing the intensity of HSC activating signals.

FGF19 has beneficial effects on the metabolic syndrome: mitigating dyslipidemia, improving glucose homeostasis, reducing total body weights, and reducing body fat mass. Overexpression of FGF19 reduces serum triglyceride and total cholesterol levels.[146] In mice fed a diet high in fat, fructose, and cholesterol, FGF19 overexpression reduced triglyceride, total cholesterol, and LDL levels.[147] Conversely, FGF15 deficiency in mice increases serum triglyceride levels induced by HFD.[149] Fasting serum glucose and insulin levels are decreased by FGF15 and FGF19. Mice overexpressing FGF19 had reduced fasting serum insulin, glucagon, and glucose levels.[146, 147] These mice also had improved responses during insulin and glucose tolerance tests.[146, 147] Homeostatic model assessment of β cell function and insulin resistance (HOMA-IR), an indicator of insulin resistance, was reduced in transgenic mice.[147] The reverse was observed in FGF15 deficient mice which had increased fasting glucose levels and worsened glucose tolerance.[149, 152] FGF19 also affects glucose homeostasis in the body by regulating hepatic gluconeogenesis and glycogenesis. In the liver, FGF19 activation of FGFR4-βKL causes the dephosphorylation and inactivation of the cAMP response element binding protein (CREB) and consequently leads to the down-regulation of *Pgc1α* expression. The lower levels of PGC1α decreases the expression of *Pepck* and *G6Pase*, genes involved in gluconeogenesis. Knockout of *Fgf15* increased *Pgc1α*, *Pepck*, and *G6Pase* expression.[153] Liver glycogenesis is also regulated by FGF15 and FGF19. Liver homogenates from FGF19 treated mice had increased glycogen synthase activity and increased levels of glycogen, whereas FGF15 deficient mice had reduced glycogenesis post glucose challenge.[152] The mechanism by which FGF19 increases

hepatic glycogenesis is shown to be dependent upon ERK signaling and independent of insulin signaling.[152]

FGF19 also affects NASH and metabolic disease development by its effects peripherally on adipose and muscle tissue. Adipose tissue does not express FGFR4 and regulation of adipose tissue by FGF19 is mediated by FGFR1-βKL.[11, 146] Treatment of mice with FGF19 and transgenic overexpression of FGF19 reduces body fat mass and total body weight.[146, 147, 154] When fed a HFD, FGF19 transgenic mice resisted body weight gain and expansion of retroperitoneal and epididymal white adipose tissue.[146] Correspondingly, knockout of *Fgf15* increased fat mass and total body weight during high fat feeding.[148] FGF19 transgenic mice have shown to have increased brown adipose tissue, thermogenesis, and energy expenditure.[146, 155]

In addition to its effects on adipose tissue, FGF19 also regulates muscle tissue. Treatment of mice with FGF19 increased soleus, tibialis anterior, and gastrocnemius muscle weights in a βKL dependent manner; the number of muscle fibers were not altered by FGF19 but instead fiber area was increased.[154] Concordantly, human myotubes treated *in vitro* with FGF19 have increased area. FGF19 also protects against dexamethasone, obesity, and age induced muscle atrophy. Reductions in atrophy by FGF19 further manifested as improvements in grip strength, an indicator of muscle strength.[154]

FGF19 not only regulates body weight and glucose homeostasis peripherally but also acts centrally in the brain. A study using radiolabeled iodinated FGF19 examined its pharmacokinetic properties after intravenous injection. After 10 minutes, radiolabeled intact ^{125}I-FGF19 was present in the brain though at low levels. Brain perfusion indicates that FGF19 does cross the blood brain barrier (BBB), but to a limited extent.[156] It is important to note that FGF15 and FGF19 are expressed in the developing fetal

brain, however, is not expressed in the adult brain.[7, 157, 158] It is therefore likely that FGF15 and FGF19 exert their central effects not by crossing the BBB but instead by interacting with neurons that have projections that traverse the BBB. One such neuron type being the agouti-related peptide (AGRP)/ neuropeptide Y (NPY) neurons.[159] In the arcuate nucleus of the hypothalamus, AGRP/NPY neurons express FGFR1, FGFR2, and FGFR3 but not FGFR4.[160] As shown by immunofluoresence, intraperitoneal injection of FGF19 in mice increased phosphorylation of the FGFR secondary messenger ERK in NPY neurons in the hypothalamic arcuate nucleus.[161] FGF19 signaling decreases the activation of AGRP/NPY neurons.[161] Expression of c-Fos is a marker of neuron activation.[162] HFD fed mice and ob/ob mice have increased NPY/c-Fos co-positive cells in the hypothalamus. FGF19 given by intracerebral ventricular injection (*i.c.v.*) decreased the number of NPY/c-Fos positive cells in HFD mice.[161] The effects of *i.c.v.* FGF19 on metabolic disease development has been studied in both ob/ob and HFD mouse models.[155, 161, 163] In these studies, *i.c.v.* FGF19 reduced food intake and body weight gain, improved glucose and insulin tolerance, and decreased fasting insulin levels. Inhibition of FGFR in the brain via *i.c.v.* injection of FGFR inhibitor PD173074 had the opposite effects: increased food intake, total body weight, and worsened insulin tolerance.[163] Taurocholic acid feeding was shown to increase FGF15 levels and increased glucose tolerance. Tissue-specific knockout of *Fgfr1* in AGPR neurons prevented the improvement of glucose tolerance by TCA. These findings indicate the beneficial central effects of FGF15 and FGF19 on glucose homeostasis are likely mediated by FGF19 activation of FGFR1 centrally.[160]

A bi-specific activating antibody (bFKB1) targeting FGFR1-βKL has been designed and tested in mice and cynomolgus monkeys.[164, 165] As the effects of FGF19 on adipose tissue and brain are mediated by FGFR1-βKL, the effects of bFKB1 should

mirror the extrahepatic effects of FGF19 but not the hepatic FGFR4 mediated effects. As expected, bFKB1 decreased body weight while increasing browning of adipose tissue, thermogenesis, and energy expenditure. Treatment with bFKB1 also reduces blood glucose and insulin levels, improved glucose tolerance, reduced hepatic triglycerides, and reduced serum lipids. Interestingly, the effects of bFKB1 on brown fat thermogenesis were still present in adipocyte-specific FGFR1 deficient mice and in uncoupling protein 1 (UCP1) deficient mice indicating the effects on thermogenesis may be mediated indirectly.[164] In both mice and cynomolgus monkeys, bFKB1 treatment led to inductions of high molecular weight adiponectin. Changes in body weight and energy expenditure are also independent of effects on adiponectin; body weight and energy expenditure changes were also present in adiponectin deficient mice.[165] It is possible that the effects of bFKB1 are mediated centrally. Of importance, treatment with bFKB1 did not induce phosphorylation of ERK in the liver.[165] This is promising as one of the potential liabilities of FXR agonists and FGF19 analog therapeutics is FGF19-FGFR4 driven hepatocellular carcinoma (See later section - Safety concerns of FXR agonist therapy).

1.5.2 Progress of human clinical trials:

1.5.2.1 FXR agonists:

The development of FXR agonists for the treatment of NASH is currently a hotbed of research. Several compounds currently in human clinical trials and one compound, OCA, has already been approved for the treatment of another liver disease. These agonists have both steroidal and nonsteroidal pharmacophores and activate FXR systemically. Current progress of these compounds in clinical trials is described below and summarized in Table 1.

OCA received accelerated approval for the treatment of PBC in 2016. The accelerated approval was based upon reductions in alkaline phosphatase (ALP) in PBC patients and was given with the condition that improvements in survival or disease outcomes be established.[166] To ascertain this information, the FDA required three additional studies; 1) a pharmacokinetic, safety and efficacy study in PBC patients with Child-Pugh classes B and C, 2) a safety and efficacy study of OCA for the monotherapy of PBC in patients intolerant or unresponsive to ursodeoxycholic acid, and 3) a study in PBC patients demonstrating that observed decreases in ALP are associated with changes in clinical progression to cirrhosis, transplant, decompensation, or death.[167] These trials are to be completed by the end of 2022.[167] For the treatment of NASH, OCA has completed both Phase II and Phase III (FLINT) trials with additional Phase III trials underway (REGENERATE and REVERSE).[168-171]

In the Phase II study, the safety and efficacy of OCA was investigated in patients with NAFLD and type 2 diabetes mellitus.[168] 64 patients were randomized to placebo (n = 23), 25 mg of OCA (n = 20), and 50 mg of OCA (n = 21). The primary endpoint was changes in insulin sensitivity determined by glucose infusion rate during 2-step euglycemic clamp procedure. Insulin sensitivity was improved in patients in the low dose group and trended for improved in the high dose group. Many additional secondary endpoints were also measured including changes in body weight, serum biomarkers of liver injury, serum biomarkers of BA homeostasis, and fibrosis biomarkers. As expected, OCA increased serum FGF19 levels, suppressed BA synthesis indicated by decreased serum C4 levels (intermediate of BA synthesis used as biomarker of BA synthesis), and reduced serum BA concentrations. OCA had many beneficial effects in patients including reduced body weights, serum triglyceride levels, serum alanine aminotransferase (ALT) and γ-glutamyl-transferase (GGT) activities, and reduction in

fibrosis biomarkers. However, of potential concern, OCA increased levels of serum LDL while lowering HDL. Serum ALP levels were also increased in OCA treated patients.[168]

The "FXR ligand obeticholic acid for non-cirrhotic, non-alcoholic steatohepatitis trial" (FLINT) was a multi-center, randomized, placebo controlled Phase III study.[169] 142 and 141 patients were randomized to placebo or 25 mg of OCA, respectively, and treated for 72 weeks. The primary outcome of the study was improvement in liver histology defined as a decrease in NAS score by at least 2 points. A greater percentage of patients in the OCA arm compared to the control arm had improved NAS scores and histology scores regarding steatosis, hepatic inflammation, fibrosis, and hepatocyte ballooning. In concordance with the Phase II study, OCA reduced body weights, and serum activities of ALT and GGT.[168] There was also a modest decrease in systolic blood pressure in OCA treated patients. Also corresponding to the Phase II trial, OCA increased serum activities of ALP and levels of LDL while decreasing levels of HDL. Contrary to the Phase II study findings, fasting insulin and HOMA-IR were increased in OCA treated patients. The most common side effect was pruritis (23.4% vs 6.3% in placebo), which led to some patients receiving antipruritic mediation or temporary discontinuation of OCA.

Two additional Phase III trials are currently underway investigating the effects of OCA for the treatment of NASH. The REGENERATE trial is a multi-centered, randomized, double blinded, placebo controlled trial that began in September 2015 and is currently recruiting patients. This study aims to follow 2370 participants treated with either placebo, 10 mg of OCA, or 25 mg of OCA for 18 months. Participants will be non-cirrhotic NASH patients with fibrosis scores of 2 or 3. The primary endpoints under investigation are improvements in liver histology and progression to disease related events including common liver complications, HCC, liver transplantation, and death. As

the FLINT and REGENERATE trials investigated and will investigate OCA in non-cirrhotic NASH, the REVERSE trial will study the effects of OCA in compensated cirrhotic NASH patients. This trial is a multicenter, randomized, double blinded, placebo controlled study that began in August 2017 and has a targeted estimated enrollment of 540 participants. Patients will be randomized to placebo, 10 mg of OCA, or 25 mg of OCA. The primary endpoint is the percentage of patients with histologic improvement of fibrosis by a score of 1 or more using the NASH Clinical Research Network scoring system. The expected completion dates of the REVERSE and REGENERATE trials are in 2020 and 2022 respectively.

Several non-steroidal FXR agonists have reached clinical trials. Compounds in this class are named using the drug suffix –fexor (i.e. tropifexor, nidufexor, turofexorate). The compound WAY-362450 described in the animal studies above was developed under the name FXR450 or turofexorate. A Phase I study using turofexorate was completed but development was discontinued thereafter.[172] The compounds tropifexor (LJN452), nidufexor (LMB763), and EDP305 have completed Phase I trials and are currently in Phase II trials.[173-176] A Phase II study was recently completed on GS-9674 (previously known as Px-104 and Px-102), and is currently under investigation in two additional Phase II studies.[177-179] GS-9674 is a close analogue of GW4064.[180] See Table 1 for a summary of completed and on-going trials with FXR agonists.

1.5.2.2 FGF19 modified protein:

An analog of FGF19, NGM282, is currently in human clinical trials. A Phase I safety and tolerability study of NGM282 in adults has been completed as well as a 12 week-long Phase II safety, tolerability and efficacy study in NASH patients.[181, 182] Findings from the Phase II study mirrored results from preclinical animal studies. NGM282 decreased body weight and body mass index. While no changes in

hemoglobin A1c were observed, NGM282 reduced serum insulin levels and improved insulin sensitivity as evident by decreased HOMA-IR. NGM282 reduced absolute lipid content in the liver and reduced serum liver injury biomarkers ALT and AST. The levels of serum fibrosis biomarkers (pro-C3, PIIINP, and TIMP1) were reduced by NGM282. Fibrosis severity measured by multiparametric MRI was also decreased by NGM282. Histologic assessment of liver biopsies found that 84% of patients had improved NAS scores and 42% of patients had improved fibrosis stage. The primary difference of the findings from the Phase II study from preclinical animal studies pertains to serum lipid levels. NGM282 increased serum LDL levels in patients, however, concurrent treatment with a statin brought LDL levels back to baseline.[183] Common adverse reactions were diarrhea (41% and 36%; 3 mg and 6 mg doses respectively), abdominal pain (30% and 18%; 3 mg and 6 mg doses respectively), and nausea (33% and 14%, 3 mg and 6 mg doses respectively). Due to adverse effects, 32% of patients treated with 6 mg of NGM282 had to interrupt or discontinue therapy.[181]

As described previously, a FGFR1-βKL bi-specific activating antibody would be expected to have effects comparable to FGF21 and the extrahepatic effects of FGF19 mediated through FGFR1-βKL. NGM313 is an FGFR1-βKL bi-specific activating antibody currently in Phase I trials. NGM313 has already completed a Phase I trial in healthy adults and is now being studied in a Phase I trial in obese individuals.[184, 185]

1.5.3 Safety concerns of FXR agonist therapy

1.5.3.1 Experiences with OCA

OCA is currently the only approved FXR agonist on the market and is approved for the treatment of PBC. In September 2017, just under a year and a half after its accelerated approval, an FDA safety communication was released regarding OCA.[186]

This report described 11 cases of severe liver injury and 19 cases of death associated with OCA therapy. The communication described how these adverse outcomes appear to be due to excessive dosing, in particular frequency of dosing. In the OCA package insert, it is stated that in patients with moderate and severe liver injury, Child-Pugh Class B and C, the serum levels of OCA increase 4 and 17 fold respectively.[186] Hence, dose adjustment is required for these patients; the medication is to be dosed weekly instead of daily.[166] In the 19 cases of death associated with OCA, 8 cases reported the cause of death. Of these 8 cases, 7 cases involved the daily dosing of OCA in patients with moderate and severe liver injury instead of the recommended weekly dosing. Of the 11 reports of severe liver injury induced by OCA, 6 were cases of patients with moderate or severe liver injury receiving daily dosing of OCA. The safety communication reminded health care providers to assess liver function in all patients before treating with OCA and to follow recommended dose adjustments. In February 2018, a follow-up safety communication was released stating that a black box warning was added to the OCA prescribing information.[187] This black box warning highlights the importance of screening liver function, properly selecting dose, and performing monitoring after initiation of therapy.[166] This communication urged prescribers to follow dosing on labeling, perform routine biochemical monitoring, re-calculate Child-Pugh class, and adjust dosage accordingly when warranted.[187]

A second safety concern regarding OCA was identified during Phase II and Phase III NASH clinical trials.[168, 169] In both trials, OCA treatment increased serum LDL levels while lowering HDL levels. As most NASH patients have underlying metabolic syndrome and higher rates of cardiovascular disease morbidity and mortality, these changes in serum lipid levels may lead to detrimental consequences. The on-going Phase III REGENERATE trial will study the effects of 18 month long OCA therapy in a

targeted 2370 patients with NASH.[170] OCA had beneficial effects on liver histology in NASH patients during the FLINT trial and therefore the benefit of OCA may outweigh potential cardiovascular risks. It will be of interest to see how OCA effects the development of NASH and cardiovascular outcomes in the large REGENERATE trial and the risk-benefit of OCA treatment.

1.5.3.2 Carcinogenicity of FGF19 and relevance of animal carcinogenicity studies

In multiple mouse models, it has been demonstrated that activation of FGFR4/βKL by FGF19, but not FGF15 or NGM282, is carcinogenic.[188-191] While FGF15 and FGF19 are orthologs they only share 50% amino acid sequence homology.[7, 8] Additionally, FGF15 has an unpaired cysteine not present in the sequence of FGF19. It has been proposed that the unpaired cysteine in FGF15 forms an intermolecular disulfide bond leading to the formation of FGF15 homodimers. In non-reducing gels, it was shown that anti-FGF15 antibodies detect only FGF15 dimers, whereas in reducing gels anti-FGF15 antibodies detect only FGF15 monomers. In both non-reducing and reducing gels, FGF19 is detected as a monomer. This study proposed that FGF15 circulates as a homodimer and therefore may lead to different signaling outcomes than those induced by FGF19. The authors further speculated that the altered configuration of FGF15 is responsible for its lack of carcinogenicity.[188] The stark differences in carcinogenicity of FGF15 and FGF19 raise the concern that there is a lack of animal model able to adequately assess the carcinogenicity of FXR agonists. If a FXR agonist is found to be non-carcinogenic in rodent models, one must consider if this is indeed due lack of carcinogenic risk or due to the fact that rodents express non-carcinogenic FGF15 and not carcinogenic FGF19.

1.6 AIMS OF DISSERTATION

Our central hypothesis was that FGF15 and FGF19 promote liver fibrosis by both direct and indirect pathways: activation of FGFRs in HSCs and reduction of FXR activation in HSCs by decreasing BA levels (Figure 1.4). The aims in this dissertation tested this hypothesis using both *in vitro* and *in vivo* approaches. Data from these studies may have important implications and therapeutic applications for the treatment of hepatic fibrosis as compounds targeting FXR and FGF19 pathways are currently in late phase clinical trials for many forms of liver diseases.

Aim 1 - Determine the effects of FGF15 deficiency on the development of fibrosis in a HFD-induced NASH model (Chapter 2). WT and *Fgf15* knockout (*Fgf15*$^{-/-}$) mice were fed a HFD for 6 months to induce a NASH phenotype. A glucose tolerance test was conducted after 5 months of feeding to ensure the development of metabolic syndrome. Effects of FGF15 deficiency on each of the key characteristics of NASH---steatosis, inflammation, and fibrosis---as well as signs of metabolic syndrome, were determined.

Aim 2 - Assess the effects of FGF19 and FXR activation on the human HSC line LX-2 (Chapter 3). In order to determine the direct effects FGF19 and FXR have on HSC activation and proliferation, LX-2 cells were cultured with and without recombinant FGF19 and CDCA. LX-2 cells and recombinant FGF19 were selected for this aim as they are of human origin and thus have greater relevance to human health. CDCA was chosen as the FXR agonist for this aim as it is the strongest endogenous agonist of FXR. Effects of FGF19 and FXR signaling on hepatocytes has been studied previously, therefore the human hepatoma cell line HepG2 was treated with the recombinant FGF19 as a positive control ensuring the functionality of the recombinant protein when used *in vitro*. The effects of FGF19 on the phenotype and proliferation of LX-2 cells was determined.

Aim 3 - Differentiate the effects of FGF15 from those of BA levels on HSC activation *in vivo* using the CCl_4 hepatic fibrosis model in conjunction with BA supplementation or sequestration (Chapter 4). *Fgf15*$^{-/-}$, Fgf15 overexpressing transgenic (FABP1-Fgf15; TG), and WT mice were treated with CCl_4 chronically to induce liver fibrosis. To determine if the observed differences in fibrogenesis were due to alterations in FGF15 levels or BA levels, mice were also assigned a specific diet which modulated the size of the BA pool. As *Fgf15*$^{-/-}$ mice have increased BA pools, *Fgf15*$^{-/-}$ mice were fed either a chow diet or a diet containing cholestyramine, a BA sequestrant. As the TG mice have decreased BA pools, TG mice were fed either a chow diet or a diet supplemented with CA. These treatment groups provided multiple combinations of *Fgf15* expression and TBAP sizes, allowing for the identification of the BA dependent and independent effects on hepatic fibrosis.

FIGURES

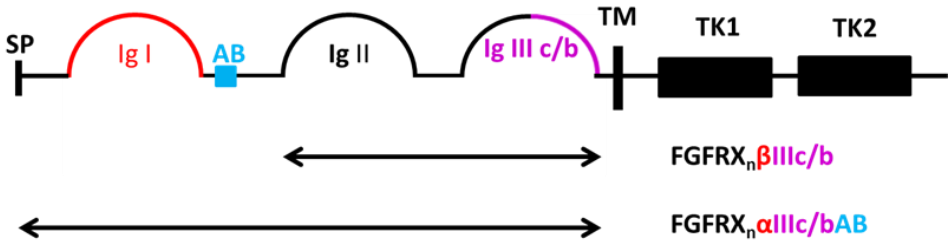

Figure 1.1. *Structure of FGFRs.* Ig I domain is present in α but not β variants (red). Splice variation in the Ig III loop distinguishes b and c type receptors (purple). Acid box is present in AB variants (blue). AB = Acid Box, Ig = Immunoglobulin-like domain, SP = Signal peptide, TM = Transmembrane domain, TK = Tyrosine kinase domain.

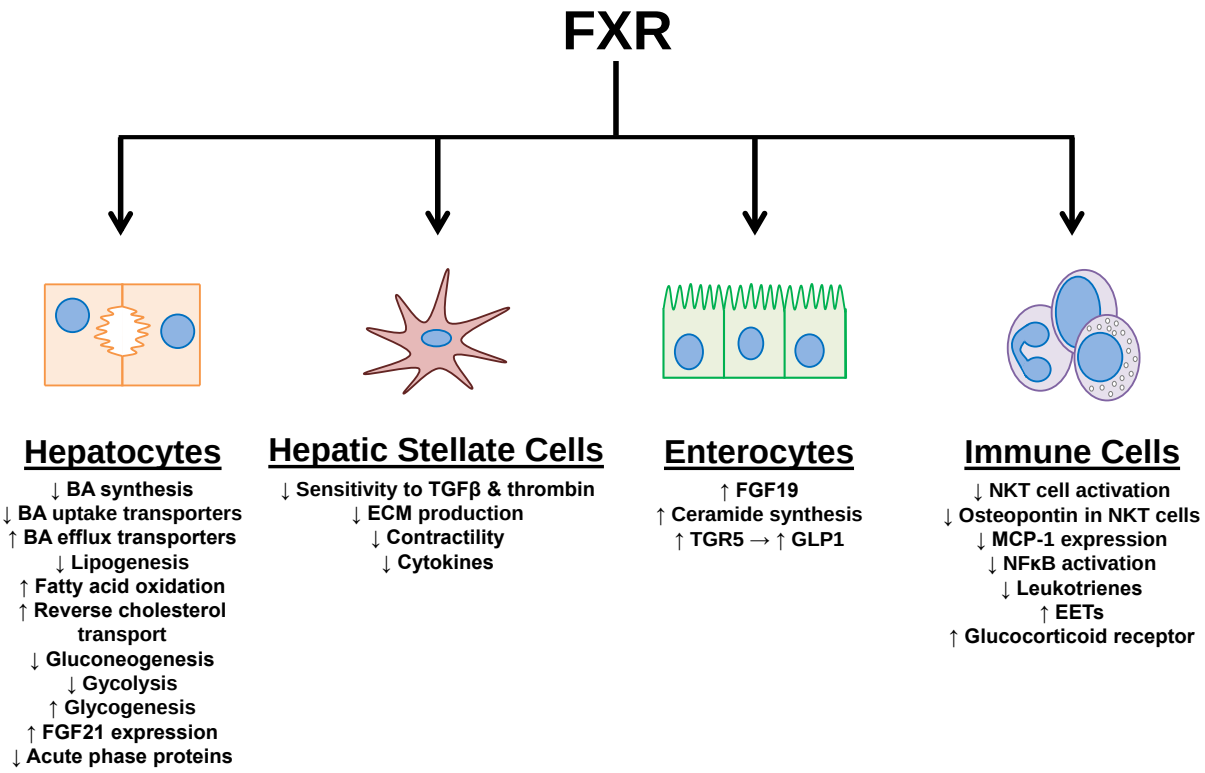

Figure 1.2. *Summary of the effects of FXR activation in specific cell types.*

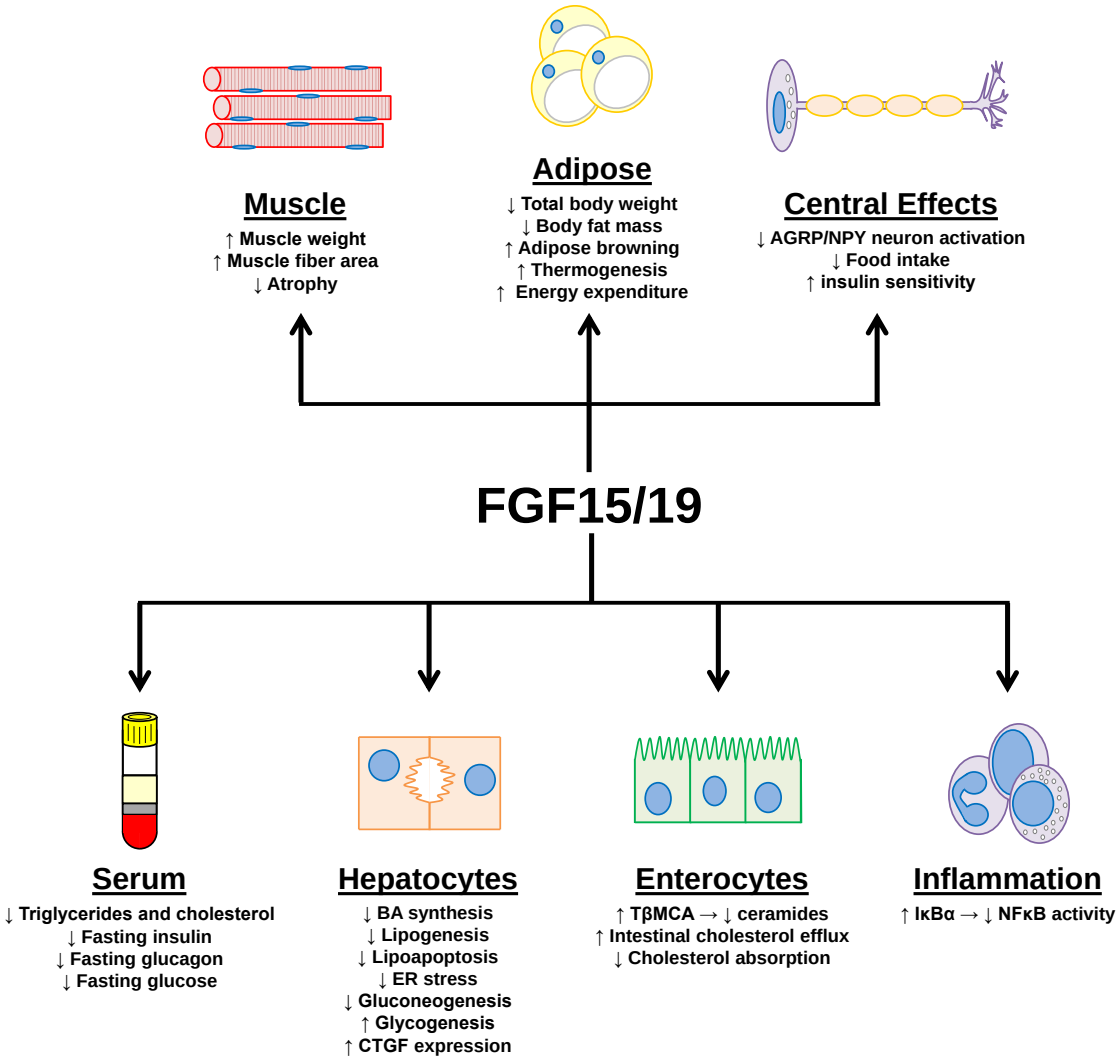

Figure 1.3. *Summary of the effects of FGF15/19 signaling in specific cell types, tissues, and processes.*

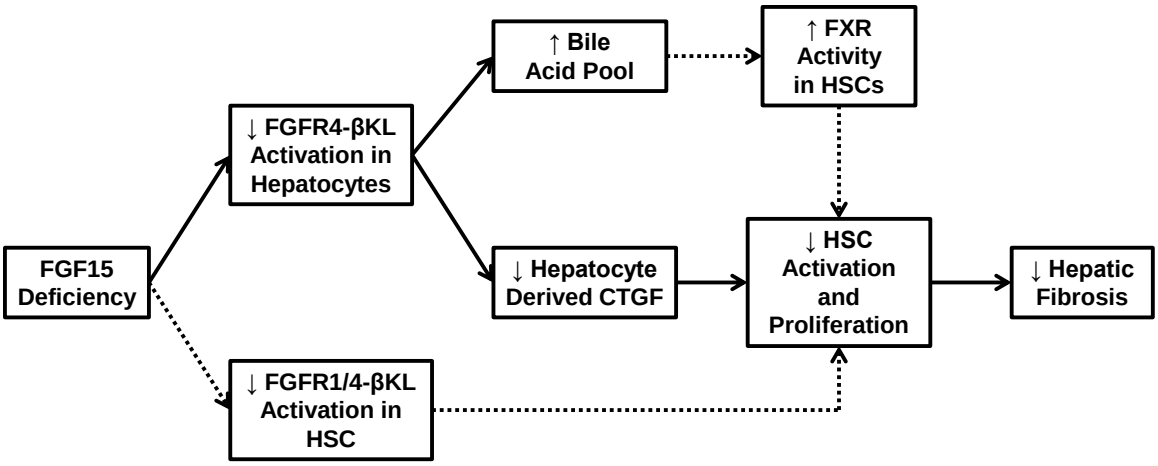

Figure 1.4. *Hypothesized mechanism by which FGF15 deficiency protects against the development of hepatic fibrosis.* Solid lines represent previously published effects whereas dotted lines represent hypothesized effects.

TABLES

FGF subfamily	Study	Findings
FGF1 subfamily	Lin et al.	FGF2 induces collagen 1α1 and αSMA in HSCs in vitro. FGF2 increases HSC proliferation mediated by MEK/ERK signaling.
	Nakamura et al.	FGF2 increases proliferation of Lx-2 cells. Inhibition of FGFR1 does not alter αSMA induction in Lx-2 cells treated with TGFβ.
	Yu et al.	Single and double knockout of FGF1 and FGF2 decrease CCl_4 induced hepatic fibrosis. Single and double FGF1 and FGF2 knockout mice have reduced collagen 1α1 expression but not αSMA. Desmin expression in the liver is remained constant in FGF1 and FGF2 deficient mice indicating FGF1 and FGF2 do not affect HSC proliferation.
	Antione et al.	FGF2 treatment fails to affect the proliferation of Lx-2 cells or primary rat HSCs in vitro.
	Rosenbaum et al.	TGFβ increases the expression of FGF2 by MFLCs. FGF2 mediates TGFβ induced HSC proliferation but does not alter expression of fibronectin.
FGF7 subfamily	Steiling et al.	FGF7 is expressed in fibrotic livers but not healthy controls. FGF7 expression is co-localized with αSMA in stained liver sections.
	Otte et al.	IHC of liver sections from rats treated with phenobarbitone and CCl_4 revealed FGF7 is exclusively expressed by HSCs in fibrotic foci. Severity of hepatic fibrosis correlated positively to FGF7 expression.
	Tsai et al.	FGF7 accelerates DNA incorporation of BrdU and expression of PCNA in hepatocytes after partial hepatectomy.
FGF9 subfamily	Antione et al.	FGF9 is expressed in hepatocytes and HSCs basally but greatly up-regulated in HSCs after CCl_4 exposure. FGF16 and FGF20 expression has not been detected in HSCs. FGF9 induces hepatocyte proliferation but not HSC proliferation.
FGF19 subfamily	Uriarte et al.	FGF15 deficiency reduces hepatic fibrosis in mice treated with DEN and CCl_4. Collagen 1α1, Timp1, αSMA, and CTGF expression induced by CCl_4 is mitigated in FGF15 knockout mice. CCl_4 treatment of transgenic mice overexpressing FGF15 have had 3 fold higher expression of TGFβ and CTGF compared to WT mice. FGF15 signaling increases CTGF release from hepatocytes leading to the paracrine activation of HSCs.
	Xu et al.	DMN treated mice co-treated with FGF21 have had reduced fibrosis and mitigated expression of collagen 1α1, αSMA, and TGFβ. FGF21 reduced TGFβ signaling is observed as a decrease in pSmad2/3:Smad2/3 ratio. FGF21 attenuates DMN induced hepatic inflammation and reduces TNFα, IL-6, and IL-1β expression. In vitro treatment of T6 cells with FGF21 decreases alcohol and PDGF inductions of collagen 1α1, αSMA, and TGFβ. FGF21 reduces Bcl-2/Bax ratio in vitro in cultured T6 cells.
	Fisher et al.	FGF21 deficient mice fed a MCDD have increased fibrosis with increased expression of collagen 1α1, αSMA, and TGFβ. MCDD fed FGF21 knockout mice have increased hepatic inflammation with increased expression of MCP-1, MIP1α, IL-1β, and CD36. The increased expression of pro-fibrotic and pro-inflammatory genes in FGF21 deficient mice is reversible by continous subcutaneous infusion of FGF21.

Table 1.1. *Regulation of HSCs and development of hepatic fibrosis by various FGF isoforms.*

Mechanism	Compound	Phase	Study Title	Start Date	End Date	NCT ID#
FXR agonist	OCA	3	Randomized Global Phase 3 Study to Evaluate the Impact on NASH With Fibrosis of Obeticholic Acid Treatment (REGENERATE)	9/2015	10/2022	NCT02548351
		3	Study Evaluating the Efficacy and Safety of Obeticholic Acid in Subjects With Compensated Cirrhosis Due to Nonalcoholic Steatohepatitis (REVERSE)	8/2017	7/2021	NCT03439254
		2	The Farnesoid X Receptor (FXR) Ligand Obeticholic Acid in NASH Treatment Trial (FLINT)	3/2011	9/2014	NCT01265498
		1	Obeticholic Acid in Morbidly Obese Patients and Healthy Volunteers (OCAPUSH)	8/2015	10/2019	NCT02532335
		1	Hepatic Impairment Trial of Obeticholic Acid	6/2013	10/2013	NCT01904539
		1	Effect of Food on Pharmacokinetics of Obeticholic Acid	8/2013	11/2013	NCT01914562
		1	Single Dose and Multiple Dose Trial to Assess Pharmacokinetics of Obeticholic Acid	10/2013	11/2013	NCT01933503
	Tropifexor (LJN452)	2	Safety, Tolerability, and Efficacy of a Combination Treatment of Tropifexor (LJN452) and Cenicriviroc (CVC) in Adult Patients With Nonalcoholic Steatohepatitis (NASH) and Liver Fibrosis (TANDEM)	8/2018	6/2020	NCT03517540
		2	Study of Safety and Efficacy of Tropifexor (LJN452) in Patients With Non-alcoholic Steatohepatitis (NASH) (FLIGHT-FXR)	8/2016	9/2019	NCT02855164
	EDP305	2	A Study to Assess the Safety, Tolerability, Pharmacokinetics and Efficacy of EDP-305 in Subjects With Non-Alcoholic Steatohepatitis	4/2018	4/2019	NCT03421431
		1	Drug-drug Interaction Study Between EDP-305, Intraconazole and Rifampin in Healthy Volunteers	7/2017	9/2017	NCT03213145
		1	A Study of EDP-305 in Subjects With Mild and Moderate Hepatic Impairment Compared With Normal Healthy Volunteers	6/2017	9/2017	NCT03207425
		1	Drug-drug Interaction Study Between EDP-305, Midazolam, Caffeine and Rosuvastatin in Healthy Volunteers	5/2017	6/2017	NCT03187496
		1	A Study of EDP 305 in Healthy Subjects and Subjects With Presumptive NAFLD	9/2016	6/2017	NCT02918929
	GS-9674	2	Safety and Efficacy of Selonsertib, GS-0976, GS-9674, and Combinations in Participants With Bridging Fibrosis or Compensated Cirrhosis Due to Nonalcoholic Steatohepatitis (NASH) (ATLAS)	3/2018	4/2020	NCT03449446
		2	Safety, Tolerability, and Efficacy of Selonsertib, GS-0976, and GS-9674 in Adults With Nonalcoholic Steatohepatitis (NASH)	7/2016	7/2019	NCT02781584
		2	Evaluating the Safety, Tolerability, and Efficacy of GS-9674 in Participants With Nonalcoholic Steatohepatitis (NASH)	10/2016	1/2018	NCT02854605
		1	Pharmacokinetics and Pharmacodynamics of GS-9674 in Adults With Normal and Impaired Hepatic Function	7/2016	12/2018	NCT02808312
		1	Study in Healthy Volunteers to Evaluate the Safety, Tolerability, Pharmacokinetics and Pharmacodynamics of GS-9674, and the Effect of Food on GS-9674 Pharmacokinetics and Pharmacodynamics	1/2016	7/2016	NCT02654002
	Nidufexor (LMB763)	2	Safety, Tolerability, Pharmacokinetics and Efficacy of LMB763 in Patients With NASH	10/2016	3/2019	NCT02913105
	Turofexorate (FXR450)	1	Study Evaluating the Safety of FXR-450 in Healthy Subjects	10/2007	2/2008	NCT00499629
	EYP001	1	Study Evaluating Safety, Tolerability and Pharmacokinetics of EYP001a in Healthy Male Subjects	8/2016	3/2017	NCT03110276
FGF19 analog	NGM282	2	Study of NGM282 in Patients With Nonalcoholic Steatohepatitis (NASH)	5/2015	9/2019	NCT02443116
		1/2	Study of NGM282 in Subjects With Functional Constipation and Healthy Individuals	12/2015	1/2017	NCT02649062
		1	SAD and MAD Study of NGM282 in Healthy Adult Participants	1/2013	7/2013	NCT01776528
FGFR1-βKL activating antibody	NGM313	1	Study of NGM313 in Obese Participants	9/2017	12/2018	NCT03298464
		1	Study of NGM313 in Healthy Adult Participants	2/2016	4/2017	NCT02708576

Table 1.2. *List of completed and on-going clinical trials investigating the use of FXR agonists and FGF19 analogs for the treatment of NASH.*

CHAPTER 2:

EFFECT OF FIBROBLAST GROWTH FACTOR 15 DEFICIENCY ON THE DEVELOPMENT OF HIGH FAT DIET-INDUCED NON-ALCOHOLIC STEATOHEPATITIS

2.1 ABSTRACT

Non-alcoholic steatohepatitis (NASH) is a form of non-alcoholic fatty liver disease (NAFLD) characterized by steatosis, inflammation, and fibrosis often associated with metabolic syndrome. Fibroblast growth factor 15 (FGF15), an endocrine factor mainly produced in the distal part of small intestine, has emerged to be a critical factor in regulating BA homeostasis, energy metabolism, and liver regeneration. We hypothesized that FGF15 increases the severity of each of the listed features of NASH. To test this hypothesis, four-week old male $Fgf15^{-/-}$ and their corresponding wild-type (WT) mice were fed either a high fat diet (HFD) or a control chow diet for six months. The results confirmed that HFD feeding for six months in WT mice recapitulated human NASH phenotype, including macrovesicular steatosis, inflammation, and fibrosis. Whereas FGF15 deficiency had no effect on the severity of liver steatosis or inflammation, it was associated with decreased liver fibrosis. Furthermore, FGF15 deficiency resulted in abnormal BA homeostasis, increased insulin resistance, increased HFD-induced serum triglycerides, decreased induction of hepatic cholesterol content by HFD, and altered gene expression of lipid metabolic enzymes. These data suggest that FGF15 improves lipid homeostasis and reduces BA synthesis, but may promote fibrosis during the development of NASH.

2.2 INTRODUCTION

NASH is a more severe stage within the spectrum of NAFLD characterized by steatosis, inflammation, and fibrosis and is often associated with metabolic syndrome. NASH can progress in severity leading to the development of end-stage liver diseases such as cirrhosis and HCC. The prevalence of NASH is currently on the rise and in 2011, it was estimated that NASH afflicts 3-5% of people in the United States. [192] Unfortunately, there are currently no approved therapeutics for the treatment of NASH. To address this problem, intense research efforts are ongoing with a few compounds currently in clinical trials. Several of these compounds modulate the functions of a nuclear receptor, FXR, and its response gene, *FGF19*.

FGF15 is a member of the family of FGFs and its human orthologue is FGF19. Though FGF15 and FGF19 are orthologues they share only 50% amino acid sequence homology.[7, 8] Unlike most other FGFs, FGF15 does not bind extracellular heparin sulfate and can travel through systemic circulation to affect functions in distal organs. For this reason, FGF15 is known as an endocrine FGF.[20] Upon activation of FXR in the ileum, FGF15 is induced in enterocytes and secreted into the portal circulation. In the liver, FGF15 binds to its predominant receptor, FGFR4, a tyrosine kinase receptor, which then activates the mitogen-activated protein kinases (MAPK) signaling pathway. This results in down-regulation of the expression of *Cyp7a1* which encodes a rate-limiting enzyme for BA synthesis.[6, 10, 13, 193] Therefore, FGF15 acts as a negative feedback factor maintaining BA homeostasis. Activation of FGFR4 by FGF15 is dependent upon the presence of βKL, a binding partner of FGFR4, which serves as an obligate co-receptor for FGF15.[20, 194] In addition to MAPK signaling, FGFR4 activation induces other signaling pathways including phosphoinositide 3-kinase-Protein Kinase B, Rat sarcoma viral oncogene homolog (RAS), signal transducer and activator of transcription (STAT),

and phospholipase C-γ pathways. [20] FGFR4 has also been shown to antagonize the pathways mediated by NF-κB[151] and CREB-PGC1α.[153] FGF15 may also bind the FGFR1c/βKL dimer, but to a lesser extent. [11]

In addition to maintaining BA homeostasis, FGF15/19 signaling plays a role in a number of other metabolic functions. For example, in transgenic gain-of-function studies, FGF19 increases insulin sensitivity, decreases serum cholesterol and triglyceride levels, and aids in weight loss.[146, 155] FGF15/19 also regulates cellular energy homeostasis by decreasing gluconeogenesis,[153] while increasing protein and glycogen synthesis.[152] Additionally, FGF15 strongly enhances cell proliferation, stimulating HCC development [72] and liver regeneration.[195, 196] Recent studies have also shown that FGF15 may enhance the development of CCl_4 induced liver fibrosis.[72] However, the role of FGF15 in NAFLD and NASH development has not been clarified. In the current study, we analyzed the effects of FGF15 deficiency in mice on the development of NASH with a focus on steatosis, inflammation, and fibrosis. A long-term HFD feeding model was selected as it best recapitulates symptoms of metabolic syndrome in humans.

2.3 METHODS

Animals and Treatment:

A whole body *Fgf15* KO mouse strain (*Fgf15*$^{-/-}$) was used with a mixed 75% A129/25% C57BL/6J background.[195] WT mice with the same genetic background were used as controls. Briefly, homozygous KO and wild-type (WT) colonies were littermates obtained from heterozygous breeders (Fgf15$^{+/-}$) on a mixed 75% A129/25% C57BL/6J background. The established homozygous KO and WT colonies were expanded with similar genetic background. Four week old male KO and WT mice were fed a HFD (60% calories from lard, 0.2796% cholesterol, 20% calories from carbohydrate, Research

Diets catalog # D12492, New Brunswick, NJ; n = 5 for WT and n = 4 for KO) or control diet (10% calories from lard, 0.00136% cholesterol, 70% calories from carbohydrates, Research Diets catalog # D12450J; n = 4 for both WT and KO). Mice were group-housed and provided food and water *ad libitum*. Total body weights were measured weekly. Five months after commencing the designated diet, an oral glucose tolerance test was performed. Animals were euthanized at the end of the sixth month of feeding. Blood, liver and ileum samples were collected as previously described.[100] The animal protocols conducted in this study were approved by the Rutgers Institutional Animal Care and Use Committee.

Serum biochemical parameters and hepatic lipid composition:

Serum levels of triglyceride, cholesterol, BAs, ALT activity, and ALP activity were measured using commercially available kits according to the manufacturers' instructions (triglycerides, cholesterol, ALT, and ALP kits - Pointe Scientific, Canton, MI; total BAs kit - Bioquant, San Diego, CA). Tissue lipid extracts were generated by homogenizing 100 mg of tissue in a buffer containing 18 mM Tris (pH 7.5), 300 mM mannitol, 50 mM EGTA, and 0.1 mM phenylmethylsulfonyl fluoride. The homogenate was incubated overnight in 2:1 chloroform-methanol solution with gentle shaking. Water was added to the mixture and the samples were centrifuged to separate the aqueous and lipid phases. The lipid phase was collected and dried via vacuum. The concentrated lipids were dissolved in 60% tert-butanol and 40% Triton X-114/methanol (2:1) mix and analyzed for triglyceride and cholesterol using the previously described kits.

Histology:

Frozen liver samples were sectioned and stained with hematoxylin and eosin (H&E) or Sirius Red and severity scored for histomorphological characteristics of

NAFLD. Fibrosis was represented as the percent of tissue area positive for Sirius Red staining determined using ImageJ software.[197] Liver sections were immunohistochemically stained for desmin (PIPA519063; Thermo Fisher Scientific, Waltham, MA) with percent positive stained cells calculated with Image Pro Plus (Media Cybernetics Inc., Rockville, MD). Images were captured with a VS120 Slide Scanner (Olympus, Center Valley, PA).

Gene expression:

Total RNA was extracted from homogenized frozen tissue samples in TRIzol Reagent (Thermo Fisher Scientific; Waltham, MA). 2 µg of isolated total RNA was reverse transcribed to cDNA. Relative expression of genes of interest was determined via RT q-PCR with Sybr Green chemistry. Primer sequences are listed in Table 2.1. Expression of *β-actin* was used to normalize mRNA levels.

Protein Analysis:

Crude membrane fractions were prepared to determine relative bile salt export pump (BSEP) protein levels in the liver by western blot. Crude membrane fractions were prepared as previously described.[198] Protein concentration of the crude membrane faction was measured by BCA assay (Pierce Biotechnology, Rockford, IL) and 50 µg of protein was resolved in a 10% polyacrylamide gel. Protein was transferred to a polyvinylidene difluoride (PVDF) membrane and blocked in 5% nonfat dry milk for 2 hours. Membranes were incubated with anti-BSEP primary antibodies (K44, 1:3000) overnight followed by a 1-hour incubation in a species-specific secondary antibody conjugated to horseradish peroxidase. Bands were detected using Pierce ECL western blotting substrate (Pierce Biotechnology, Rockford, IL). Membrane were stripped (Restore Western Blot Stripping Buffer; Thermo Scientific, Waltham, MA) and re-probed

with anti-β-actin antibody (1:1000; JLA20, EMD Millipore, Temecula, CA) as a loading control.

Statistical Analysis:

The data are expressed as mean ± standard deviation (SD). Comparison of the multiple treatment groups was performed using two-way ANOVA followed by post-hoc Tukey's HSD. The result was considered significant with *P*-value less than 0.05. Correlations between ALT and lipid levels were analyzed using simple linear regression and F-test.

2.4 RESULTS

Effects of FGF15 deficiency on metabolic syndrome development, liver steatosis, and lipid homeostasis:

FGF15 deficient mice fed the chow diet were found to have increased insulin resistance when compared to WT mice, revealed by the glucose tolerance test (Figure 2.1A). A trend was seen for worsened insulin resistance in KO mice fed the HFD compared to WT mice (Area under the curve from glucose tolerance test; p-value = 0.06). The effects on insulin resistance were not associated with differences in weight gain as at no point were total body weights found to be different between WT and KO mice on matching diets (Figure 2.1B). As early as day 7 after initiation of the study, both WT and KO mice fed the HFD had significantly increased body weights compared to mice on the control diet. Six months of HFD, but not the control chow diet, induced hepatic steatosis in WT mice (Figure 2.2A and 2.2B). FGF15 deficiency did not affect the severity of hepatic steatosis revealed by staining with Oil Red O. Furthermore, the hepatic triglyceride content measured in liver homogenates from *Fgf15*$^{-/-}$ mice was not different from those measured in WT mouse livers fed a matching diet (Figure 2.2C).

There were decreased hepatic total cholesterol levels in KO versus WT mice fed a HFD (Figure 2.2C).

In WT mice, HFD increased serum total cholesterol levels but did not affect serum triglycerides (Figure 2.2D). In contrast to WT mice, KO mice on HFD had increased serum triglycerides. No differences in serum total cholesterol levels were found between WT and KO mice on either diet.

Although differential effects of FGF15 deficiency on steatosis were not observed histologically or in measurements of hepatic triglyceride content, the expression of genes involved in lipid homeostasis was altered (Figure 2.2E). In WT mice HFD resulted in down-regulation of mRNA expression of the *fatty acid synthase* (*Fas*) and *acyl-CoA synthetase short-chain 2* (*Acss2*). This was not observed in KO mice fed the HFD, and in fact, expression of these two genes was up-regulated. Basal mRNA levels of *microsomal triglyceride transfer protein* (*Mtp*) were reduced in the KO mice. HFD led to decreased *Mtp* mRNA levels in WT comparable to those of KO. *Cd36* encodes for uptake transporter for lipoproteins [199] and long-chain fatty acids.[200] HFD increased mRNA levels of *Cd36* in both WT and KO mice. There was greater *Cd36* expression in KO mice on both diets compared to WT mice.

Effects on hepatic inflammation and serum biomarkers:

WT mice on HFD had mild histomorphologic characteristics and scores of hepatic inflammation (Figure 2.3A and 2.3B). In WT mice, HFD led to elevations in ALT and ALP activities, indicating hepatocellular and biliary epithelium injury. (Figure 2.4A and 2.4B). Although the KO mice had higher basal ALP activities, the increase in ALT and ALP following HFD was not seen in KO mice. Knockout of *Fgf15* did not significantly

alter the expression of the inflammatory mediators *Tnfα* and *intercellular adhesion molecule 1* (*Icam1*) (Figure 2.4D).

As shown in Figure 2.4E and 2.4F, in WT mice, HFD led to an increase in *Fgf15* mRNA expression in ileum, and a decrease in hepatic mRNA expression of the genes encoding *Bsep* and *Cyp7a1*. These changes in gene expression were not observed in KO mice fed the HFD at the RNA level. Both chow and HFD fed KO mice had greater *Cyp8b1* expression than WT mice. Total serum BA levels were greater in HFD-fed KO mice compared to WT mice (Figure 2.4C). The relative mRNA levels of *ileal bile acid binding protein* (*Ibabp)* were increased in KO HFD mice compared to WT mice indicating greater activation of ileal FXR (Figure 2.4E).

A linear regression analysis comparing ALT to serum and hepatic triglyceride and total cholesterol levels was performed (Figure 2.5). The results showed strong correlations of ALT to both hepatic total cholesterol ($R^2 = 0.57$, $p < 0.001$) and serum total cholesterol levels ($R^2 = 0.54$, $p = 0.001$). A weaker correlation was found when correlating ALT to hepatic triglyceride content ($R^2 = 0.33$, $p = 0.02$), and no correlation was observed with serum triglycerides ($R^2 = 0.01$, $p = 0.7$).

Effects on hepatic fibrosis:

Long-term HFD caused moderate fibrosis in WT mice, however, in this NASH-induced fibrosis model, KO mice were protected from fibrosis (Figure 2.6A and 2.6B). FGF15 deficiency reduced HFD-induced fibrosis similar to that of WT mice on the control diet. There was also a basal decrease in collagen in *Fgf15*$^{-/-}$ mice fed the chow diet. In agreement with the Sirius Red staining, the gene expression of *Col1α1* and *Timp1* was markedly induced by HFD in WT mice (Figure 2.6C). Moreover, the chow diet fed KO mice had similar *Timp1* but lower *Col1α1* expression compared to the WT mice. The

HFD-induced *Col1α1* was much smaller in KO mice. There was a trend for decreased *αSma* (*p = 0.06*) and *Timp1 (p=0.06)* expression in KO mice fed the HFD compared to WT mice. The hepatic expression of *Tgfβ* was not changed regardless of diet or FGF15 deficiency. HFD decreased expression of *Ctgf* but no difference in expression was observed between WT and KO mice. IHC staining for the HSC marker, desmin, revealed that the HFD increased the percentage of desmin-positive cells in the livers of WT but not KO mice (Figure 2.7).

2.5 DISCUSSION

In this chapter, we analyzed the effects of FGF15 deficiency in mice on NASH development. The role of FGF15 in maintaining BA homeostasis has been previously described.[193] Briefly, activation of FXR in ileal enterocytes leads to the production and secretion of FGF15 into the hepatic portal circulation. FGF15 travels to the liver and activates its predominant receptor, FGFR4, on hepatocytes, which subsequently suppresses BA synthesis through the down-regulation of the gene expression of *Cyp7a1.*[193] In agreement, these FGF15-mediated negative feedback mechanisms on BA production were observed in our studies. HFD in WT animals resulted in up-regulation of *Fgf15* in the ileum. This is correlated with down-regulation of hepatic mRNA expression of *Cyp7a1* and *Bsep*. Knockout of *Fgf15* removed this negative feedback regulation and the expression of *Cyp7a1*, *Cyp8b1*, and *Bsep* remained constant or higher during HFD feeding, manifesting as an increase in total serum BA concentrations. Counterintuitively, the levels of *Cyp7a1* expression in control fed KO mice were not elevated compared to WT. The reason is not clear but we speculate an age-related propensity for increased liver inflammation,[201] or other factors of the KO mice at the end of this long-term feeding may have contributed to the lack of *Cyp7a1* induction as we normally show in younger KO mice.

Previous reports have shown that FGF15/19 regulates glucose homeostasis. Postprandial secretion of FGF15 has been found to repress hepatic gluconeogenesis via inhibition of the CREB-PGC-1α pathway.[153] Transgenic overexpression of FGF19 in the muscles of mice led to increased basal metabolic rates.[146] These transgenic mice were resistant to HFD-induced weight gain and also had enhanced insulin sensitivity. Similar findings were observed in a study with HFD in *ob/ob* mice supplemented with FGF19, which showed that daily administration of FGF19 for one week led to increased metabolic rates, improved insulin sensitivity, and weight loss.[155] Corresponding to the findings of these FGF19 gain-of-function studies, in our loss-of-function study we observed that *Fgf15*$^{-/-}$ mice exhibited exacerbated insulin resistance. Furthermore, supplementation of *ob/ob* mice with recombinant FGF19 led to decreased serum triglyceride and cholesterol levels.[155] Similarly, basal serum cholesterol levels in our *Fgf15* KO mice were elevated compared to WT mice. Whereas no effect was observed on basal serum triglyceride levels in *Fgf15*$^{-/-}$ mice, there were increased triglycerides in WT mice compared to KO when fed a HFD.

The HFD in our study led to the development of hepatic steatosis in WT mice and a compensatory decrease in expression of genes involved in lipid synthesis, *Fas* and *Acss2*. Knockout of *Fgf15* prevented this compensatory decrease as the expression of *Fas* and *Acss2* in chow fed and HFD fed *Fgf15*$^{-/-}$ mice was the same. Additionally, *Fgf15*$^{-/-}$ mice fed the control diet had decreased expression of *Mtp,* which is involved in VLDL secretion from the liver, compared to WT. Based on these findings, it is to be expected that *Fgf15*$^{-/-}$ mice would have exacerbated steatosis as there would be increased lipid synthesis and reduced triglyceride efflux from the liver. However, we found that knockout of *Fgf15* had no effect on the severity of steatosis observed histologically or on hepatic lipid compositions. It is possible that FGF15 protects the liver

from the development of steatosis and that our model of six months of HFD may have overwhelmed this protective effect. In a similar study to ours, transgenic expression of FGF19 in HFD fed *ob/ob* mice led to decreased hepatic triglyceride and cholesterol content.[155] Based on these findings, we speculate that a study with a shorter duration may allow for enhanced understanding of how FGF15 signaling mitigates the development of hepatic steatosis.

Currently, there are two models which attempt to describe the etiology of NASH. The first model, the "two-hit" model, proposes that NASH is the result of two sequential events: the accumulation of hepatic lipids followed by an inflammatory insult.[35] In this model, the accumulation of intrahepatic triglycerides is believed to predispose the liver to injury by a subsequent insult. The second model proposes that NASH is a sequelae of systemic inflammation similar to atherosclerosis.[202] In this model, the accumulation of lipids and immune cell activation occur simultaneously rather than as separate events. Elevations in cholesterol are thought to result in aggravated liver injury in NASH. Results from the regression analysis performed in our study are in agreement with the model of systemic inflammation-induced NASH. Both serum and hepatic total cholesterol levels were identified to have strong, positive, linear correlations to ALT. Only a weak correlation was found when comparing hepatic triglyceride content to ALT and no correlation was found between ALT and serum triglyceride levels. We believe these correlations, though not a novel concept, help provide further supporting evidence for a role of cholesterol in the progression of NASH.

In our HFD induced NASH model, deficiency of FGF15 appeared to be protective against the development of fibrosis; it also decreased basal levels of liver collagen. The induction of two fibrotic genes, *Col1α1* and *Timp1*, was not evident in *Fgf15*$^{-/-}$ mice. FGF15 may also affect the proliferation of HSCs as the percent of the liver

cell population that was positive for desmin increased in WT mice fed the HFD but not in KO mice. The expression of *Tgfβ1* was not altered in *Fgf15*$^{-/-}$ mice. It is possible that the long study duration allows for the expression levels of *Tgfβ* to normalize after development of fibrosis. A future time course study may provide valuable insight into mechanisms underlying the protective effects of FGF15 deficiency on liver fibrosis. Overall, the findings in these studies indicate that FGF15 plays a significant role in the development of fibrosis during HFD-induced NASH.

Mechanisms underlying the protective effect of FGF15 deficiency on the development of liver fibrosis do not appear to be mediated via reduction of hepatic inflammation. No differences were noted in hepatic expression of the inflammatory mediators, *Tnfα* or *Icam1,* or in inflammation assessed by histopathological examination. However, hepatic inflammation involves numerous cell types and mediators. Therefore, our initial assessment of the effects of FGF15 on hepatic inflammation is basic and further more in-depth studies are of interest. A recent study reported that deletion of *Fgf15* in mice mitigated CCl_4 induced liver fibrosis.[72] Expression of *Fgfr4* and *βKL* was relative low in HSCs compared to hepatocytes. Treatment of multiple hepatocyte cell lines resulted in up-regulation of *Ctgf,* suggesting that the mechanism by which FGF15 may enhance the development of fibrosis is indirect through induction of CTGF production in hepatocytes followed by a subsequent activation of HSCs via CTGF.[72] Interestingly in our study, we found no differences in the expression of *Ctgf* between WT and KO mice, indicating another mechanism may be at play.

Although FGFR4 is the primary receptor of FGF15, FGFR1 can also be activated by FGF15.[72] Despite the lower expression of *Fgfr4* in HSCs compared to hepatocytes, HSCs have a higher levels of *Fgfr1* compared to hepatocytes. Additionally, another study found that hypoxia induced transdifferentiation of LX-2 cells, a human HSC cell

line, and increased the expression of *FGFR4* by 2.47 fold.[71] Combined, these observations suggest that FGF15 may have direct effects on HSCs which warrants further studies to test this possibility. It is also possible that FGF15 affects the development of fibrosis through both indirect and direct mechanisms; indirect activation of HSCs via inducing hepatocyte derived CTGF and direct activation of FGFR4 and FGFR1 on HSCs.

In conclusion, the 6 month HFD study model was able to induce the key features of NASH, including steatosis, inflammation, fibrosis, and metabolic syndrome, in our WT mice. Deficiency of FGF15 had both beneficial and detrimental effects on these characteristics of NASH. *Fgf15*$^{-/-}$ mice fed the HFD had increased insulin resistance, higher levels of serum triglycerides, and abnormal BA homeostasis. Additionally, the FGF15 deficient mice did not have altered severity of steatosis or inflammation but were protected against the development of liver fibrosis. Based on our findings and those of a previous study,[196] we speculate that FGF15 promotes liver fibrosis through both direct and indirect mechanisms; activation of FGFR on HSCs and indirectly through induction of hepatocyte derived CTGF.

FIGURES

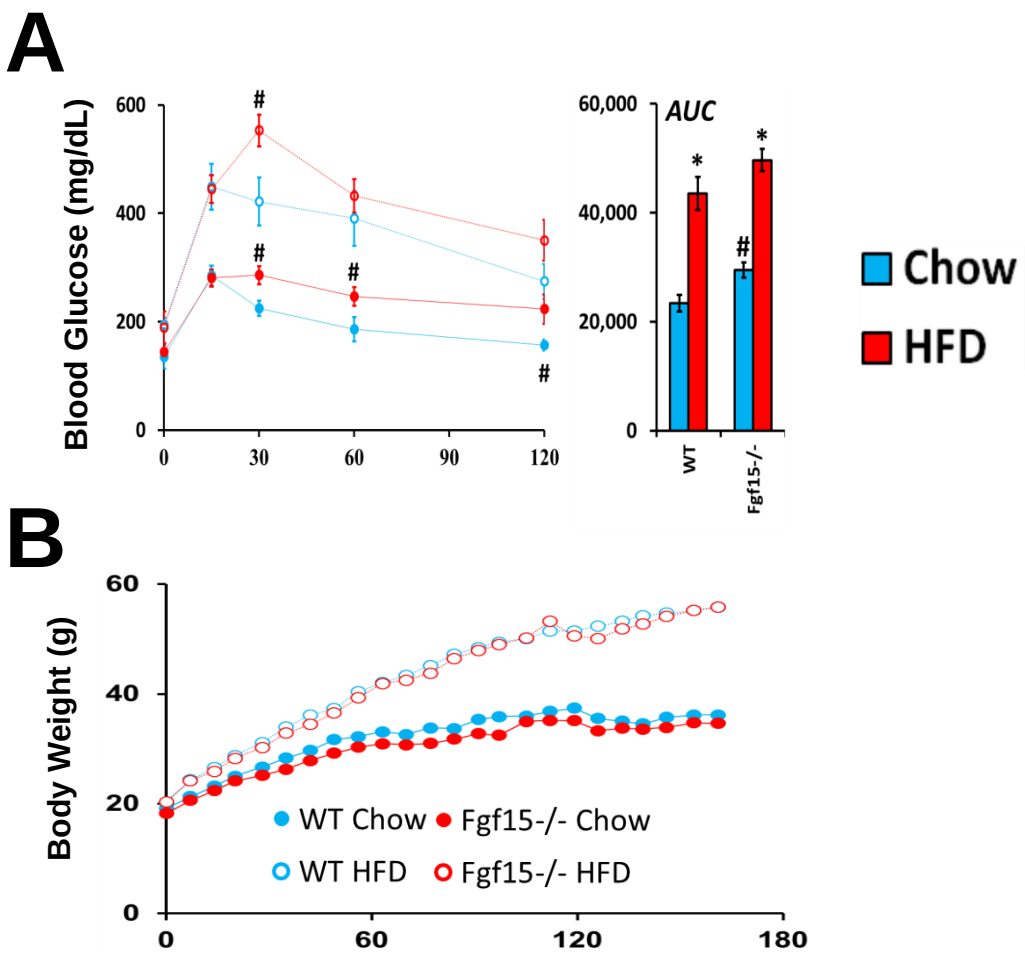

Figure 2.1. *Effects of FGF15 deficiency on glucose tolerance and body weight.* (A) Blood glucose levels were measured after administering an oral glucose challenge. The area under the curve (AUC) from the glucose-time graph was calculated for each group. (B) Body weights were measured weekly after initiating the assigned diet. Body weights of both WT and KO mice fed the HFD were significantly greater when compared to chow diet fed mice as early as day 7. *Statistical significance between diets; #Statistical significance between WT and KO mice on corresponding diets ($p \leq 0.05$).

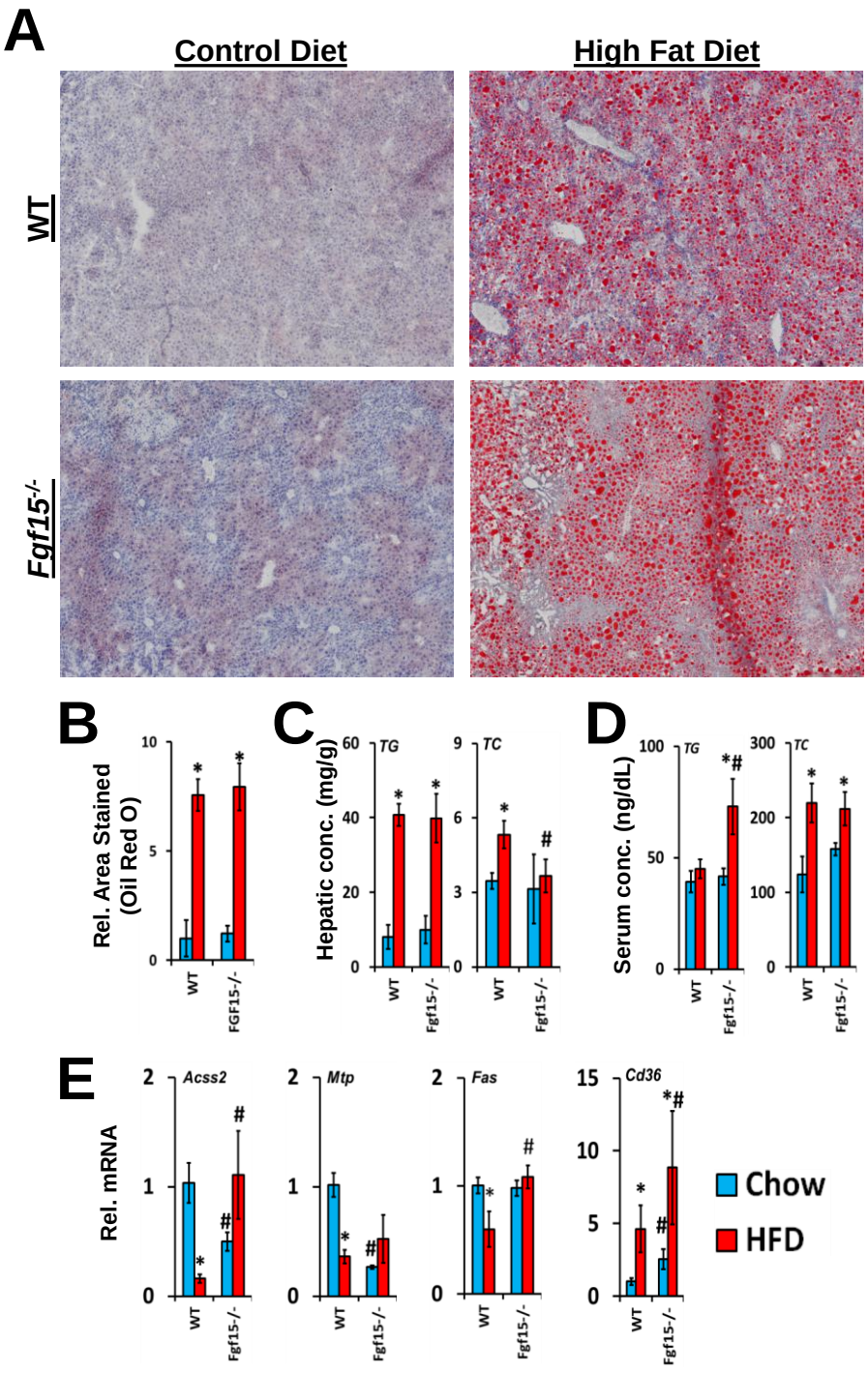

Figure 2.2. *Effect of FGF15 deficiency on steatosis and expression of genes involved in lipid homeostasis.* (A) Isolated frozen liver sections were stained with Oil Red O, imaged at 40x magnification, and (B) relative area stained quantified. (C) Hepatic and (D) serum

concentrations of total cholesterol and triglycerides were measured. (E) The relative mRNA expression of genes involved in lipid homeostasis was altered in Fgf15$^{-/-}$ mice. *Statistical significance between diets; #Statistical significance between WT and KO mice on corresponding diets ($p \leq 0.05$).

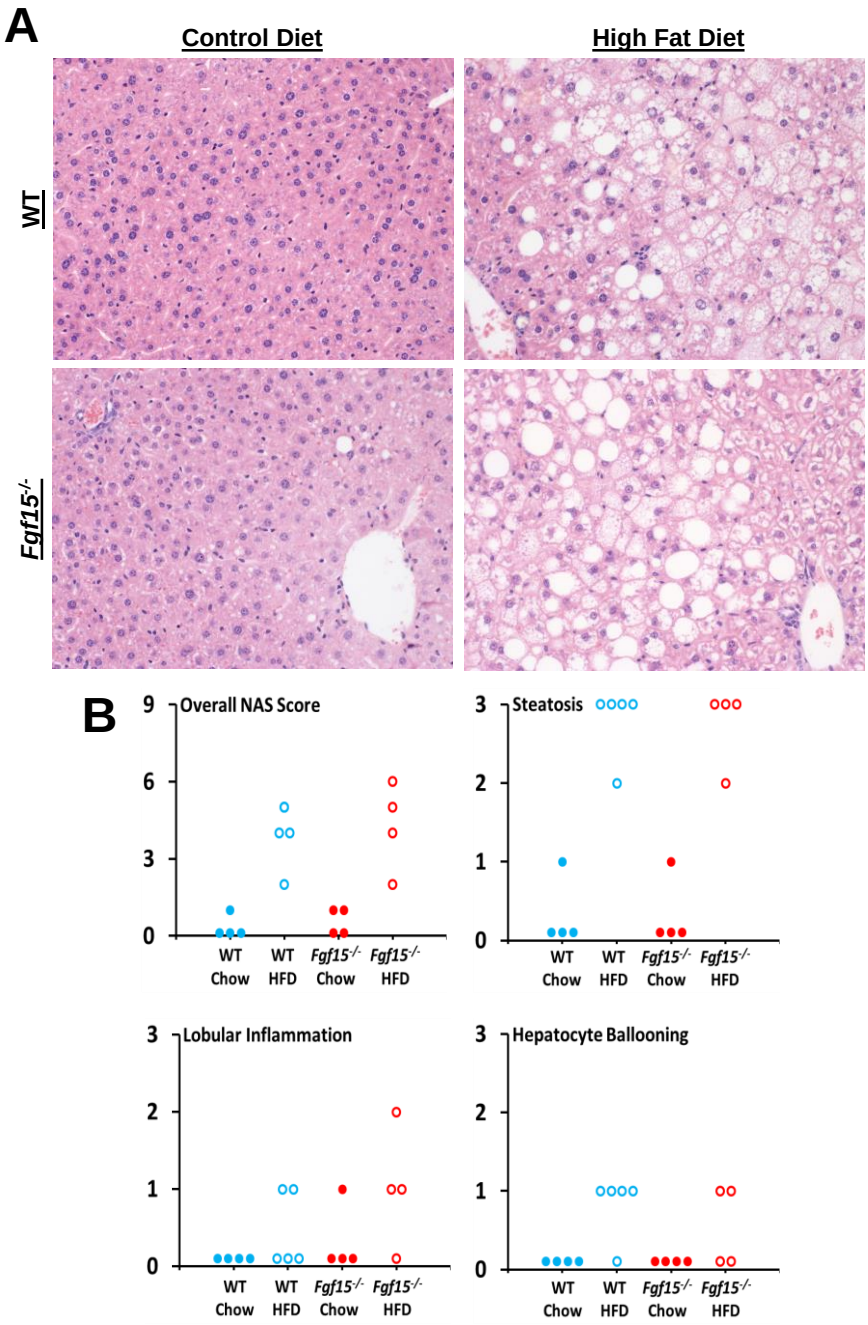

Figure 2.3. *Effect of FGF15 deficiency on liver histology.* (A) Liver sections were stained with HE, imaged at 100x magnification, and (B) scored based on NAS criteria.

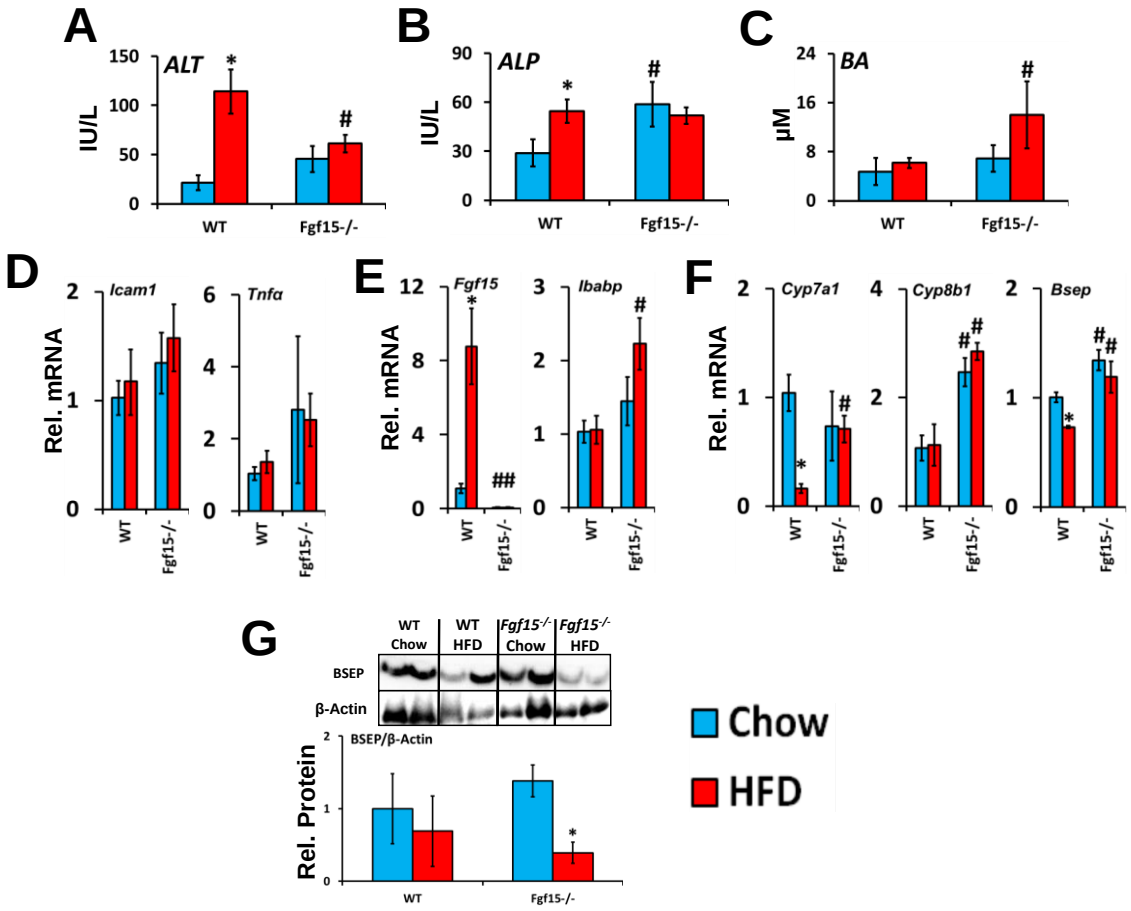

Figure 2.4. *Effects of FGF15 deficiency on serum biomarkers, hepatic inflammatory gene expression, and bile homeostasis.* (A and B) FGF15 deficiency led to a basal increased in ALP but attenuated the HFD induced increase in ALT. (C) KO mice fed the HFD had greater serum BA levels than WT mice. (D) No differences were observed in the relative mRNA expression of *Tnfα* and *Icam1* in KO mice. (E) Relative mRNA expression of ileal *Fgf15* and *Ibabp*, and (F) hepatic *Cyp7a1*, *Cyp8b1*, and *Bsep* was determined. (G) Relative levels of BSEP protein was measured by Western blot. *Statistical significance between diets; #Statistical significance between WT and knockout mice on corresponding diets ($p \leq 0.05$).

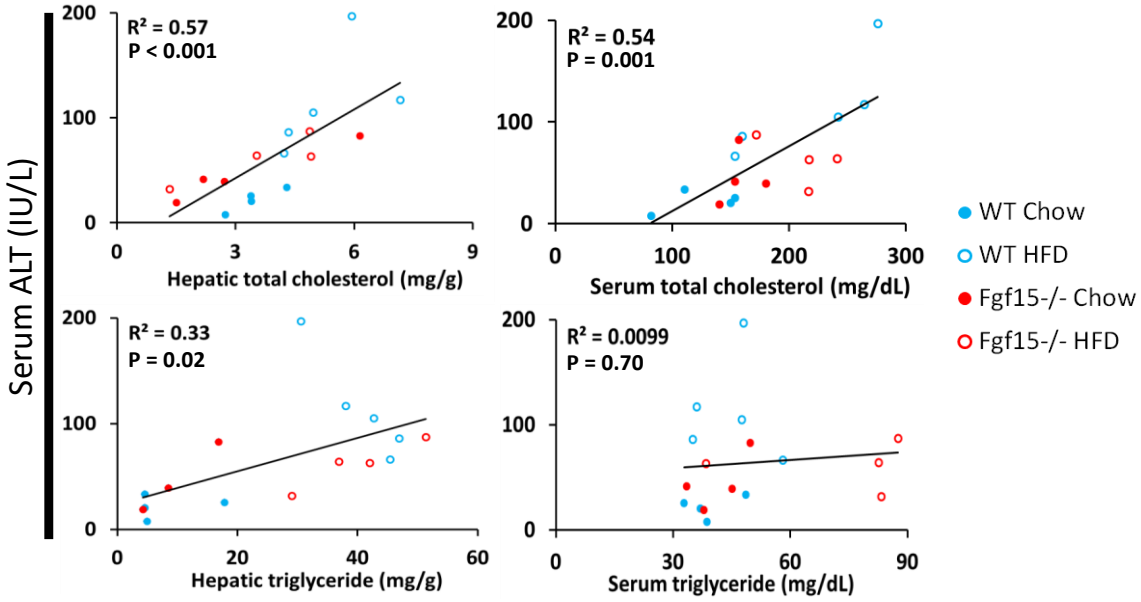

Figure 2.5. *Strong linear correlation between hepatic and serum cholesterol content and serum ALT.* Linear regression analysis comparing serum ALT to serum and hepatic total cholesterol and triglycerides was performed. Displayed p-values were calculated by F-test. The scatterplots include datum points from all study animals and are colored based on the group of the respective mouse**.**

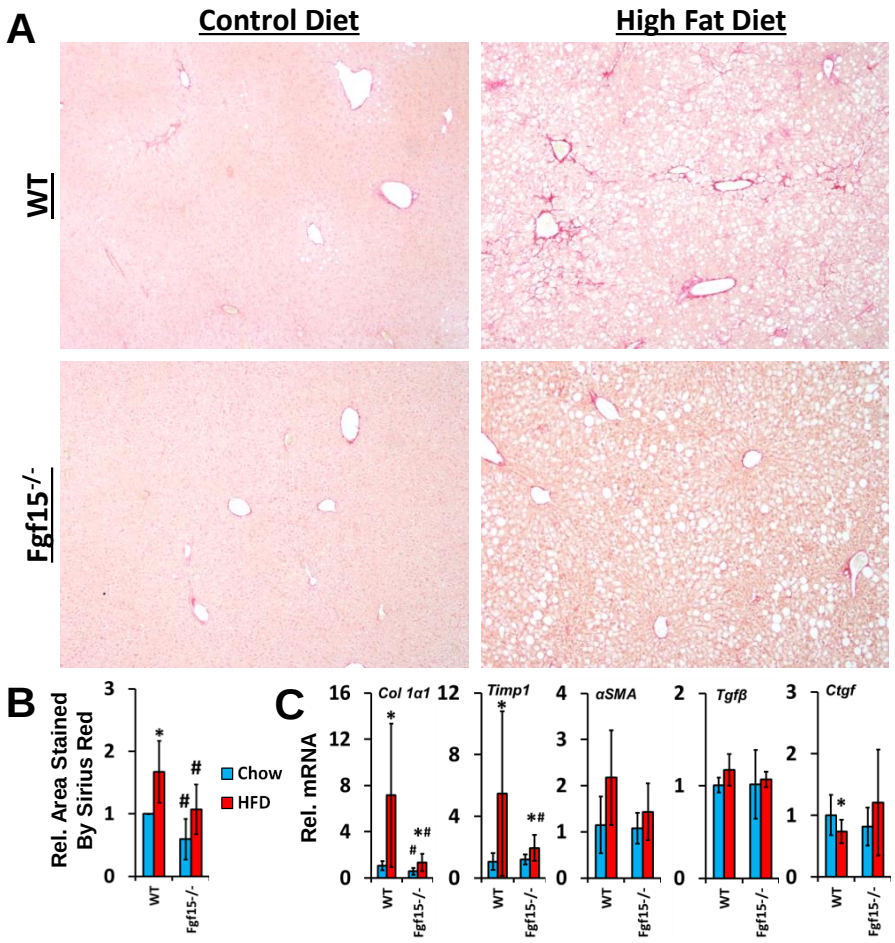

Figure 2.6. *Deficiency of FGF15 attenuates both basal collagen levels and HFD induced liver fibrosis.* (A) Liver sections were stained with Sirius Red, imaged at 40x magnification, and (B) the relative area of the liver stained was quantified. (C) The relative mRNA expression of *Col1α1* and *Timp1* was decreased in HFD fed *Fgf15*$^{-/-}$ mice compared to WT mice while expression of *Tgfβ1* and *Ctgf* was not altered. There was a trend for decreased *αSMA* in HFD-fed KO mice compared to WT mice. *Statistical significance between diets; #Statistical significance between WT and KO mice on corresponding diets ($p \leq 0.05$).

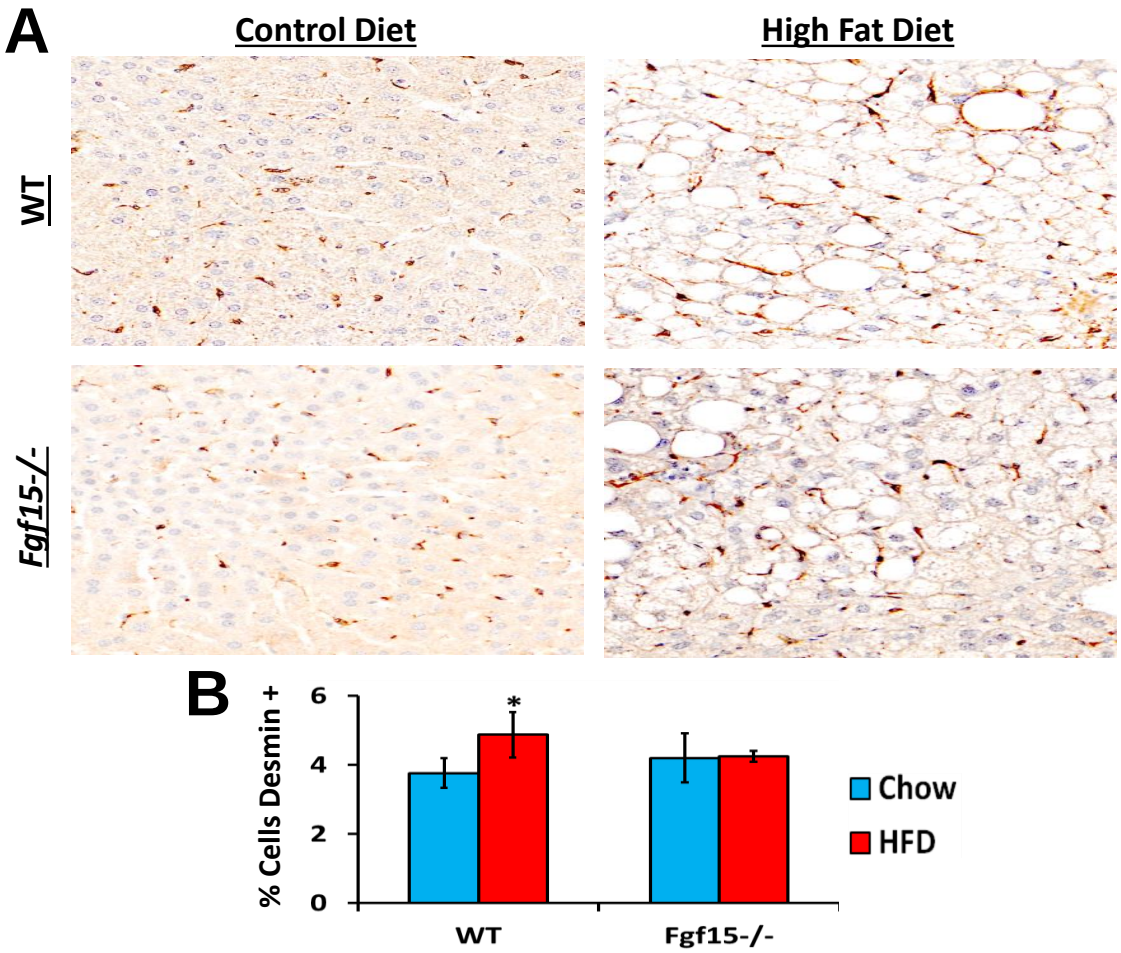

Figure 2.7. *Effects of FGF15 deficiency on the number of HSC in the liver.* (A) Liver sections were stained using IHC targeting the HSC marker desmin. Images shown at 200x magnification. (B) HFD lead to an increased percentage of desmin positive cells in livers of WT mice but not of FGF15 deficient mice. *Statistical significance between diets; #Statistical significance between WT and KO mice on corresponding diets ($p \leq 0.05$).

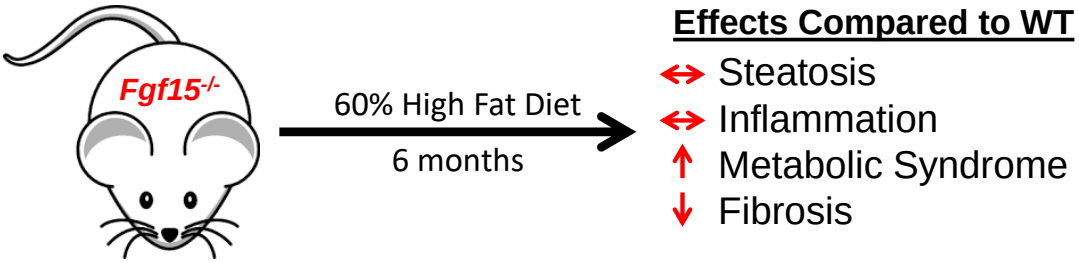

Figure 2.8. *Graphical abstract of Chapter 2.*

TABLES

	Forward Primer	Reverse Primer
β-Actin	5'- GCGTGACATCAAAGAGAAGC- 3'	5'- CTCGTTGCCAATAGTGATGAC- 3'
αSMA	5'- CCTGACGGGCAGGTGATC- 3'	5'- ATGAAAGATGGCTGGAAGAGAGTCT- 3'
Acss2	5'- AAACACGCTCAGGGAAAATCA- 3'	5'- ACCGTAGATGTATCCCCCAGG- 3'
Bsep	5'- TGAATGGACTGTCGGTATCTGTG- 3'	5'- CCACTGCTCCCAACGAATG- 3'
Cd36	5'- GATGACGTGGCAAAGAACAG- 3'	5'- TCCTCGGGGTCCTGAGTTAT- 3'
Col1α1	5'- GAGAGAGCATGACCGATGGATT- 3'	5'- TGTAGGCTACGCTGTTCTTGCA- 3'
Ctgf	5'- GGCCTCTTCTGCGATTTCG- 3'	5'- CCATCTTTGGCAGTGCACACT- 3'
Cyp4a10	5'- TTCCCTGATGGACGCTCTTTA- 3'	5'- GCAAACCTGGAAGGGTCAAAC- 3'
Cyp7a1	5'- AACAACCTGCCAGTACTAGATAGC- 3'	5'- GTGTAGAGTGAAGTCCTCCTTAGC- 3'
Cyp8b1	5'- AGTACACATGGACCCCGACATC- 3'	5'- GGGTGCCATCCGGGTTGAG- 3'
Fas	5'- GCTGCGGAAACTTCAGGAAAT - 3'	5'- AGAGACGTGTCACTCCTGGACTT - 3'
Fgf15	5'- GCCATCAAGGACGTCAGCA- 3'	5'- CTTCCTCCGAGTAGCGAATCAG- 3'
Fxr	5'- TCCGGACATTCAACCATCAC- 3'	5'- TCACTGCACATCCCAGATCTC- 3'
Ibabp	5'-CCCCAACTATCACCAGACTTC - 3'	5'- ACATCCCCGATGGTGGAGAT- 3'
Icam1	5'- CAGTCCGCTGTGCTTTGAGA- 3'	5'- CGGAAACGAATACACGGTGAT- 3'
Mtp	5'- CAAGCTCACGTACTCCACTGAAG- 3'	5'- TCATCATCACCATCAGGATTCCT- 3'
Tgfβ1	5'- TTGCCCTCTACAACCAACACAA- 3'	5'- GGCTTGCGACCCACGTAGTA- 3'
Timp1	5'- CCTTGCAAACTGGAGAGTGACA- 3'	5'- AGGCAAAGTGATCGCTCTGGT- 3'
Tnfα	5'- ACAAGGCTGCCCCGACTAC- 3'	5'- TTTCTCCTGGTATGAGATAGCAAATC- 3'

Table 2.1. List of primers used in Chapter 2.

CHAPTER 3: REGULATION OF HEPATIC STELLATE CELL FUNCTION AND PROLIFERATION BY FXR AND FGF19

3.1 ABSTRACT

Mice deficient in FGF15, ortholog of human FGF19, are resistant to the development of hepatic fibrosis in both high fat diet induced NASH model and CCl_4 fibrosis model. As HSCs are the primary producers of ECM during the development of hepatic fibrosis, we aimed to determine to what extent that FGF19 acts as a profibrogenic or mitogenic factor to HSCs. We treated a human HSC line, LX-2, with recombinant FGF19 protein and measured the effects on FGFR activation by changes in secondary messenger phosphorylation, gene expression of HSC phenotypic markers, and proliferation. We also treated LX-2 cells with a natural primary BA FXR agonist, CDCA, to determine to what degree FXR signaling affects FGFR expression. FGF19 treatment activated FGFR in LX-2 cells evident by the increase in pSTAT3 and pJNK. FGF19 modestly decreased the expression of *COL1α1* after 48 hours of treatment and mitigated the induction of *COL1α1* by TGFβ. Cell proliferation was decreased by FGF19 evident as lowered cell counts and decreased expression of Cyclin D after 48 hours of treatment. NFκB signaling in LX-2 cells was suppressed by FGF19. Correspondingly, gene expression of the cytokines *IL1β*, *IL6*, *IL8* was reduced by FGF19. CDCA treatment up-regulated the expression of *βKL* and *FGFR1.* When co-treated with FGF19, CDCA prevented the compensatory down-regulation of FGFR induced by FGF19 treatment. In summary, this study suggests that FGF19 activates FGFR in human HSCs and reduces inflammatory gene expression via reduced NFκB signaling, but does not function as a profibrotic mediator or mitogen.

3.2 INTRODUCTION

Deficiency of FGF15, ortholog of human FGF19, has been shown to be protective against the development of hepatic fibrosis in both a HFD model of NASH and in a CCl_4 model of liver fibrosis.[72, 149] In the CCl_4 model of fibrosis, it was found that FGF19 induces the production of CTGF in HepG2 cells. Correspondingly, it was reported that treatment with CCl_4 led to induction of CTGF in WT but not *Fgf15*$^{-/-}$ mice. Therefore, it was concluded that the effects of fibrosis protection offered by FGF15 deficiency was due to decreased HSC activation by hepatocyte-derived CTGF. Interestingly, no differences in *Ctgf* expression were observed in the study using the HFD-induced NASH model. Additionally, the protective effect of FGF15 deficiency on the development of fibrosis was present despite a trend for increased inflammation in FGF15 deficient mice. Based on the findings from these two studies, we hypothesized that additional mechanisms underlie the regulation of hepatic fibrogenesis by FGF15 and FGF19.

FGF19 has been shown to increase the proliferation of hepatocytes.[188, 189, 195, 196] Furthermore, FGF2, which activates the same receptors as FGF19 but with different co-factors, has been shown to induce activation and proliferation of HSCs.[203] We therefore hypothesized that FGF15 and FGF19 may act as a fibrogenic factor that directly modulates HSC activation and proliferation. To test this hypothesis, we treated a human HSC cell line, LX-2, with recombinant FGF19 protein. As FGF19 strongly regulates BA homeostasis and FXR activation in HSC has been shown to affect HSC phenotype, we also aimed to identify how FXR signaling integrates with FGF19 signaling in HSCs. Therefore, FXR was also activated in LX-2 cells by treatment with a natural primary BA FXR ligand, CDCA.

3.3 METHODS

Cell culture and treatments:

LX-2 and HepG2 cells were cultured according to vendor's protocols. Recombinant FGF19 protein was generated as previously described[204]. Protein was isolated from HepG2 cells treated with 0.5, 5, and 50 ng/mL FGF19 for 60 minutes and HepG2 cells treated with 50 ng/mL FGF19 for 15, 30, and 60 minutes. Total RNA was isolated from HepG2 cells treated with 0.5, 5, and 50 ng/mL FGF19 for 24 hours. LX-2 cells were treated with 50 ng/mL FGF19 for 15 and 30 minutes and protein was isolated. LX-2 cells were treated with 500 pM recombinant TGFβ and/or 50 ng/mL FGF19 for 24 hours, after which time RNA was isolated. LX-2 cells were also treated with 50 ng/mL FGF19 for 8 hours and RNA was isolated. Lastly, LX-2 cells were treated with 50 ng/mL FGF19 and/or 100 μM CDCA for 48 hours for gene expression analysis. All protein isolation was performed using RIPA buffer containing protease and phosphatase inhibitors (1 mM phenylmethane sulfonyl fluoride, 50 mM sodium fluoride, 10 mM sodium orthovanadate). RNA isolation was performed using TRIzol Reagent (ThermoFisher Scientific, Waltham, MA).

Cell proliferation:

The effect of FGF19 on the proliferation of LX-2 cells was investigated via cell counts, viability, and Alamar Blue assay. LX-2 cells were seed at 5,000 cells per well and treated with 50 ng/mL FGF19 for 48 hours. Cells were then either counted using hemocytometer or analyzed by Alamar Blue assay. For the Alamar Blue assay, cells were washed in Hanks Balanced Salt Solution and then incubated in 1 mg/mL resazurin. Fluorescence was measured using an excitation wavelength of 560 nm and emission wavelength of 600 nm.

Western Blot:

The concentration of protein isolates was determined using Pierce BCA Protein Assay kit according to manufacturer’s protocol (ThermoFisher Scientific; Waltham, MA).

Gels were loaded with 20 µg of protein and separated by electrophoresis. Protein was transferred to a PVDF membrane, blocked with 5% milk, and incubated overnight in primary antibody (See Table 3.1 for primary antibody information). Membranes were then incubated with species-specific secondary antibody and signals detected by enhanced chemiluminescence (Pierce ECL Western Blotting Substrate; ThermoFisher Scientific, Waltham, MA). Relative protein levels were determined using densiometry and normalized to levels of Tubulin or β-Actin.

Gene expression:

2 µg of isolated total RNA was reverse transcribed to cDNA and analyzed by RT-qPCR using Sybr green chemistry. Primer sequences used in this study are listed in Table 3.2. Expression of genes of interest were normalized against the expression of *β-Actin.*

Statistical tests & analysis

Data are presented as mean + SD. Statistical analyses were selected based upon variable type, number of variables, and number of groups. Comparison between two groups was performed using Student's T-test. Analysis of of 3 or more groups within the same variable was performed using One-Way ANOVA with post-poc Duncan's Multiple Range Test. Findings from both Student's T-tests and ANOVA with post-hoc Duncan's Multiple Range Tests were considered significant when $P \leq 0.05$.

3.4 RESULTS

Recombinant FGF19 protein is functional and activates FGFR on LX-2 cells

The recombinant FGF19 protein was created as previously described.[204] We treated HepG2 cells with FGF19 at 0.5, 5, and 50 ng/mL. The levels of phosphorylated ERK (pERK), a known secondary messenger of activated FGFR, were increased in HepG2 cells treated with 50 ng/mL of FGF19 (Figure 3.1B). Subsequently, the expression of hepatocyte FGF19 response genes, *CYP7A1 and CYP8B1*, was down-

regulated in a dose dependent fashion (Figure 3.1C). The time dependent increase in pERK and phosphorylated STAT3 (pSTAT3) following treatment with 50 ng/mL FGF19 further confirmed the functionality of the recombinant FGF19 *in vitro (*Figure 3.2). In previous reports, FGF19 treatment of HepG2 cells was found to up-regulate the expression of *CTGF* after 5 hours of treatment.[72] In our hands, after 24 hours of treatment with FGF19, the expression of *CTGF* and *TGFβ* in HepG2 cells was unchanged (Figure 3.3).

The relative expression of FGF19 receptors in LX-2 cells compared to HepG2 cells was identified. Both LX-2 and HepG2 cells express *FGFR1*, *FGFR4*, and *βKL* but to varying extents. In LX-2 cells the Ct values (+/- SD) for *FGFR1*, *FGFR4*, and *βKL* were 20.97 (+/- 0.53), 26.61 (+/- 0.50), and 26.07 (+/- 0.43) respectively. In HepG2 cells, the Ct values for *FGFR1*, *FGFR4*, and *βKL* were 23.79 (+/- 0.48), 21.35 (+/- 0.47), and 23.98 (+/- 0.33). Based on these values, *FGFR1* expression in LX-2 cells is 49.7 fold higher than that of *FGFR4.* Conversely, *FGFR1 expression in* HepG2 cells is 5.4 fold lower than that of *FGFR4*. The expression of *FGFR1* is 7.1 fold higher in LX-2 cells compared to HepG2, whereas, the expression of *FGFR4* and *βKL* is 38.2 and 4.26 fold lower in LX-2 cells than HepG2 cells, respectively.

To determine if FGF19 can activate FGFRs on HSCs, LX-2 cells were treated with 50 ng/mL FGF19 for 0, 15, and 30 minutes with changes in secondary messenger phosphorylation measured. Levels of pSTAT3 and pJNK, but not pERK, were increased (Figure 3.4). As FGFR4 activation has been shown to antagonize the NFκB pathway by increasing the levels of chaperone protein IκBα, phosphorylated and unphosphorylated IκBα were detected. After 15 and 30 minutes of treatment, levels of IκBα were increased and the ratio of pIκBα/IκBα was reduced (Figure 3.4).

FGF19 reduces cytokine expression in LX-2 cells but does not alter LX-2 collagen expression

LX-2 cells were treated with 500 pM TGFβ and/or 50 ng/mL FGF19 for 24 hours and total RNA was collected for gene expression analysis (Figure 3.5). Treatment with TGFβ was performed as a positive control for LX-2 cell activation. As expected, TGFβ increased the expression of both *COL1α1* and *COL4α1* while reducing the expression of *PPARγ* and its response genes *abhydrolase domain containing 5* (*ABHD5)*, *adipose triglyceride lipase* (*ATGL)*, and *CCAAT enhancer binding protein alpha* (*CEBPα*). *FXR* was down-regulated by TGFβ and was associated with a reduced expression of *SHP*. Treatment of LX-2 cells with 50 ng/mL FGF19 for 24 hours did not alter *COL1α1* expression and led to a modest decrease in *αSMA* and PPARγ response gene expression (*ABHD5*, *ATGL*, *CEBPα*). Expression of *FXR* and FXR response gene *SHP* were decreased by FGF19. Additionally, although FGF19 treatment alone did not reduce *COL1α1* expression, FGF19 modestly decreased the induction of *COL1α1* by TGFβ.

Effects of FGF19 on gene expression in LX-2 cells were also investigated after 48 and 8 hours of treatment. Unlike at 24 hours, after 48 hours of FGF19 treatment expression of *COL1α1* was decreased (Figure 3.6A). The decreased expression of PPARγ response genes caused by 24 hours of FGF19 treatment was also observed after 48 hours of treatment. Additionally, FGF19 reduced the expression of genes encoding cytokines IL1β, IL6, and IL8 after 48 hours of treatment. After 8 hours of treatment with FGF19, there was a trend for decreased expression of *IL8*. No changes in gene expression were otherwise observed at the 8 hour time point (Figure 3.7).

As levels of IκBα were increased 30 minutes after FGF19 treatment, we sought to determine if IκBα levels were still elevated 72 hours after treatment and if this may contribute to the reduction in cytokine expression. Indeed, levels of IκBα were still increased 72 hours after treatment with FGF19. Moreover, levels of phosphorylated p65 were reduced (Figure 3.6B).

FGF19 does not stimulate LX-2 proliferation

LX-2 cells were treated with 50 ng/mL FGF19 for 48 hours and effects on proliferation were investigated via cell counts, Alamar Blue assay, and expression of genes involved in regulating cell cycle progression. For the cell count and Alamar Blue assay, wells were seeded with 5000 cells. After 48 hours, there was an average of 9,375 cells in wells treated with vehicle (Figure 3.8A). These data agree with the reported doubling time, 2-3 days of LX-2 cells. LX-2 cells treated with FGF19 did not proliferate. Wells treated with 50 ng/mL FGF19 contained an average of roughly 4,700 cells. FGF19 treatment was not toxic as viability of the treated cells was 97% (Figure 3.8B). Corresponding to decreased proliferation, the gene expression of *Cyclin D1* was reduced (Figure 3.8C). Cyclin D1 is critical for G1 to S phase transition during cell cycle progression. Interestingly, despite the decreased cell count observed after FGF19 treatment, no effect of FGF19 on proliferation was observed in the Alamar Blue assay (Figure 3.8D). Treatment of LX-2 cells for 48 hours with 100 μM of CDCA led to decreased cell numbers. The reduction in cell count may have been result of increased cell death as viability was reduced to 78%. Additionally, expression of *Cyclin D1* was reduced by CDCA.

FXR regulates FGF19 receptor expression in HSCs

We then determined to what extent FGF19 and BAs affect the expression of their receptors in HSCs. LX-2 cells were treated with CDCA for 24 hours and with CDCA, FGF19, or both CDCA and FGF19 for 48 hours. Treatment of LX-2 cells with CDCA for 24 hours induced the expression of FXR response gene *SHP* and increased *FGFR1, βKL,* and *TGR5* expression (Figure 3.9A). The expression of the FGF19 receptors, *FGFR1, FGFR4, and βKL,* underwent compensatory down-regulation in response to 48 hours of FGF19 treatment (Figure 3.9B). This down-regulation, as well as the down-regulation of *TGR5,* was prevented by co-treatment with CDCA.

3.5 DISCUSSION

HepG2 cells were treated with recombinant FGF19 produced in our lab to ensure the functionality of the protein in the *in vitro* experiments. The effect of FGF19 on BA synthesis has been well studied; activation of FGFR4-βKL co-receptor by FGF19 activates ERK and JNK pathways and subsequently leads to the down-regulation of *CYP7A1* and *CYP8B1* gene expression. Accordingly, in our study, the treatment of HepG2 cells with FGF19 led to a dose-dependent increase in pERK and reduction in mRNA levels of *CYP7A1* and *CYP8B1*. This indicates that the recombinant FGF19 is functional. As the high dose, 50 ng/mL, of FGF19 was more efficacious in stimulating ERK activation compared to all other concentrations, the 50 ng/mL dosage was selected for later studies with LX-2 cells. It has been previously reported that FGF19 induces *CTGF* expression in HepG2 cells[72]. In our study, FGF19 did not alter *CTGF* or *TGFβ* expression in HepG2 cells. This discrepancy between our study and that previously reported may be due to differences in time points investigated.

Prior to performing FGF19 treatments of LX-2 cells, we aimed to determine the relative expression of FGF19 receptors, including FGFR1, FGFR4, and βKL, in LX-2 and HepG2 cells. We found that both LX-2 and HepG2 cells express *FGFR1*, *FGFR4* and *βKL*, but to varying extents. Align with previous reports, HepG2 cells express predominantly FGFR4 compared to FGFR1. Conversely, LX-2 cells express predominantly FGFR1 compared to FGFR4. The expression of *FGFR4* in LX-2 cells is much lower than in HepG2 cells whereas the expression of *FGFR1* is higher in LX-2 cells. These findings suggest regulation of HSCs by FGF19 is plausible and would likely be mediated through FGFR1.

To determine to what extent FGF19 activates FGFRs on HSCs, LX-2 cells were treated with 50 ng/mL FGF19 and the effects on secondary messenger activation over

the course of an hour were measured. FGF19 was found to activate both STAT3 and JNK signaling pathways but did not alter ERK activity. This indicates that FGF19 can indeed activate FGFRs on LX-2 cells, however, FGF19 activates different signaling pathways in LX-2 cells compared to those in HepG2 cells. FGFR4 has also been shown to mediate the activity of the NFκB pathway[151]. In brief, FGFR4 activation stimulates the interaction of IκBα kinase (IKK) with FGFR4 and thereby prevents the phosphorylation of IκBα by IKK. This leads to increased levels of IκBα and reduced activation of p65[151]. Correspondingly, FGF19 treatment increased IκBα levels in LX-2 cells 15 and 30 minutes after treatment. This further supports that FGF19 activates FGFRs on LX-2 cells and that this activation may have anti-inflammatory effects.

We treated LX-2 cells with TGFβ as a positive control to verify we could activate LX-2 cells consistently in culture. As expected, TGFβ induced collagen expression and reduced PPARγ activity observed as a decrease in expression of PPARγ target genes, including *ABHD5*, *ATGL*, and *CEBPα*. *FXR* expression has been shown to be drastically down-regulated during HSC activation. In the current study, we showed that *FXR* expression was reduced by TGFβ. Therefore, we hypothesize that one of the mechanisms by which HSC activation suppresses FXR expression is via TGFβ. The activation of LX-2 cells with our positive control, TGFβ, demonstrates that we could activate LX-2 cells by profibrotic mediators treatment. This would allow for the investigation of the potential profibrotic effects of FGF19.

Evident that FGF19 activates FGFR on LX-2 and that in our hands, we are capable of consistently activating LX-2 cells in culture with test compounds, we sought to identify the effects of FGF19 on HSC phenotype and proliferation. FGF19 did not increase HSC activation as initially hypothesized. Expression of *αSMA*, a marker of an activated HSC, was slightly decreased at 24 hours but not 8 or 48 hours. Additionally,

FGF19 treatment decreased *COL1α1* expression modestly at 48 hours and mitigated the induction of *COL1α1* by TGFβ. Expression of *PPARγ*, a marker of a quiescent HSC, was not altered by FGF19 treatment. However, PPARγ activity may have been slightly decreased as expression of PPARγ target genes were slightly decreased after 24 and 48 hours of treatment. Overall, the changes in expression of HSC phenotypic marker genes in response to FGF19 treatment were modest and indicating no change in HSC phenotype to either an activated or quiescent state.

As FGF19 increased IκBα levels, we measured the expression of inflammatory mediators. Indeed, the expression of *IL1β*, *IL6*, and *IL8* was reduced by FGF19 after 48 hours of treatment. Additionally, we found that the increase in IκBα was sustained for 72 hours after treatment with FGF19. At this time point, decreased levels of phosphorylated p65 revealed NFκB activity was decreased. Pathways activated by FGF19 in LX-2 cells, STAT3 and JNK, are known to be positive regulators of cytokine expression. Therefore, it is unlikely that these pathways are responsible for the down-regulation of cytokines in LX-2 cells and likely the down-regulation is resultant of reduced NFκB activity.

Like FGF19, FGF2 activates both FGFR1 and FGFR4 however does not require βKL as an obligate co-receptor. FGF2 has been reported to function as a mitogen for HSCs.[77] We therefore hypothesized that FGF19 may serve as a mitogen for HSCs. However, we observed the opposite; FGF19 reduced cell counts and expression of *Cyclin D1*. The decreased cell count appears not to be due to toxicity as the viability of LX-2 cells treated with FGF19 was 97%. Disagreeing with our cell count data, FGF19 treatment had no effect in the Alamar Blue assay. However, the Alamar Blue assay is dependent upon metabolic rate in addition to the number of cells present. FGF19 has been shown to alter energy utilization.[115] Therefore, the discrepancy between the observations on cell count and in the Alamar Blue assay may possibly be attributed to

altered metabolism in LX-2 cells by FGF19. FGF2 was shown to increase HSC proliferation through activation of the ERK pathway subsequent up-regulation of Cyclin D1.[77, 205] In our study, FGF19 did not increase ERK signaling and decreased *Cyclin D1* expression. Therefore, the lack of ERK activation by FGF19 may be the reason for the differences in mitogenicity of FGF2 and FGF19.

We must be cautious when translating the *in vitro* FGF19 treatment findings to *in vivo* effects on fibrosis. Though FGF19 did not induce LX-2 activation it did activate STAT3 and JNK pathways. STAT3 signaling has been shown to be a key regulator of HSC activation. Additionally, though LX-2 cells are a useful tool to study HSC function they are not quiescent and express markers of both quiescent and activated HSCs. Therefore, from our data, it is not possible to determine if FGF19 may affect HSC transdifferentiation from a quiescent to an activated phenotype.

FIGURES

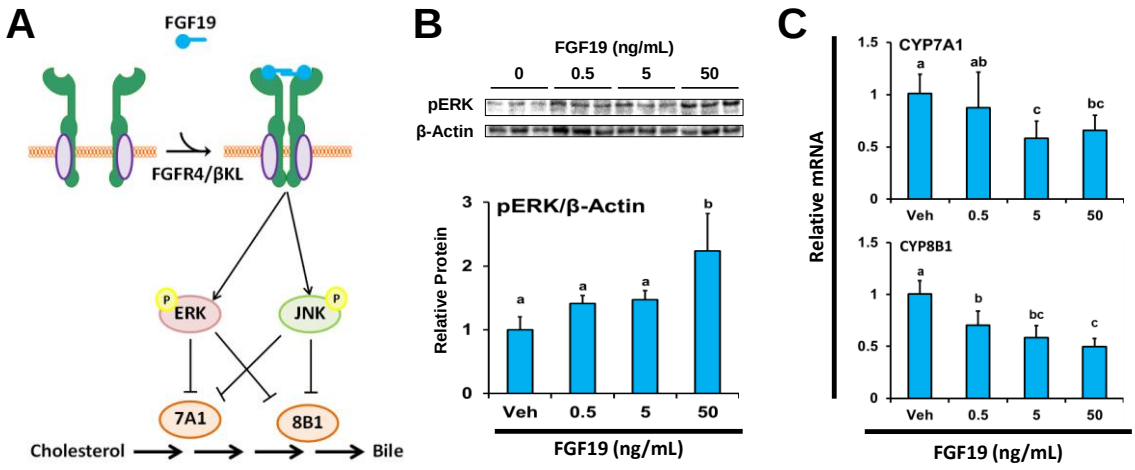

Figure 3.1. *Recombinant FGF19 protein is functional and activates FGFR4 on HepG2 cells.* (A) Mechanism by which FGF19 suppresses BA synthesis in hepatocytes. FGF19 led to the activation of FGFR4 on HepG2 cells evident by (B) increase in ERK phosphorylation after 1 hour treatment and (C) down-regulation of *CYP7A1* and *CYP8B1* mRNA levels after 24 hours of treatment. Data are presented as mean + SD and analyzed by one-way ANOVA with post-hoc Duncan's Multiple Range Test.

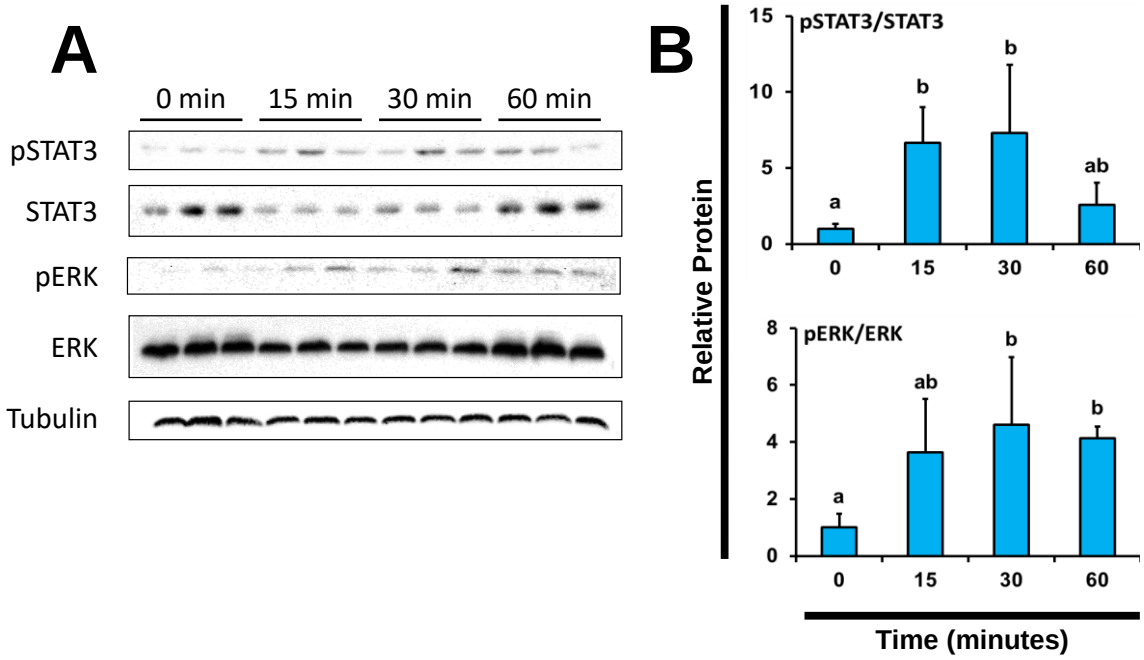

Figure 3.2. *Time course of FGFR secondary messenger activation in HepG2 cells following treatment with FGF19.* (A) Relative levels of pSTAT3, STAT3, pERK, and ERK in HepG2 cells treated with 50 ng/mL FGF19 for 0, 15, 30, and 60 minutes were detected by Western Blot and (B) semi-quantified. Data are presented as mean + SD and analyzed by one-way ANOVA with post-hoc Duncan's Multiple Range Test.

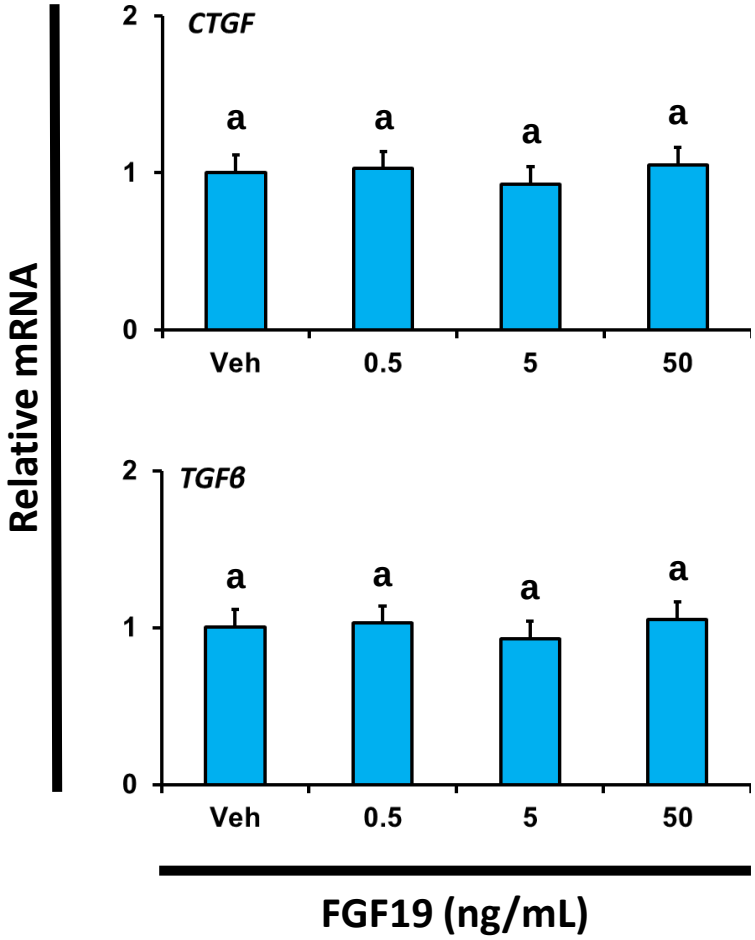

Figure 3.3. *Treatment of HepG2 cells with FGF19 for 24 hours did not alter CTGF or TGFβ expression.* Data are presented as mean + SD and analyzed by one-way ANOVA with post-hoc Duncan's Multiple Range Test.

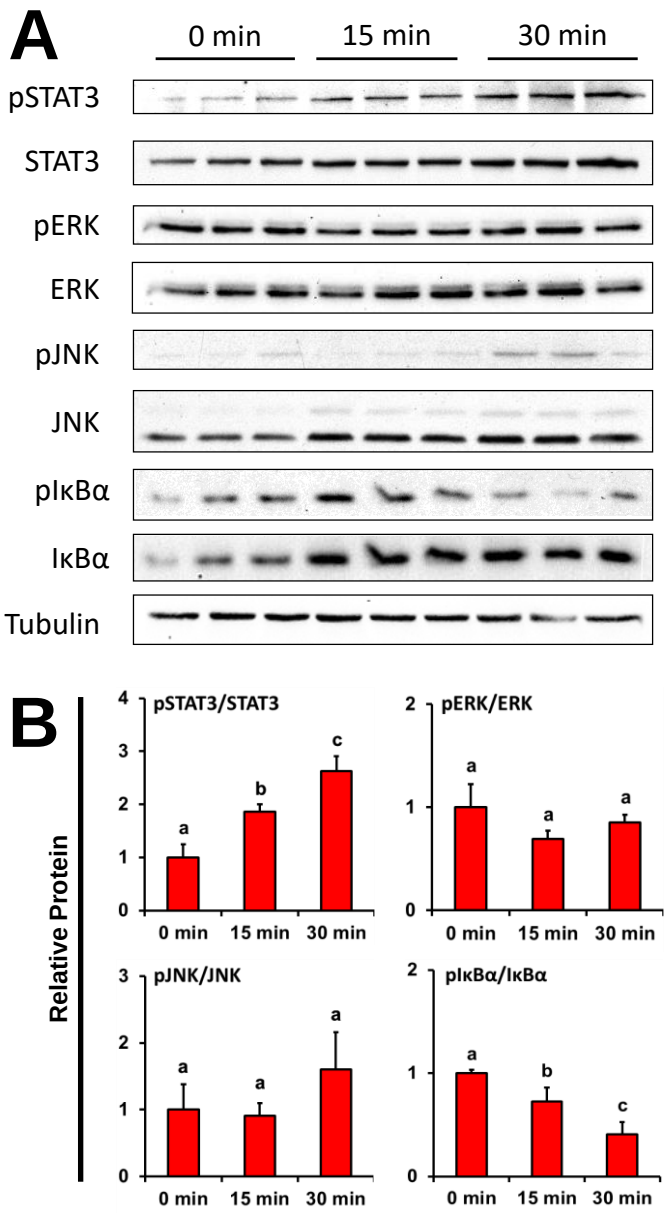

Figure 3.4. *FGF19 activates FGFRs on HSCs.* (A) Relative levels of phosphorylated and total FGFR secondary messengers in LX-2 cells treated with 50 ng/mL FGF19 were detected by Western Blot and (B) semi-quantified. As FGFR4 activation has been shown to antagonize NFκB signaling by increasing IκBα levels, phosphorylated and unphosphorylated IκBα levels were measured as well. Data are presented as mean + SD and analyzed by one-way ANOVA with post-hoc Duncan's Multiple Range Test.

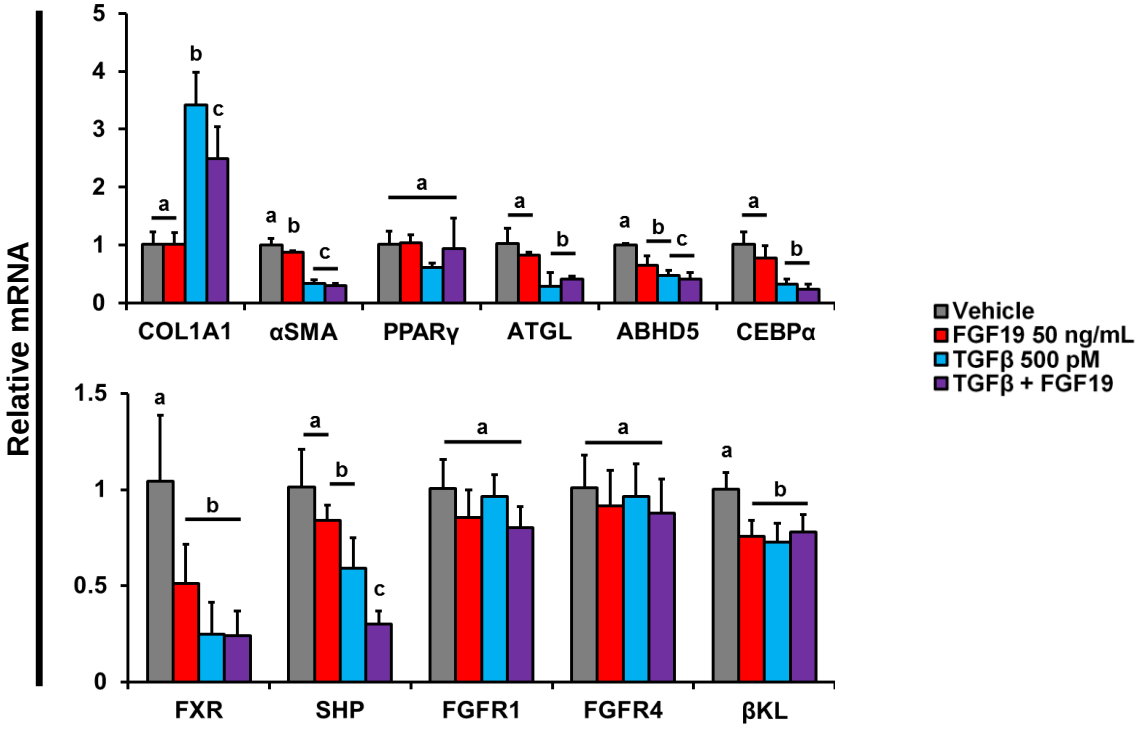

Figure 3.5. *Treatment of LX-2 cells with FGF19 and TGFβ for 24 hours.* LX-2 cells were treated with 50 ng/mL FGF19 and/or 500 pM of TGFβ for 24 hours and changes in gene expression of *COL1α1*, *αSMA*, *PPARγ*, PPARγ target genes (*ABHD5*, *ATGL*, *CEBPα*), FGF19 receptors, and BA receptors were measured. Data are presented as mean + SD and analyzed by one-way ANOVA with post-hoc Duncan's Multiple Range Test.

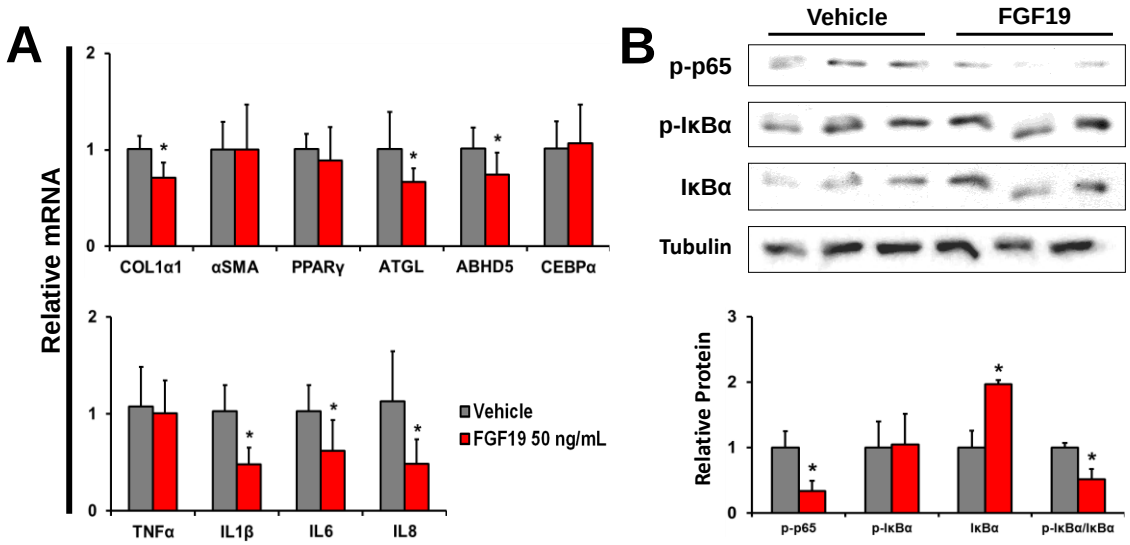

Figure 3.6. *FGF19 treatment for 48 hours did not alter LX-2 activation but reduced inflammatory gene expression.* (A) LX-2 cells were treated with 50 ng/mL of FGF19 for 48 hours and changes in gene expression of *COL1α1*, *αSMA*, *PPARγ*, PPARγ target genes (*ABHD5*, *ATGL*, *CEBPα*), inflammatory mediators (*TNFα*, *IL1β*, *IL6*, and *IL8*), and cell cycle regulators (*Cyclin D1* and *Cyclin E1*) were measured. (B) *R*elative levels of p-p65, pIκBα, and IκBα in LX-2 cells treated with 50 ng/mL FGF19 for 72 hours were detected by Western Blot and semi-quantified. Data are presented as mean + SD and analyzed by Student's T-test. * indicates significance compared to vehicle ($p \leq 0.05$).

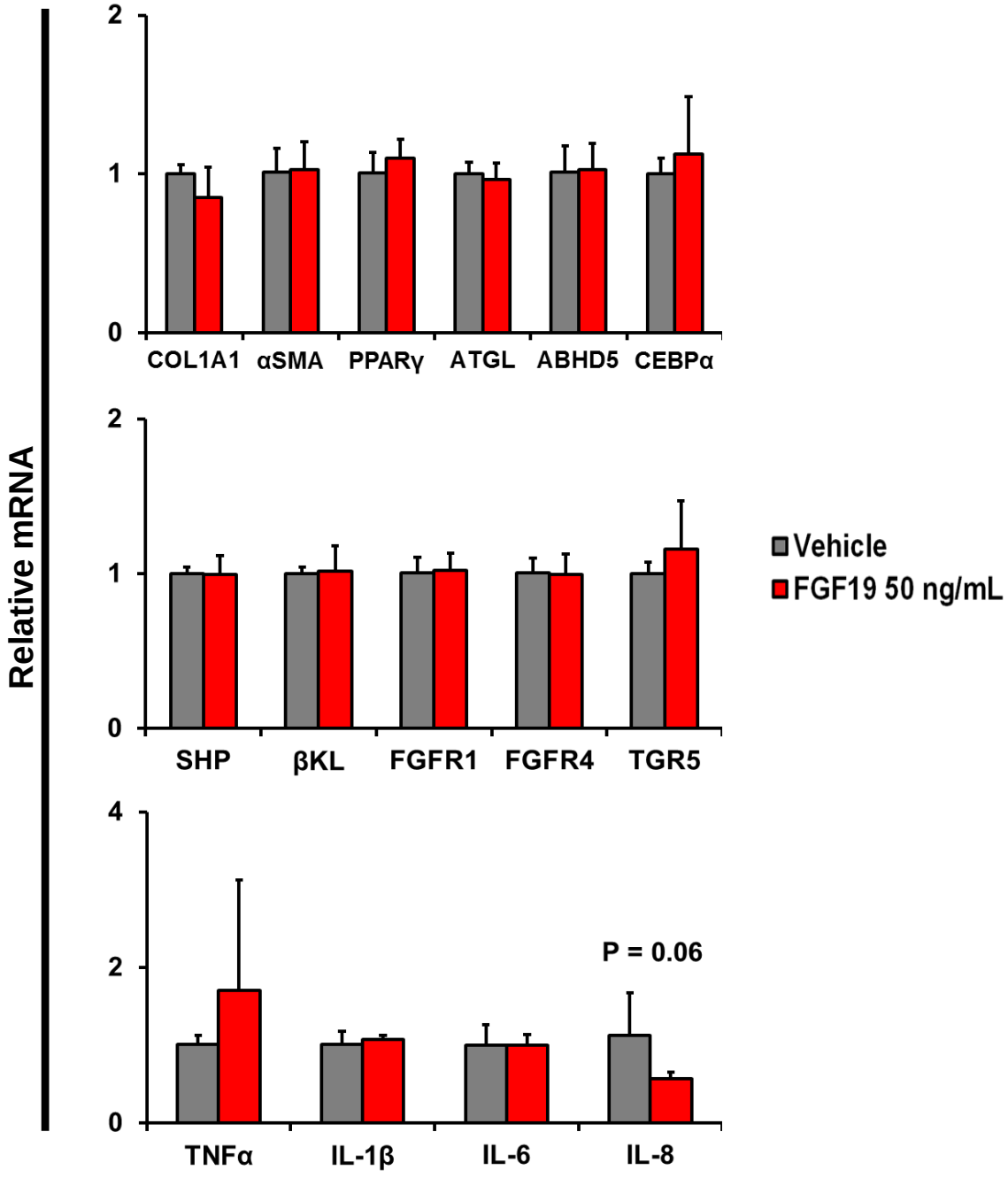

Figure 3.7. *Gene expression in LX-2 cells after 8 hours treatment with 50 ng/mL FGF19.* Data are presented as mean + SD and analyzed by Student's T-test. * indicates significance compared to vehicle ($p \leq 0.05$).

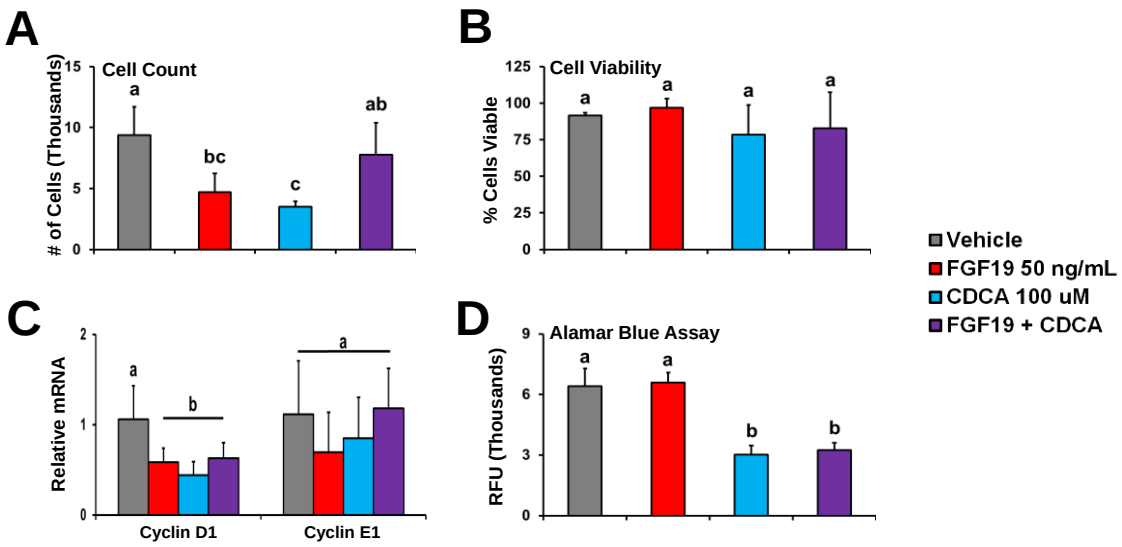

Figure 3.8. *Effect of FGF19 and CDCA on the proliferation of LX-2 cells.* 5,000 LX-2 cells were seeded into each well and treated with 50 ng/mL FGF19 and/or 100 μM of CDCA for 48 hours. (A) Cells were counted and (B) viability assessed via trypan blue. (C) Expression of genes involved in cell proliferation was measured. (D) Alamar blue assay was performed and relative fluorescence measured. Data are presented as mean + SD and analyzed by one-way ANOVA with post-hoc Duncan's Multiple Range Test.

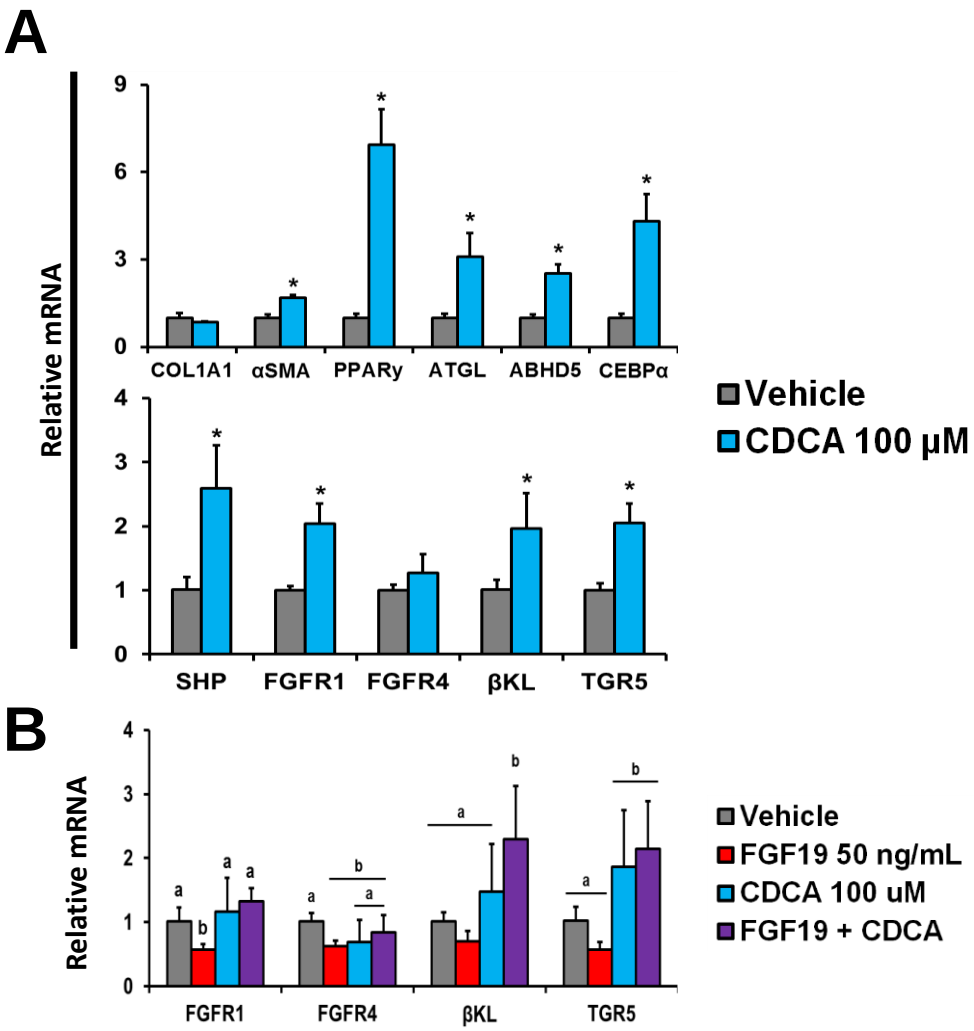

Figure 3.9. *FXR activation in LX-2 cells increases PPARγ activity, increases the expression of FGF19 receptors, and prevents the compensatory down-regulation of FGF19 receptors induced by FGF19 treatment.* (A) LX-2 cells were treated with 100 µM CDCA for 24 hours with changes in gene expression measured. Data are presented as mean + SD and analyzed by Student's T-test. * indicates significance compared to vehicle ($p \leq 0.05$). (B) LX-2 cells were treated with FGF19, CDCA, and both FGF19 and CDCA for 48 hours and effects on the expression of *FGFR1*, *FGFR4*, *βKL*, and *TGR5* were measured. Data are presented as mean + SD and analyzed by one-way ANOVA with post-hoc Duncan's Multiple Range Test.

TABLES

Target	Manufacturer	Cat #	Dilution
ERK	Cell Signaling Technology	9102S	1:1000
IκBα	Cell Signaling Technology	4812S	1:1000
JNK	Cell Signaling Technology	9252S	1:1000
STAT3	Cell Signaling Technology	4904	1:1000
p-ERK @ Thr202 and Thr 204	Cell Signaling Technology	9101	1:1000
p-IκBα @ Ser32	Cell Signaling Technology	2859S	1:1000
p-JNK @ Thr183 and Tyr185	Cell Signaling Technology	9251S	1:1000
p-p65 @ Ser536	Cell Signaling Technology	3033S	1:1000
p-STAT3 @ Ser727	Cell Signaling Technology	9134	1:1000
Tubulin	DSHB	12G10	1:100
β-Actin	DSHB	JLA20	1:200

Table 3.1. *List of antibodies used in Chapter 3.*

Gene	Sense	Antisense
ABHD5	CCGGCTTCGAGATAAGTCCC	GCCAACCAGTTAGCCATCCT
ATGL	ACCAGCATCCAGTTCAACCT	ATCCCTGCTTGCACATCTCT
CEBPα	TGTATACCCCTGGTGGGAGA	TCATAACTCCGGTCCCTCTG
COL1α1	AGTGGTTTGGATGGTGCCAA	GCACCATCATTTCCACGAGC
COL4α1	ACTCTTTTGTGATGCACACCA	AAGCTGTAAGCGTTTGCGTA
CTGF	GGCCTCTTCTGCGATTTCG	CCATCTTTGGCAGTGCACACT
CYCLIN D1	AGGTCTGCGAGGAACAGAAGTG	TGCAGGCGGCTCTTTTTC
CYCLIN E1	ATCCTCCAAAGTTGCACCAG	AGGGGACTTAAACGCCACTT
CYP7A1	TGTCCTGGAAGATTGTTCGCT	GGACATTTAGCTTGGCCCTCT
CYP8B1	AGTACACATGGACCCCGACATC	GGGTGCCATCCGGGTTGAG
FGFR1	GTCTGCTGACTCCAGTGCAT	CTCCCAGGGGTTTGCCTAAG
FGFR4	CAAAGACAACGCCTCTGACA	CACCAAGCAGGTTGATGATG
FXR	AACATAGCTTCAACCGCAGACG	GAAATGGCAACCAATCATGTACA
IL1β	AACAGGCTGCTCTGGGATTCTCTT	ATTTCACTGGCGAGCTCAGGTACT
IL6	TGACAAACAAATTCGGTACATCC	ATCTGAGGTGCCCATGCTAC
IL8	CACTGCGCCAACACAGAAATTA	ACTTCTCCACAACCCTCTGCAC
PPARγ	GTCGTGTCTGTGGAGATAAA	ACATGATGGCATTATGAGAC
SHP	AGCTGGAAGTGAGAGCAGATCC	AGAAGTGCGTAGAGAATGGCG
TGFβ	TTGCCCTCTACAACCAACACAA	GGCTTGCGACCCACGTAGTA
TGR5	CAGTGTCGACCTGGACTTGA	TAACGGCCAGAGGAGCTTTA
TNFα	AGGACGAACATCCAACCTTCCCAA	TTTGAGCCAGAAGAGGTTGAGGGT
αSMA	CCGGGACTAAGACGGGAATC	CACCATCACCCCCTGATGTC
β-Actin	TGAGCTGCGTGTGGCTCCC	AGGGATAGCACAGCCTGGATAGCA
βKL	GCAGTCAGACCCAAGAAAATACAGA	CCCAGGAATATCAGTGGTTTCTTC

Table 3.2. *List of primers used in Chapter 3.*

CHAPTER 4: REGULATION OF CARBON TETRACHLORIDE INDUCED HEPATIC FIBROSIS BY BILE ACIDS AND FGF15

4.1 ABSTRACT

Background: Fibroblast growth factor 15 (FGF15, ortholog to human FGF19) is a key regulator of bile acid (BA) homeostasis that inhibits the expression of genes critical in BA synthesis; *Fgf15*$^{-/-}$ mice have increased total bile acid pool (TBAP) size. FGF15 deficiency protects mice from liver fibrosis. FXR is a nuclear receptor activated by BAs and its activation in HSCs has been shown to reduce fibrotic gene expression.

Objective/Hypothesis: We sought to identify the mechanism by which FGF15 deficiency is protective against liver fibrosis. We hypothesized that increased BA levels in *Fgf15*$^{-/-}$ mice leads to stronger FXR activation in HSCs and subsequently reduces fibrosis.

Methods: We treated WT, knockout (KO; *Fgf15*$^{-/-}$), and *Fgf15* overexpressing transgenic (TG) mice with CCl_4 for 4 weeks to induce liver fibrosis. *Fgf15*$^{-/-}$ mice were fed a 2% cholestyramine containing diet to reduce TBAP size. TG mice have smaller TBAP size which we increased via a diet containing 0.2% cholic acid (CA).

Results: *Fgf15*$^{-/-}$ mice had lower hepatic collagen levels compared to WT mice. Cholestyramine increased the basal collagen levels in *Fgf15*$^{-/-}$ mice to levels comparable to those in WT mice. With CCl_4 treatment, *Fgf15*$^{-/-}$ mice showed worsened centrilobular necrosis and inflammation compared to WT, however, no differences were observed in fibrotic gene expression or fibrosis severity. CCl_4 induced fibrosis was increased by cholestyramine in *Fgf15*$^{-/-}$ but not WT mice. TG mice had higher basal and CCl_4 induced expression of inflammatory cytokines. The fibrosis severity induced by CCl_4 was similar between TG and WT mice. The expression of *Col1α1* and amount of collagen staining in Sirius Red stained liver sections was inversely correlated to TBAP size and hepatic

Shp expression in *Fgf15*$^{-/-}$ and TG mice but not WT mice. In both WT and TG mice, co-treatment with CA and CCl_4 led to cholestasis.

Conclusion: Our findings indicate that the protective effects of FGF15 deficiency against hepatic fibrogenesis may be mediated through alterations in TBAP size and FXR activity in the liver.

4.2 INTRODUCTION

As shown in Chapter 2 and described in section 1.3.3.4, FGF15 deficiency is protective against hepatic fibrosis in both a HFD induced NASH model and CCl_4 induced hepatic fibrosis model. One study reported that the mechanism by which FGF15 deficiency ameliorated CCl_4 induced fibrosis was through the prevention of induction of CTGF in hepatocytes. Reduced hepatocyte derived CTGF led to decreased activation of HSC and subsequently reduced fibrosis.[72] However, we reported that no differences in *Ctgf* expression were observed in the HFD-induced NASH model.[206] We therefore considered that other mechanisms, in addition to reductions in hepatocyte derived CTGF synthesis, underlie the protective effect of FGF15 deficiency on fibrosis. As FXR signaling is protective against HSC activation and reduces responsiveness to profibrotic mediators, we hypothesized that the increased TBAP size in KO mice leads to enhanced FXR activation in HSCs and thereby reduced fibrosis. To test this hypothesis, we fed WT, FGF15 deficient (KO; *Fgf15*$^{-/-}$), and *Fgf15* overexpressing (TG; FABP1-Fgf15) mice diets containing either the BA sequestrant cholestyramine or supplemented with CA. Mice were then treated with CCl_4 chronically to induce fibrosis. The combinations of genotype and diet led to multiple combinations of TBAP size and *Fgf15* expression. This would allow for the identification of the BA-dependent and -independent effects of FGF15 within the CCl_4 model of fibrosis.

4.3 METHODS

Animals and treatment:

In this study, both Fgf15 deficient and overexpressing mice strains were used. Whole body Fgf15 knockout mice (Fgf15$^{-/-}$; KO) mice were raised with a mixed A129/C57BL/6J background.[149] The mixed background was necessary as knockout in a C57BL/6J background was embryonic lethal and knockout in an A129 background was not successful. Fgf15 transgenic mice (FABP1-Fgf15; TG) were raised with a C57BL/6J

background. Overexpression of Fgf15 in FABP1-Fgf15 mice was achieved through insertion of the fatty acid binding protein 1 (FABP1) promoter in front of the Fgf15 gene. This resulted in overexpression of ileal Fgf15 mRNA by over 500 fold. C57BL/6J mice were used as wild type (WT) controls.

At 8-10 weeks of age, the mice were fed either a control chow diet, 0.2% cholic acid diet (Sigma Aldrich; Cat. # C1129), or a 2% cholestyramine diet (Sigma Aldrich; Cat. # C4650). Cholic acid and cholestyramine containing diets were created by geometric dilution in powdered chow diet (PicoLab Rodent Diet 5053; LabDiet, New Brunswick, NJ). After 2 weeks on their assigned diets, the mice were treated with 1 mL/kg, i.p. CCl_4 twice a week for 4 weeks to induce liver fibrosis. The two week pre-feed period was included to allow the assigned diet sufficient time to modulate the size of the bile acid pool prior to the start of CCl_4 injections. Mice were maintained on the assigned diet during the entirety of the CCl_4 injection period.

Body and food weights were recorded twice a week during both the pre-feed and CCl_4 treatment periods. At the end of the 4 week CCl_4 treatment period, serum, gall bladder, whole GI tract, ileum, and liver tissues were collected. Animal experiments within this study were conducted with the approval of the Rutgers University Institutional Animal Care and Use Committee.

Histology and special stains:

Tissues were fixed in 4% paraformaldehyde and processed to slides. Liver tissue sections for each mouse were then stained with H&E and Sirius Red. Sections stained with H&E were scored by a pathologist for severity of biliary hyperplasia, necrosis, inflammation, and fibrosis. Biliary hyperplasia was scored based upon the number of oval or intercalated cells present in cholangioles. Centrilobular necrosis was scored corresponding to the extent of hepatocyte degradation and presence of pyknotic nuclei or cell debris. Inflammation was scored pertaining to the number of mixed inflammatory

cells present in the tissue. Lastly, hepatic fibrosis was scored according to Brunt criteria.[48] Sirius Red stained slides were imaged under polarizing light at 100x magnification and area positively staining for collagen was semi-quantified using ImageJ.[197]

Total bile acid pool measurement:

The size of the TBAP was determined by measuring BA content in the gall bladder, small intestine, liver, and serum.[207] Gall bladders were homogenized in 1 mL of PBS, homogenate diluted ten times in PBS, and BA concentration determined using commercially available kit according to the manufacturer's instructions (Total BA Assay; Diazyme, Poway, CA). A section of liver was homogenized in 0.5 mL of water and 0.5 mL of 100% ethanol added. Liver homogenates were rotated for one hour prior to centrifugation, collection of supernatant, and resuspension of pellets in 1 mL of 100% ethanol. Rotation and centrifugation was repeated, supernatants combined, and BA concentration determined using kit. Concentration of liver BAs were normalized to weight of liver section homogenized. The entire small intestine was homogenized in 3 mL of water and 2 mL of 100% ethanol was added. Intestine homogenates were rotated for one hour prior to centrifugation, collection of supernatant, and resuspension of pellets in 5 mL of 100% ethanol. Rotation and centrifugation was repeated, supernatants combined, and BA concentration determined using kit. TBAP levels were normalized to mouse total body weight.[207]

Serum biomarker measurement:

Serum ALT, ALP, and total bilirubin levels were determined using commercially available kits according to the manufacturers' instructions (Pointe Scientific, Canton, MI).

Gene expression:

Total RNA was isolated from liver and ileum samples using TRIzol Reagent (ThermoFisher Scientific, Waltham, MA). 2 µg of isolated total RNA was reverse

transcribed to cDNA and analyzed by RT-qPCR using Sybr green chemistry. Primer sequences used in this study are listed in Table 4.1. Expression of genes of interest was normalized against the expression of *β-actin.*

Statistical tests & analysis

Levene's test was performed to assess the equity of variance of each variable. Should the assumption of homogeneity of variance not be met for subsequent ANOVA tests, data were logarithmically transformed. Data were analyzed via 3-Way ANOVA and post-hoc Tukey's HSD. Significance was considered met when $P \leq 0.05$. Data in figures are presented as mean plus SD. Histology scores are presented as histology pies. Each pie is separated into slices equal to the number of mice in the respective group. Each slice is then colored based upon histologic score. Correlations between endpoints of interest and TBAP size and hepatic *Shp* expression were analyzed using simple linear regression and F-test.

4.4 RESULTS

Effect of genotype, diet, and CCl_4 on BA homeostasis

Genotype, diet, and CCl_4 affected the TBAP in mice (Figure 4.2). In WT mice, the TBAP was lowered modestly by cholestyramine and increased by the CA diet. KO mice had an increased basal TBAP, which was brought back to levels comparable to WT mice by cholestyramine feeding. Additionally, the TBAP was decreased in KO mice by CCl_4. In TG mice, the TBAP was reduced, however was greatly increased by CA feeding. Genotype and diet predominantly altered the BA concentrations in the intestine. Liver and serum BA concentrations were not affected by genotype or CCl_4 treatment alone. Cholestyramine-containing diet did not alter hepatic or serum BA concentrations in either WT or KO mice. CA diet alone increased the concentrations of BAs in the liver

and serum of TG mice but not WT mice. When co-administered with CCl_4, the CA diet increased liver and serum BAs in WT mice and further elevated serum BAs in TG mice.

Changes in BA concentration in the intestine caused by genotype and diet led to alterations in FXR activity in the ileum (Figure 4.3A). In WT mice, cholestyramine feeding did not alter ileal FXR activity as expression of FXR target genes *Fgf15*, *Shp*, and *Ibabp* remained unchanged. However, CA diet increased FXR activity and led to a 43 fold induction of *Fgf15* and trend for increased *Ibabp* expression. In KO mice, we verified that *Fgf15* was effectively knocked out. FXR activity in the intestines of KO mice was enhanced evident by increased expression of *Shp*. Cholestyramine containing diet reduced intestinal FXR activity and led to reductions in *Shp* and *Ibabp* expression. In the TG mice, *Fgf15* was overexpressed in the ileum by 578 fold. This overexpression was not further increased by CA feeding. Despite the lowered levels of BAs in the intestine, TG mice had comparable expression of FXR targets genes *Shp* and *Ibabp*.

Expression of genes involved in BA synthesis and transport in the liver were affected by genotype and diet (Figure 4.3B). In WT mice, cholestyramine led to inductions of genes involved in BA synthesis; increased *Cyp8b1* expression and a trend for increased *Cyp7a1* expression. Conversely, exogenous CA feeding suppressed the expression of *Cyp7a1*. Compared to WT, KO mice had increased, whereas TG mice had suppressed, expression levels of *Cyp7a1*. CCl_4 treatment of KO mice reduced *Cyp7a1* expression. Expression of BA transporters, *sodium taurocholate co-transporting polypeptide* (*Ntcp)* and *Bsep*, was not affected by FGF15 deficiency or cholestyramine diet (Figure 4.3B). In WT mice, CA diet led to a trend for decreased expression of *Ntcp*. CA diet alone increased *Bsep* expression in TG mice, and when combined with CCl_4, led to reductions in *Ntcp* expression.

Effect of genotype, diet, and CCl_4 on liver biomarkers and histology

Liver injury biomarkers were not affected by genotype, cholestyramine diet, or CCl_4 treatment but were elevated by CA diet (Figure 4.4). In WT and TG mice, the CA diet increased both the liver-to-body-weight ratio and activities of ALT. Co-treatment of TG mice with CA and CCl_4 led to elevations in serum total bilirubin levels. ALP activities were similar across all groups.

Livers sections were stained with H&E (Figure 4.5-4.7) and Sirius Red (Figure 4.8) and scored by a pathologist for severity of biliary hyperplasia, centrilobular necrosis, inflammation, and fibrosis (Figure 4.9). In WT mice, CCl_4 caused mild biliary hyperplasia and inflammation in a third of mice and induced fibrosis scoring either two or three (0 for no fibrosis and 4 for most severe fibrosis) in all mice. Cholestyramine diet produced mild biliary hyperplasia and inflammation in one and two out of five mice respectively. However, when given with CCl_4, cholestyramine increased frequency, but not severity, of biliary hyperplasia and inflammation. Cholestyramine did not affect fibrosis scores in WT mice. CA diet alone led to the development of biliary hyperplasia in half of the treated mice and mild fibrosis in one mouse. Co-treatment of WT mice with CA and CCl_4 led to increased severity and frequency of biliary hyperplasia, centrilobular necrosis, and inflammation than CCl_4 treatment alone. However despite the greater inflammation, fibrosis severity in these mice was reduced.

Shown in Figure 4.9, FGF15 deficiency was not protective against CCl_4 induced fibrosis with frequency and severity of fibrosis similar in KO mice compared to WT. CCl_4 caused mild to moderate centrilobular necrosis in KO mice. This differs greatly from WT mice in which no centrilobular necrosis was observed. Correspondingly, the frequency and severity of inflammation in KO mice was greater than that of WT. Mild biliary hyperplasia was also present in two thirds of the mice. Cholestyramine feeding led to mild fibrosis in half the treated KO mice. When given with CCl_4, cholestyramine

increased the severity of inflammation and fibrosis but not centrilobular necrosis. Biliary hyperplasia in KO mice caused by CCl_4 treatment was prevented by cholestyramine co-treatment.

Overexpression of FGF15 did not alter the severity of CCl_4 induced fibrosis. CA diet led to biliary hyperplasia and inflammation in all but one and two of the treated TG mice respectively. Additionally, treatment of TG mice with CA diet alone caused mild and moderate fibrosis in two mice. Lastly, TG mice fed CA were found to have steatosis, a finding not observed in any other group. Co-treatment of TG mice with CA and CCl_4 led to severe biliary hyperplasia and worsened inflammation compared to CCl_4 treatment alone. CCl_4 induced fibrosis may have been slightly reduced in TG mice by CA diet.

Effect of genotype, diet, and CCl_4 on expression of genes in hepatic inflammation and fibrosis

The presence of cholestasis in the CA treated WT and TG mice confounds the interpretation of the effects of BAs and FGF15 on CCl_4 induced inflammatory and fibrotic endpoints. Therefore, CA treated mice were excluded from subsequent analyses regarding these endpoints.

To identify effects on liver inflammation, the expression of inflammatory cytokines in the liver was measured (Figure 4.10A). Expression of *Tnfα*, *Icam1*, *Il1β*, and *Il6*, was not increased by CCl_4 in WT mice. Cholestyramine treatment of WT mice increased the expression of cytokines *Tnfα*, *Il1β*, and *Il6*. In KO mice, *Icam1* expression was increased by both cholestyramine and CCl_4 treatments. The expression of *Icam1* was greater in KO mice than WT when co-treated with cholestyramine and CCl_4. *Tnfα* expression was greater in TG mice compared to WT when treated with CCl_4.

Liver sections were stained with Sirius Red to determine relative collagen content in the liver (Figure 4.10B). Hepatic collagen levels were lower in chow fed, vehicle treated KO mice compared to WT, but were comparable between WT and TG mice. FGF15 manipulation seems to not affect the development of liver fibrosis in the CCl_4 model, as FGF15 deficiency did not reduced, nor did overexpression worsen, CCl_4 induced fibrosis; the area of positive Sirius Red staining in WT, KO, and TG mice was increased to the same extent by CCl_4. Cholestyramine feeding did not change collagen levels in WT mice but almost tripled the amount in KO mice. Treatment of WT, KO, and TG mice with CCl_4 led to comparable induction of *Col1α1* and *Timp1*(Figure 4.10C). In WT and KO mice, cholestyramine treatment led to increases in *Col1α1* and *Timp1* expression. In KO mice but not WT mice, co-treatment of cholestyramine and CCl_4 tended to further increase the induction of *Col1α1*. The expression level of *αSma* was lower in the KO and TG mice than in WT mice. None of the treatments affected *αSma* expression in WT mice, whereas expression was increased in KO by co-treatment with cholestyramine and CCl_4. Similarly, expression of *Tgfβ* was increased by CCl_4 in KO and TG mice but was not altered in WT mice by any treatment. We also assessed the expression of a FXR target gene, *Shp*, in the liver (Figure 4.10D). As expected, the KO mice had increased expression of *Shp* compared to WT mice. The pattern of *Shp* expression in the livers of KO mice followed that of the TBAP size.

The main goal of this study was to determine whether changes in BA levels and hepatic FXR activity affect hepatic inflammation and fibrosis development in FGF15 deficient and overexpressing mice. Therefore, TBAP size and expression of *Shp* in the liver were then compared to *Tnfα*, *Icam1*, and *Col1α1* expression as well as extent of Sirius Red staining by linear regression (Figures 4.11-4.14). Associations were determined for each of these variables classified by genotype. In WT mice, no

correlation was observed between TBAP and hepatic *Shp* expression to area stained by Sirius Red or *Icam1* and *Col1α1* expression. *Tnfα* expression was inversely correlated to TBAP size (R^2 = 0.193; P = 0.032) however not to hepatic *Shp* expression. In KO mice, both *Icam1* and *Tnfα* were inversely correlated to TBAP size (*Icam1* - R^2 = 0.238; P = 0.003; *Tnfα* - R^2 = 0.159; P = 0.013) and hepatic *Shp* expression (*Icam1* - R^2 = 0.393; P < 0.001; *Tnfα* - R^2 = 0.195; P = 0.009). Area stained by Sirius Red and *Col1α1* expression were also inversely correlated to both TBAP size (Sirius Red - R^2 = 0.144; P = 0.027; *Col1α1* - R^2 = 0.230; P = 0.003) and hepatic *Shp* expression (Sirius Red - R^2 = 0.285; P = 0.002; *Col1α1* - R^2 = 0.308; P = 0.001). In TG mice, *Icam1*, *Tnfα*, Sirius Red staining and *Col1α1* were not correlated to TBAP size. However, hepatic *Shp* expression was correlated to both Sirius Red stain (R^2 = 0.387; P = 0.023) and *Col1α1* (R^2 = 0.358; P = 0.031).

The correlations of *Icam1*, *Tnfα*, *Col1α1*, and Sirius Red staining to TBAP size and *Shp* expression were then repeated not classified by genotype. Each comparator was weakly and inversely correlated to TBAP size and *Shp* expression. Lines of best fit for each genotype were graphed with the line of best for the dataset as a whole. For every comparison, the line of best fit for the KO mice was nearly identical to the line of best fit for all animals analyzed together. Additionally, the regression lines comparing Sirius Red staining and *Col1α1* expression to *Shp* expression were similar for KO and TG mice.

4.5 DISCUSSION

Genotype and diets effectively modulated TBAP size

TBAP size was modulated by FGF15 deficiency and overexpression corresponding to the known role of FGF15 as a negative feedback factor of BA synthesis. In the TG mice, *Fgf15* was overexpressed by over 500 fold leading to marked

suppression of *Cyp7a1* expression. This subsequently led to decreased TBAP sizes in TG mice. In agreement, FGF15 deficiency induced the expression of *Cyp7a1* and increased TBAP size. The changes in TBAP caused by FGF15 deficiency and overexpression occurred only in the intestine with BA concentrations in the liver and serum unaltered. However, FXR activity in KO mice was increased in both the ileum and liver evident by increased expression of FXR target gene, *Shp*. The reduced TBAP in TG mice did not change *Shp* expression in either location, even though *Shp* expression was reported to be reduced in whole-body FXR deficient mice.[208]

The cholestyramine diet was well tolerated and did not increase serum liver injury biomarkers or liver-to-body weight ratio in WT and KO mice. As expected, it reduced the size of the TBAP. In WT mice, cholestyramine led to no overt toxicity observed histologically and caused mild inflammation in two of five mice. Cholestyramine only caused a modest decrease in TBAP size in the WT mice. To compensate for the sequestration of BAs, expression of *Cyp7a1* and *Cyp8b1* were induced. Treatment of KO mice with cholestyramine reduced the elevated TBAP size back to levels comparable to WT. The cholestyramine diet reduced BA levels in the intestines of WT and KO mice, but did not reduce hepatic or serum BA concentrations. Align with decreased intestinal BA levels, FXR activity in the ileum of KO mice was reduced. Although the cholestyramine diet did not reduce hepatic BA concentrations, *Shp* expression in the livers of KO mice mirrored TBAP size.

The CA diet increased TBAP size in WT, however, also led to the development of cholestasis when co-treated with CCl_4. Treatment of WT mice with only CA diet increased TBAP size but did not alter hepatic or serum BA levels. However, when WT mice were co-treated with CA and CCl_4, hepatic and serum BA levels were elevated. Though hepatic BA levels were not increased by CA diet alone, liver-to-body weight ratio

was increased as well as serum ALT activity. These liver injury markers were not further increased by CCl_4 co-treatment.

TG mice were more susceptible to CA diet-induced cholestasis than WT mice. Unlike in WT mice, CA diet alone elevated hepatic and serum BA levels in TG mice. Additionally, elevations in serum BA levels by co-treatment with CA and CCl_4 were higher in TG mice. Correspondingly, the only treatment group with increased serum total bilirubin was the CA and CCl_4 co-treated TG group. Additionally, the severity of biliary hyperplasia, a compensatory change in liver histology indicative of biliary stress and injury, was greatest in co-treated TG mice. Further evidence of cholestasis in CA treated TG mice was the induction of BA efflux transporter *Bsep* and down-regulation of uptake transporter *Ntcp*. The TG mice may have been more predisposed to CA induced injury as basal expression of *Bsep* in TG mice was 0.32 +/- 0.07 (SD) fold of that of WT mice.

Co-treatment of CA and CCl_4 likely induced cholestasis due to additive toxicity to hepatocytes. In hepatocytes CCl_4 is metabolized to a toxic carbocation which leads to lipid peroxidation and cell death.[209] Hepatocytes serve as the shuttle for BAs from the serum into bile. Therefore, CCl_4 induced hepatocyte death would lead to compromised ability of the liver to transport BAs out of the serum and into bile. The accumulated BAs could then reach a threshold of toxicity enhancing liver injury.

As mentioned in the Results section, the presence of cholestasis in the CA treated WT and TG mice confounds the interpretation of the effects of BAs and FGF15 on CCl_4 induced inflammatory and fibrotic endpoints. Therefore, CA treated mice were excluded from subsequent analyses regarding these endpoints. Even without the data from CA treated mice, the combination of the three genotypes and cholestyramine diet allowed for the dissociation of BA levels from expression of FGF15. This permitted the

determination of the BA dependent and independent effects of FGF15 on CCl_4 induced hepatic inflammation and fibrosis.

Genotype but not diet affected the severity of CCl_4 induced centrilobular necrosis

In the CCl_4 model of fibrosis, CCl_4 treatment acutely causes centrilobular necrosis. After chronic treatment with CCl_4, the severity of necrosis induced by CCl_4 decreases due to liver adaptation. No centrilobular necrosis was observed in the WT mice treated with chronic CCl_4 in our study. On the contrary, centrilobular necrosis was observed in both KO and TG mice treated with CCl_4. The effects of FGF15 deficiency on necrosis were independent of TBAP size as cholestyramine had no effect on frequency or severity of necrosis. FGF15 has been previously shown to be a regulator of hepatic rengeneration.[195, 196] Hence, we hypothesize that the necrosis in the KO mice was resultant of impaired hepatic regeneration. Both KO and TG mice had worsened CCl_4 induced inflammation compared to WT. It is hard to determine if the worsened inflammation is secondary to increases in necrosis or vice versa. Therefore, it is also possible that the increased centrilobular necrosis in KO and TG mice was the consequence of increased inflammation.

FGF15 and BAs affect the severity of CCl_4 induced inflammation

The severity of inflammation caused by CCl_4 treatment was increased by both FGF15 deficiency and overexpression. Observed histologically, CCl_4 caused only mild inflammation in two of nine WT mice. Conversely, CCl_4 treatment led to mild or moderate inflammation in eight of nine KO mice and all treated TG mice. Furthermore, cholestyramine diet worsened inflammation in WT and KO mice evident histologically and through increased expression of inflammatory mediators. It has been previously reported that FXR activation mitigates hepatic inflammation.[124, 127, 129-131] Moreover,

activation of FGFR4 by FGF15 has also been shown to reduce NFκB signaling.[151] This was also demonstrated in our treatments of LX-2 cells with FGF19. We hypothesize that both FXR activation and FGF15-FGFR antagonism of NFκB were responsible for the differences in hepatic inflammation. As WT mice have basal levels of both BAs and FGF15, they may have been protected from hepatic inflammation by both FXR and FGFR signaling. TG mice may have enhanced FGF15-FGFR antagonism of NFκB signaling, however, would have mitigated protection offered by BA signaling. KO mice would benefit from enhanced anti-inflammatory FXR signaling but not that of the FGF15-FGFR pathway.

FGF15 affects hepatic fibrogenesis by modulating BA homeostasis and subsequently hepatic FXR activity

Contrasting to previous reports, KO mice were not protected from CCl_4 induced fibrosis.[72] This may be the result of difference in CCl_4 dose as the dose in the previous study was half that used in our study. This discrepancy may also be resultant of differences in *Ctgf* expression between our studies. In the previous study, FGF15 deficiency was found to be protective against fibrosis by mitigating inductions of hepatocyte derived CTGF. In our study, *in vitro* treatment of HepG2 cells did not induce *CTGF* expression nor did we observe alterations in *Ctgf* expression in either KO or TG mice.

The severity of fibrosis in KO and TG, but not WT, mice was dependent upon TBAP size and *Shp* expression in the liver. In agreement with our previous report using FGF15 deficient mice in a HFD model of NASH, untreated KO mice had lower levels of collagen in the liver evident by Sirius Red staining.[149] Cholestyramine treatment raised the collagen levels in KO mice back to levels comparable to WT. In WT mice cholestyramine did not affect collagen levels. Similarly, cholestyramine treatment alone

increased fibrosis histology scores in KO but not WT mice. When given with CCl_4, cholestyramine increased fibrosis only in KO mice. Regression analysis was performed comparing Sirius Red staining and *Col1α1* expression to TBAP size and *Shp* expression in the liver. In WT mice, the extent of Sirius Red staining and expression of *Col1α1* were not correlated with TBAP or *Shp* expression. However in KO and TG mice, both Sirius Red staining and *Col1α1* were inversely correlated with TBAP size and hepatic *Shp* expression. The regression lines comparing *Shp* expression to Sirius Red staining and *Col1α1* expression in KO and TG mice were similar to each other as well as to the regression line for all genotypes analyzed together. The range of *Shp* expression in WT mice was much narrower than in KO and TG mice. Therefore, the lack of correlation between these comparators in WT mice may be due to tighter regulation of homeostatic BA levels, FXR activity, and expression of *Shp*.

Though in our study, FGF15 deficiency was not protective against CCl_4 induced fibrosis, our findings indicate that one of the mechanism by which FGF15 deficiency affects hepatic fibrogeneis is via alterations in BA homeostasis and subsequently alterations in FXR activity in the liver. This is aligned with the body of literature which states that FXR activation in HSCs reduces ECM production and mitigates HSC responsiveness to profibrotic signals such as TGFβ and thrombin.[61, 62]

4.6 SUMMARY

We were able to dissociate TBAP size from the expression of *Fgf15* by feeding FGF15 deficient and overexpressing mice diets containing either cholestyramine or CA. This enabled us to determine the BA dependent and independent effects of FGF15 in a CCl_4 model of hepatic fibrosis. FGF15 deficient mice had increased CCl_4 induced necrosis that was not dependent on BA levels. This further highlights the known role of FGF15 as a regenerative factor in the liver. In our hands, FGF15 deficiency did not

protect against CCl_4 induced fibrosis. However, we found that FGF15 affects both hepatic fibrogenesis, as well as inflammation, in a BA dependent manner. Furthermore, these effects were correlated to hepatic *Shp* expression. Together these findings support that FGF15 could affect hepatic inflammation and fibrosis development indirectly by regulating TBAP size and subsequently FXR activation in the liver.

FIGURES

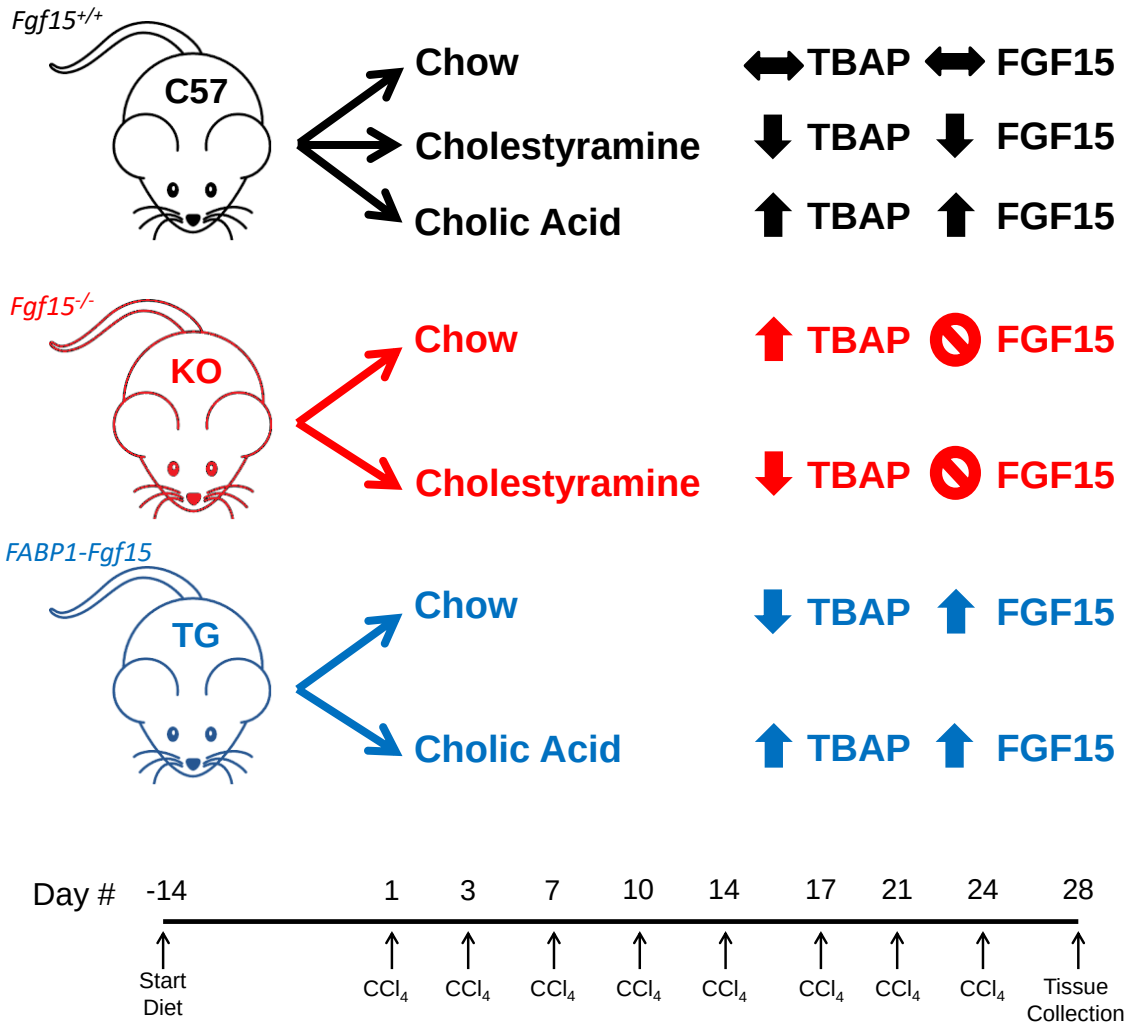

Figure 4.1. *Overview of experimental design.* The three genotypes of mice assigned to the indicated diets to create multiple combinations of TBAP size and FGF15 activity.

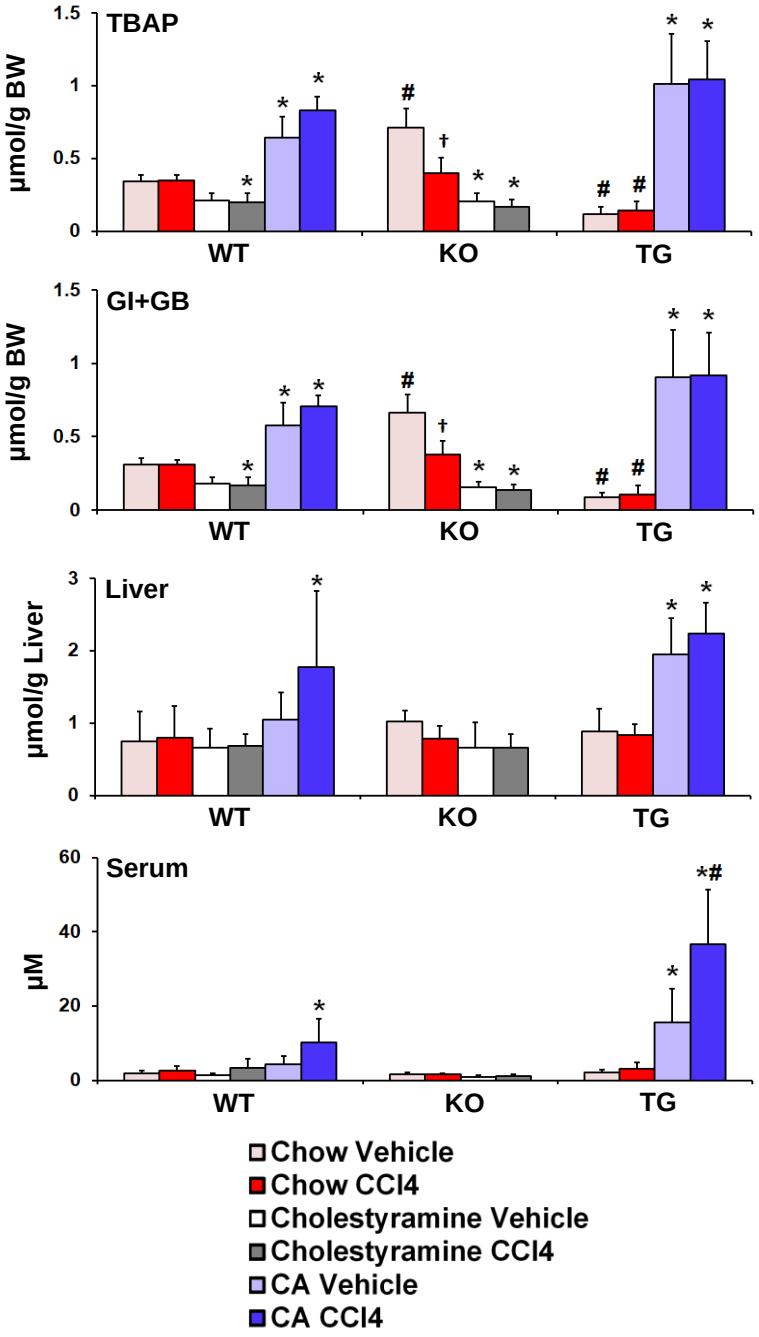

Figure 4.2. *Effect of genotype, diets, and CCl_4 treatment on TBAP size.* Data presented as mean plus SD. Data analyzed by 3-Way ANOVA followed by post-hoc Tukey's HSD. * = significant across diet; # = significant across genotype; † = significant across CCl_4 treatment ($p \leq 0.05$).

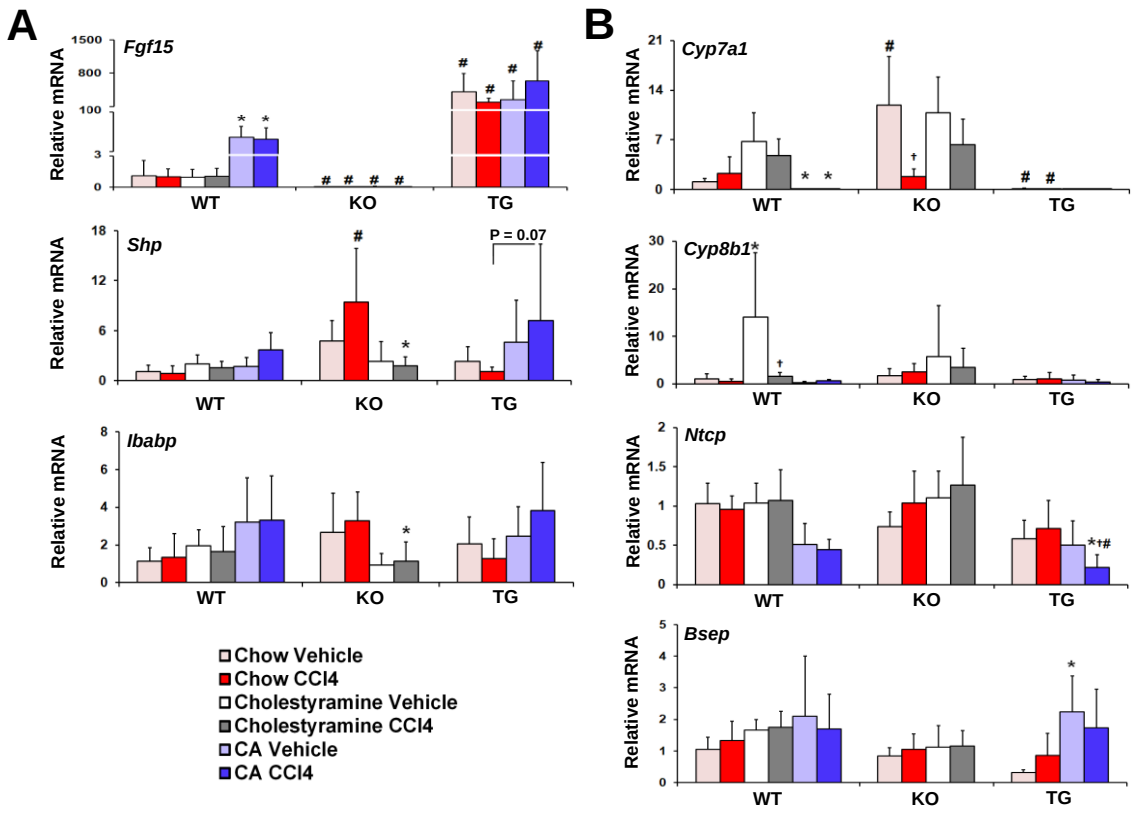

Figure 4.3. *Effect of genotype, diet, and CCl_4 treatment on expression of genes involved in BA homeostasis.* (A) Expression of FXR target genes, *Fgf15*, *Shp*, and *Ibabp*, was measured in the ileum. (B) Expression of genes regulating BA synthesis, *Cyp7a1* and *Cyp8b1*, and BA transport, *Ntcp* and *Bsep*, was measured in the liver. Data presented as mean plus SD. Data analyzed by 3-Way ANOVA followed by post-hoc Tukey's HSD. * = significant across diet; # = significant across genotype; † = significant across CCl_4 treatment ($p \leq 0.05$).

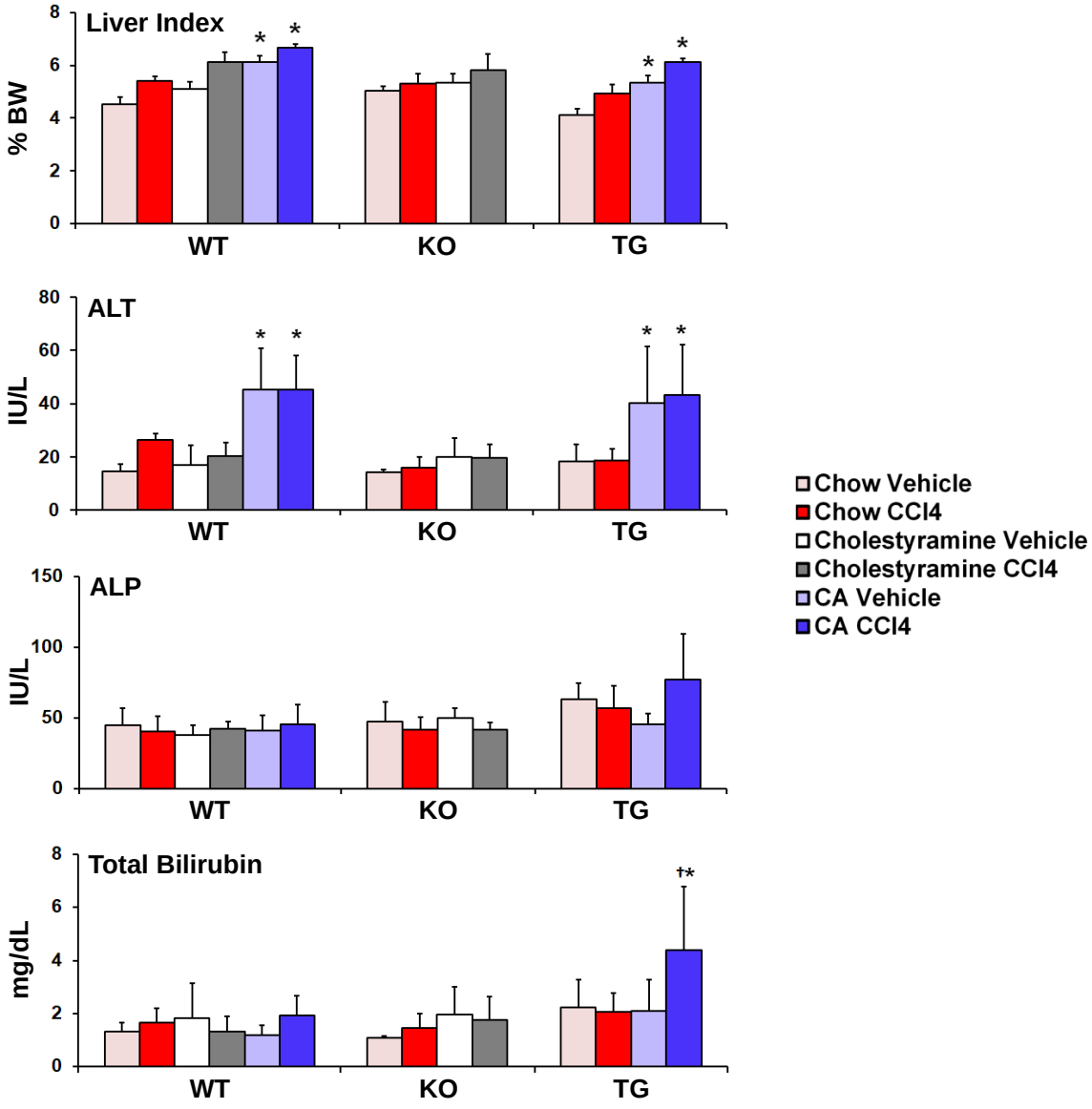

Figure 4.4. *Effect of genotype, diet, and CCl_4 treatment on indicators of liver injury.* Serum biomarkers of liver injury were measured and liver index calculated. Data presented as mean plus SD. Data were analyzed by 3-Way ANOVA followed by post-hoc Tukey's HSD. * = significant across diet; # = significant across genotype; † = significant across CCl_4 treatment ($p \leq 0.05$).

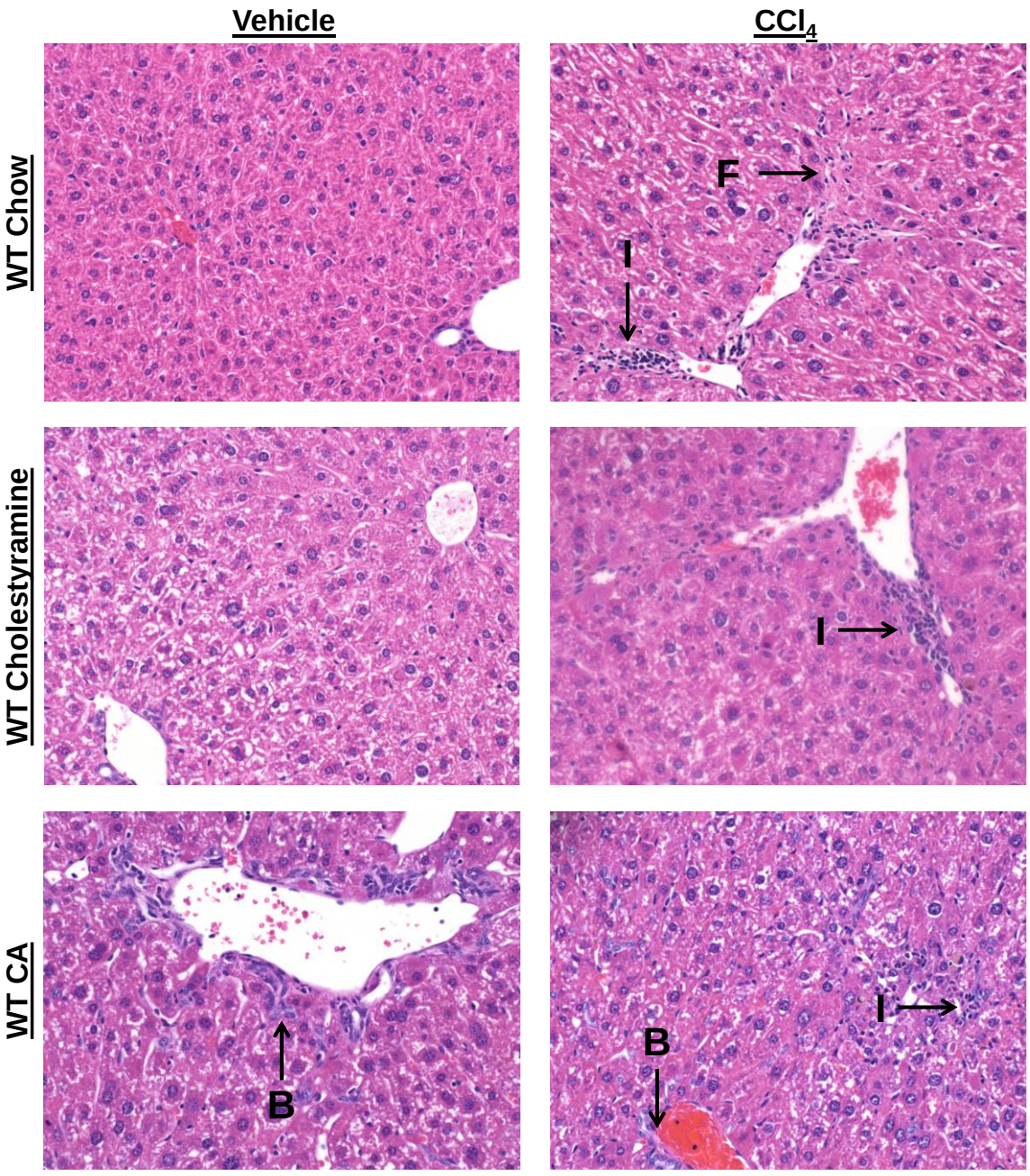

Figure 4.5. *Representative liver sections from WT animals stained with H&E and imaged at 200x magnification.* Arrows within images point to histologic findings; B = Biliary hyperplasia, F = Fibrosis, I = Inflammation.

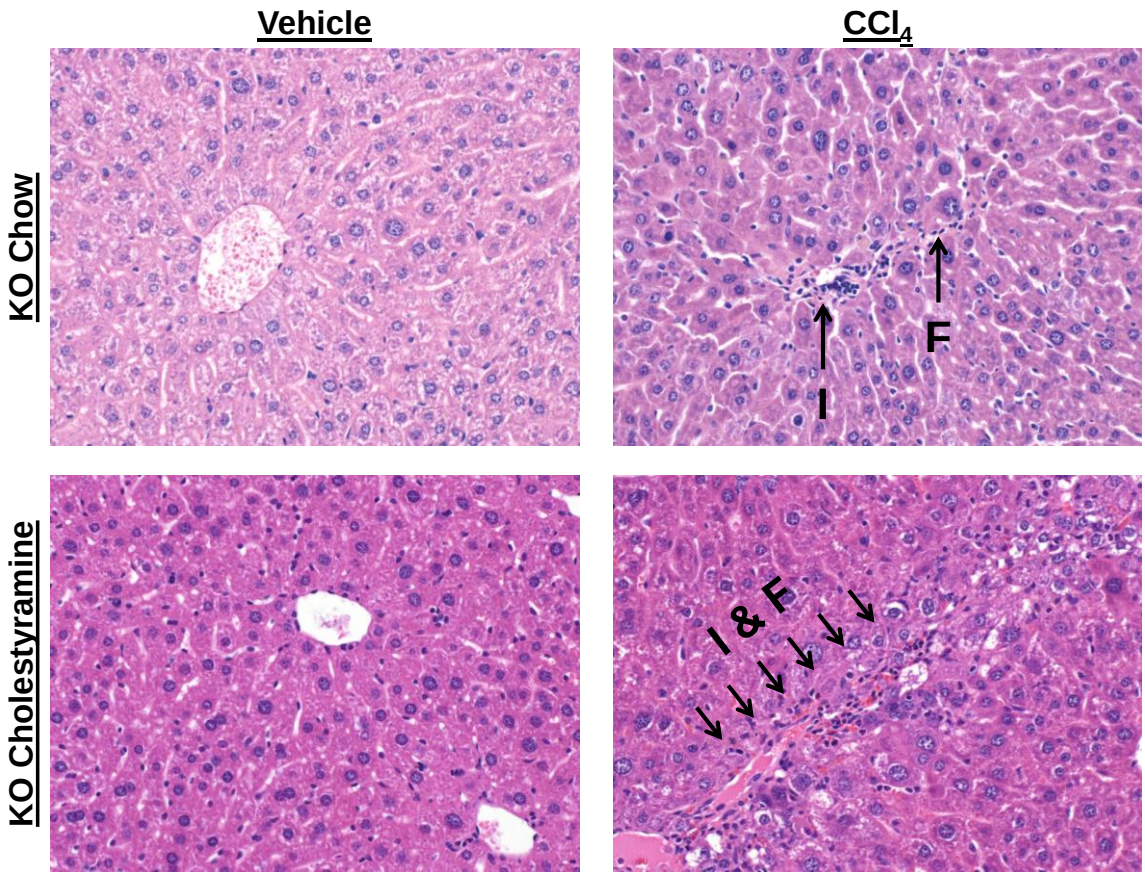

Figure 4.6. *Representative liver sections from KO animals stained with H&E and imaged at 200x magnification.* Arrows within images point to histologic findings; B = Biliary hyperplasia, F = Fibrosis, I = Inflammation.

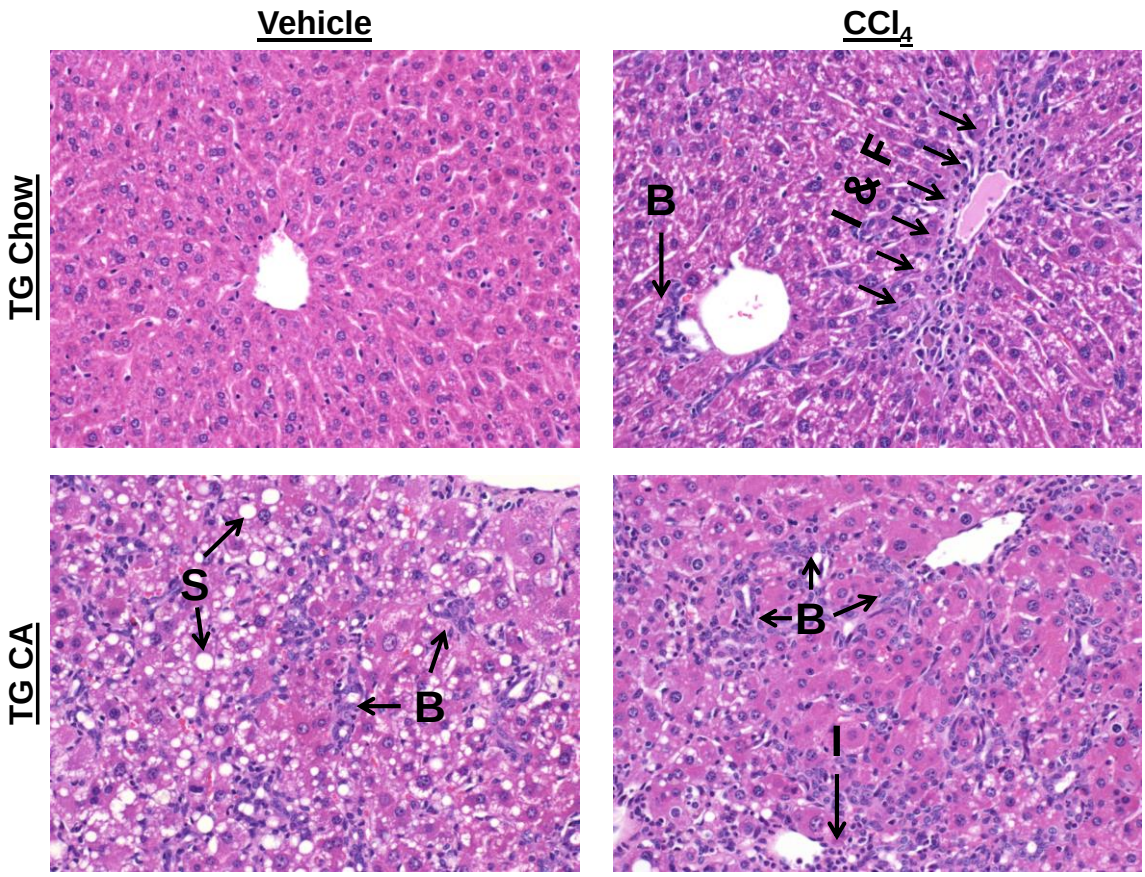

Figure 4.7. *Representative liver sections from TG animals stained with H&E and imaged at 200x magnification.* Arrows within images point to histologic findings; B = Biliary hyperplasia, F = Fibrosis, I = Inflammation, S = Steatosis.

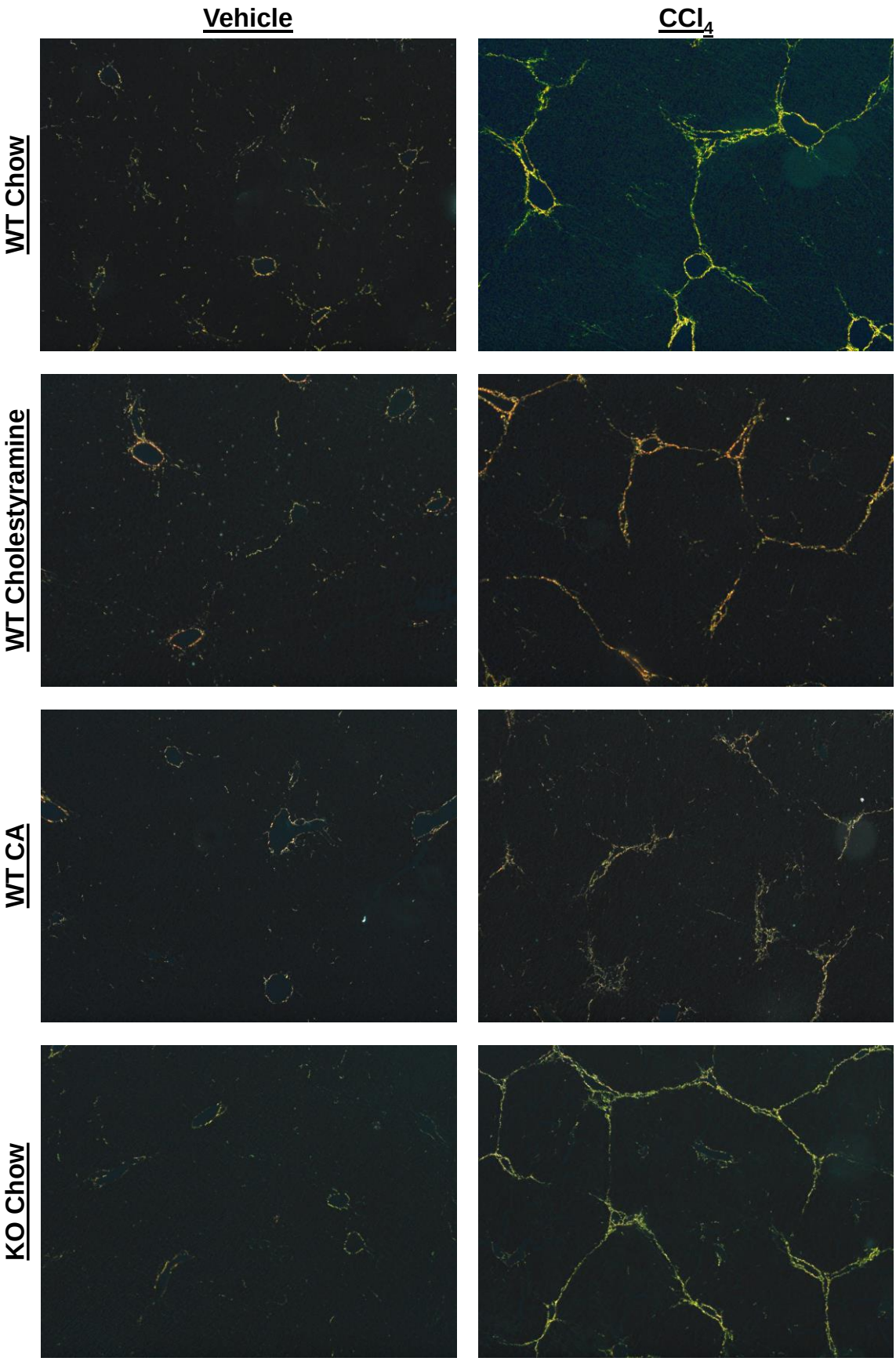
Vehicle
CCl4
WT Chow
WT Cholestyramine
WT CA
KO Chow

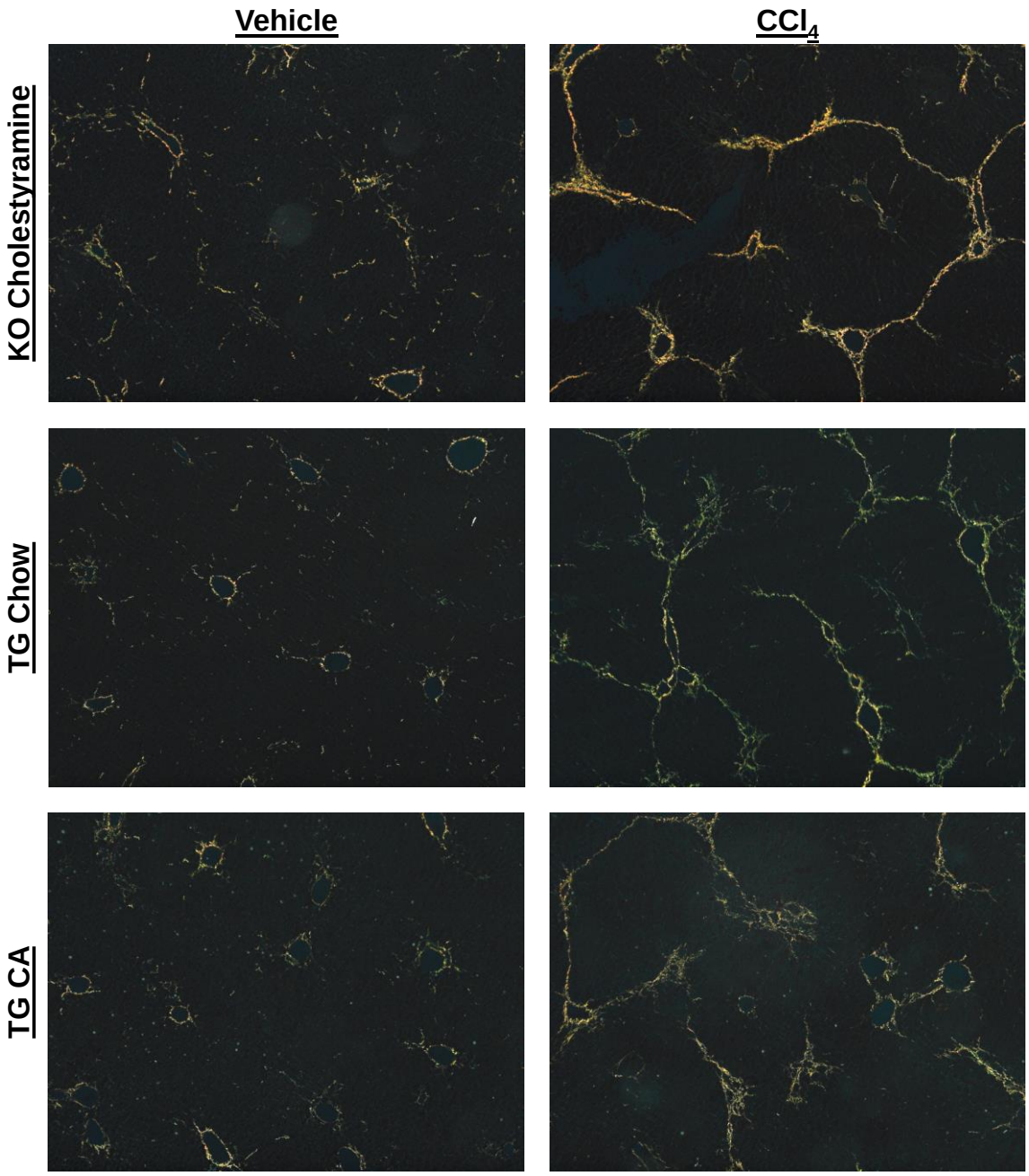

Figure 4.8. *Representative polarized images of sections stained with Sirius Red.*

Images taken at 100x magnification.

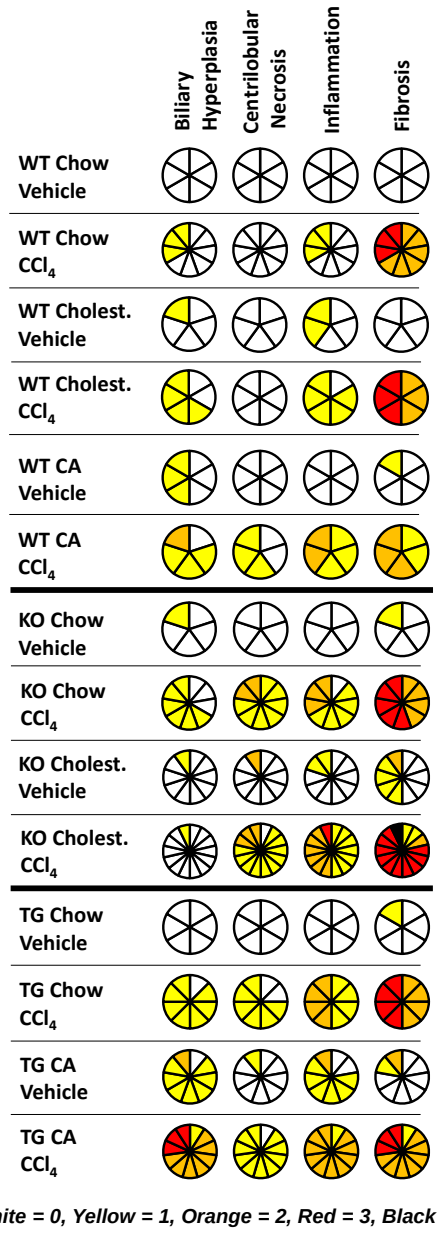

Figure 4.9. *Histology scores from H&E stained liver sections.* Sections were scored for severity of biliary hyperplasia, centrilobular necrosis, inflammation, and fibrosis. Data are presented as histology pies. Each pie is divided into slices equal to the number of mice comprising the group. Slices were colored according to histology score; white = 0, yellow = 1, orange = 2, red = 3, black = 4. Hyperplasia, centrilobular necrosis, and inflammation were scored from 0 to 3 whereas fibrosis was scored from 0 to 4.

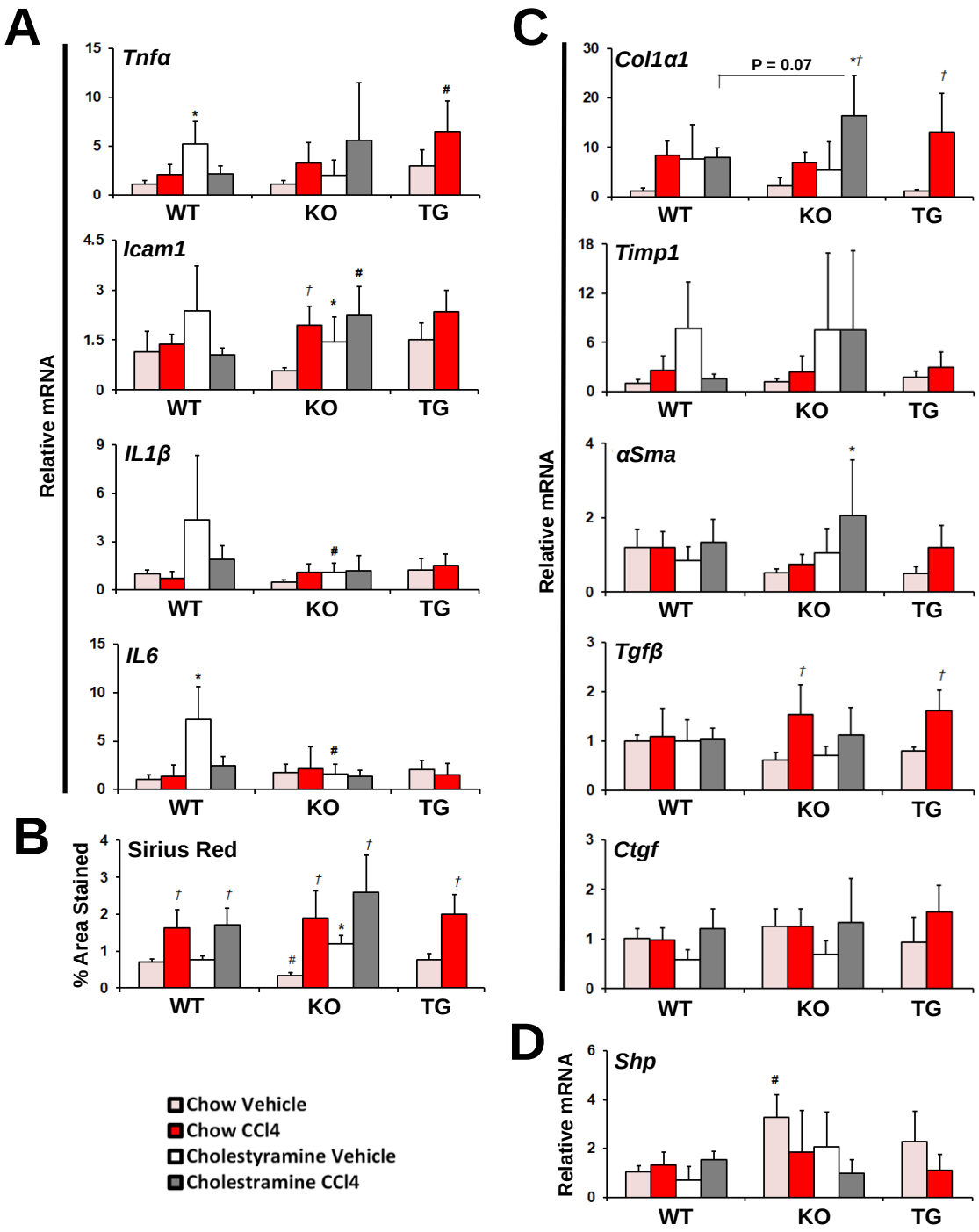

Figure 4.10. *Effect of genotype, diet, and CCl_4 treatment on hepatic inflammation and fibrosis.* (A) Expression of inflammatory mediators, *Tnfα*, *Icam1*, *Il1β*, and *Il6*, was measured. (B) The area stained in liver sections by Sirius Red was determined. (C)

Expression of fibrotic mediators *Col1α1*, *Timp1*, *αSma*, *Tgfβ*, and *Ctgf* and (D) FXR target gene was measured. Data presented as mean plus SD. Data were analyzed by 3-Way ANOVA followed by post-hoc Tukey's HSD. * = significant across diet; # = significant across genotype; † = significant across CCl_4 treatment ($p \leq 0.05$).

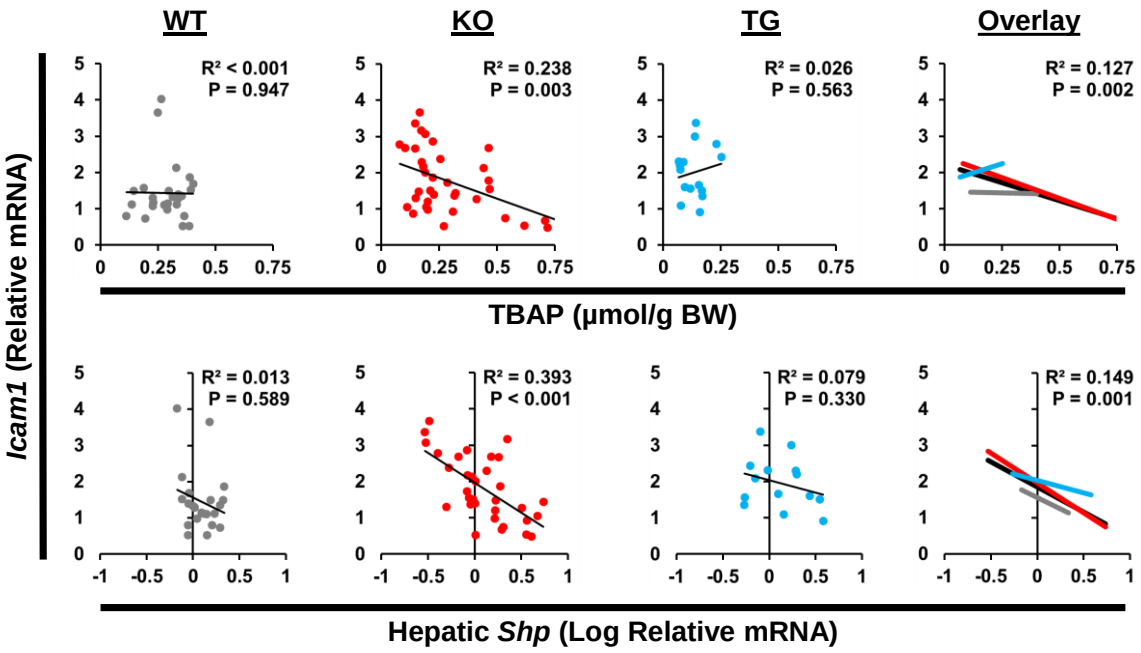

Figure 4.11. *Correlation of Icam1 expression to TBAP size and hepatic Shp expression.* Expression of hepatic *Shp* was logarithmically transformed. Data were analyzed using simple linear regression and F-test. Analyses were performed classified by genotype. Resulting R^2 and P-values are present on each respective graph. In the overlay graph, the lines of best fit from each genotype were overlaid. The overlay graph also contains the line of best fit (black regression line), R^2, and P-value for the entire dataset when analyzed across all genotypes.

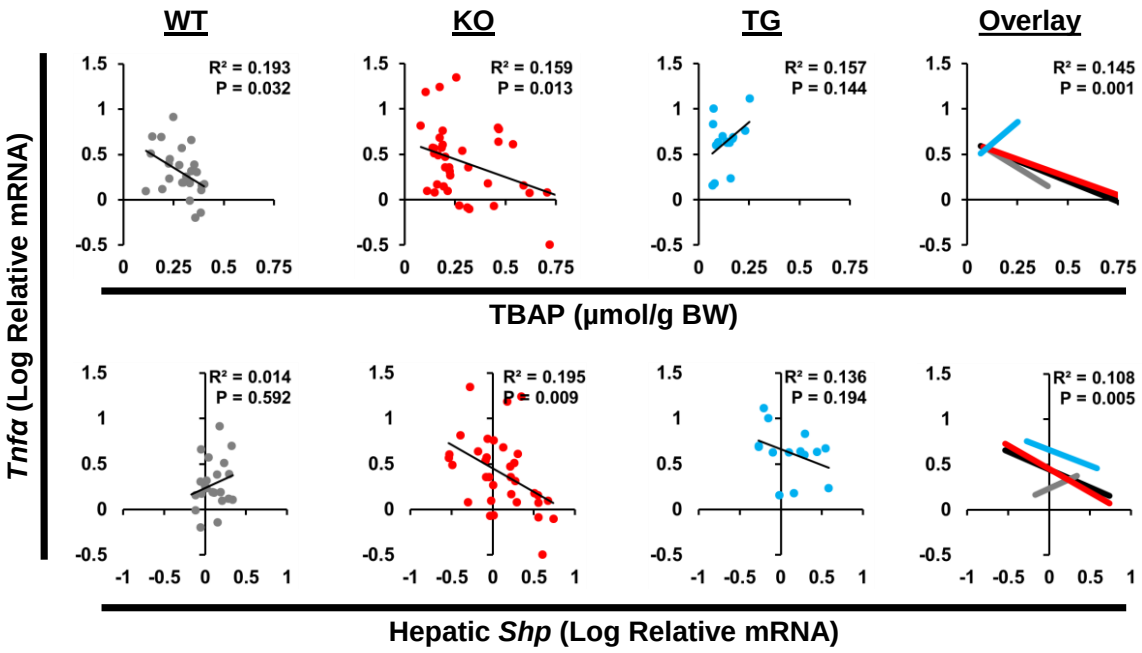

Figure 4.12. *Correlation of Tnfα expression to TBAP size and hepatic Shp expression.* Expression of hepatic *Shp* was logarithmically transformed. Data were analyzed using simple linear regression and F-test. Analyses were performed classified by genotype. Resulting R^2 and P-values are present on each respective graph. In the overlay graph, the lines of best fit from each genotype were overlaid. The overlay graph also contains the line of best fit (black regression line), R^2, and P-value for the entire dataset when analyzed across all genotypes.

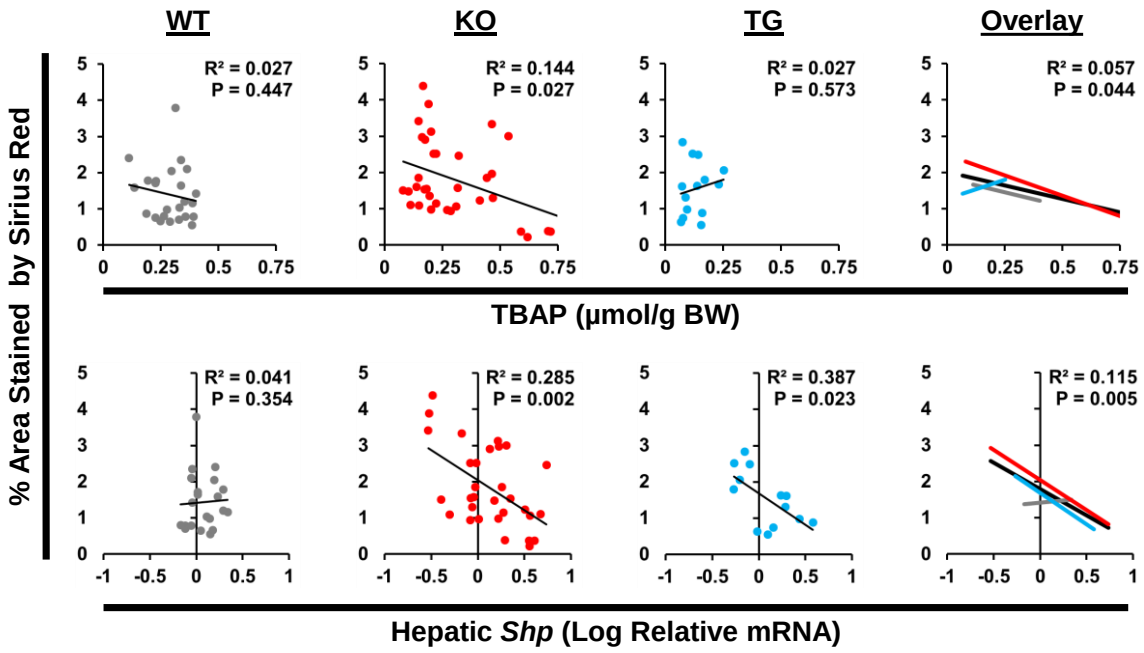

Figure 4.13. *Correlation of Sirius Red staining to TBAP size and hepatic Shp expression.* Expression of hepatic *Shp* was logarithmically transformed. Data were analyzed using simple linear regression and F-test. Analyses were performed classified by genotype. Resulting R^2 and P-values are present on each respective graph. In the overlay graph, the lines of best fit from each genotype were overlaid. The overlay graph also contains the line of best fit (black regression line), R^2, and P-value for the entire dataset when analyzed across all genotypes.

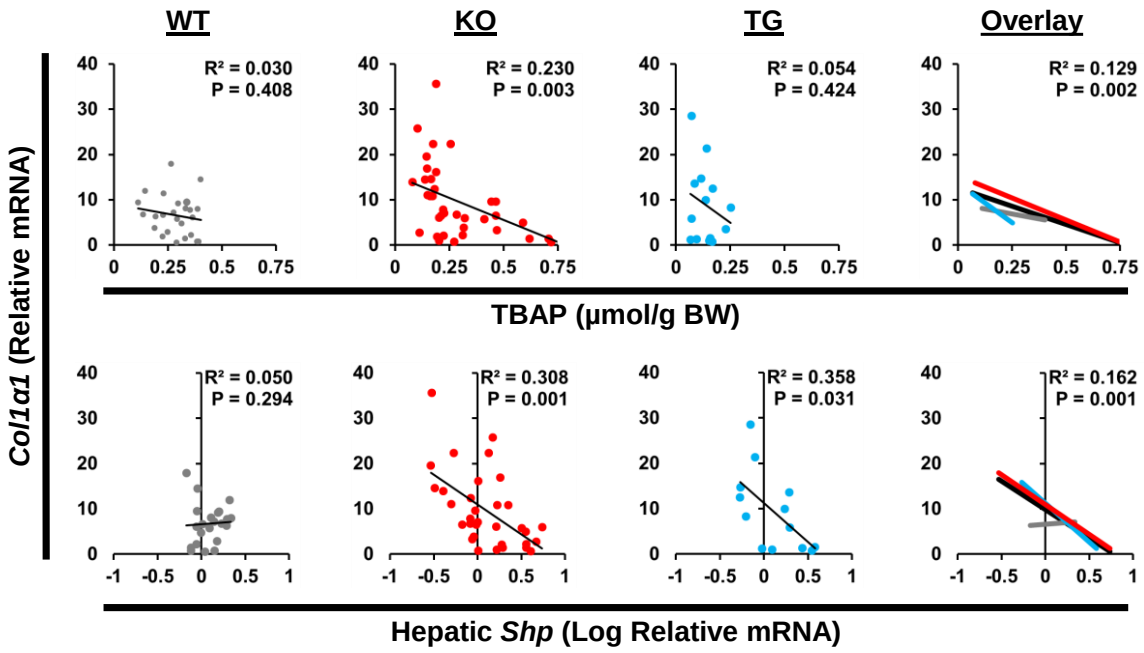

Figure 4.14. *Correlation of Col1α1 expression to TBAP size and hepatic and ileal Shp expression.* Expression of hepatic *Shp* was logarithmically transformed. Data were analyzed using simple linear regression and F-test. Analyses were performed classified by genotype. Resulting R^2 and P-values are present on each respective graph. In the overlay graph, the lines of best fit from each genotype were overlaid. The overlay graph also contains the line of best fit (black regression line), R^2, and P-value for the entire dataset when analyzed across all genotypes.

TABLES

Gene	Sense	Antisense
Bsep	CTGCCAAGGATGCTAATGCA	CGATGGCTACCCTTTGCTTCT
Col1α1	GAGAGAGCATGACCGATGGATT	TGTAGGCTACGCTGTTCTTGCA
Ctgf	GGCCTCTTCTGCGATTTCG	CCATCTTTGGCAGTGCACACT
Cyp7a1	AACAACCTGCCAGTACTAGATAGC	GTGTAGAGTGAAGTCCTCCTTAGC
Cyp8b1	AGTACACATGGACCCCGACATC	GGGTGCCATCCGGGTTGAG
Fgf15	GCCATCAAGGACGTCAGCA	CTTCCTCCGAGTAGCGAATCAG
Ibabp	CCCCAACTATCACCAGACTTC	ACATCCCCGATGGTGGAGAT
Icam1	CAGTCCGCTGTGCTTTGAGA	CGGAAACGAATACACGGTGAT
Il1β	AAGGGCTGCTTCCAAACCTTTGAC	ATACTGCCTGCCTGAAGCTCTTGT
Il6	ATCCAGTTGCCTTCTTGGGACTGA	TAAGCCTCCGACTTGTGAAGTGGT
Ntcp	GGCCACAGACACTGCGCT	AGTGAGCCTTGATCTTGCTGAACT
Shp	CGATCCTCTTCAACCCAGATG	AGGGCTCCAAGACTTCACACA
Tgfβ	TTGCCCTCTACAACCAACACAA	GGCTTGCGACCCACGTAGTA
Timp1	CCTTGCAAACTGGAGAGTGACA	AGGCAAAGTGATCGCTCTGGT
Tnfα	ACAAGGCTGCCCCGACTAC	TTTCTCCTGGTATGAGATAGCAAATC
αSma	CCTGACGGGCAGGTGATC	ATGAAAGATGGCTGGAAGAGAGTCT
β-*Actin*	GCGTGACATCAAAGAGAAGC	CTCGTTGCCAATAGTGATGAC

Table 4.1. *List of primers used in Chapter 4.*

CHAPTER 5:

DISCUSSION

AND

FUTURE DIRECTIONS

5.1 CONTRIBUTION TO THE FIELD OF RESEARCH

NAFLD has become one of the biggest medical burdens in the US with NASH and NASH associated liver fibrosis emerging to be the critical turning point for liver injury. The overarching aim of the research described in this dissertation is to determine how FGF15 and FGF19, important signal mediators of bile acid homeostasis, affect the development of NASH and hepatic fibrosis.

At the time the research in Chapter 2 was performed, the effects of FGF15/19 on hepatic steatosis, inflammation, and metabolic endpoints were only shown in gain-of-function studies using FGF19 overexpressing transgenic mice.[146] These studies focused on metabolic endpoints rather than NASH. Therefore, the role of FGF15/19 in the development of NASH was investigated by performing a loss-of-function study using FGF15 deficient mice and a HFD induced NASH model. Based upon previous gain-of-function studies with FGF19, we hypothesized that FGF15 deficiency would increase liver steatosis, inflammation, and metabolic syndrome. In addition, steatosis and inflammation in the liver is positively associated with hepatic fibrosis, therefore it was also hypothesized that FGF15 deficient mice would manifest increased hepatic fibrosis. As expected, *Fgf15*$^{-/-}$ mice showed characteristics of metabolic syndrome, including insulin resistance, obesity, and high lipid levels, as well as increased hepatic steatosis and a trend for increased inflammation. However, contrary to our hypothesis, *Fgf15*$^{-/-}$ were protected against NASH-associated liver fibrosis, suggesting that FGF15/19 may contribute to hepatic fibrosis development. An FGF19 analog protein and FXR agonists, which highly induce the expression of FGF19, are currently in human clinical trials for the treatment of cholestasis and NASH, our study raises a concern that these novel therapies may detrimentally affect fibrosis in NASH patients and that each patient needs to be thoroughly evaluated for their hepatic/biliary functions, bile acid profile and FXR

activities before administering these medications for the treatment of cholestasis or NASH.

The research in Chapters 3 and 4 was designed and conducted to identify the mechanisms by which FGF15 deficiency decreases hepatic fibrogenesis. This was of importance as it may determine to what degree the findings in our HFD-induced NASH study are clinically relevant and a potential safety signal to monitor for in relevant clinical trials. We hypothesized that FGF15 may regulate liver fibrogenesis by two mechanisms: (1) by directly acting as a profibrotic mediator to HSCs, and (2) decreasing FXR activity in HSCs by reducing TBAP size. In Chapter 3, it was determined that FGF19 can activate FGFRs in the human HSC line LX-2, however, contrary to our hypothesis, FGF19 did not increase HSC activation or proliferation. Additionally, by increasing IκBα, FGF19 treatment lowered the expression of pro-inflammatory cytokines. This finding further supports a previously published study that reported FGF19 decreases NFκB signaling in prostate cancer cells.[151] Furthermore, in a Phase II clinical trial, an FGF19 analog protein strongly decreased hepatic inflammation in NASH patients.[183] Our findings indicate that one of the mechanisms which may underlie the anti-inflammatory properties of the FGF19 analog protein may be through reduction in NFκB signaling in HSCs.

In addition to HFD-induced NASH fibrosis, CCl_4-induced liver fibrosis is also a well-established animal model to study fibrogenesis. The role of FGF15 in liver fibrosis was further determined in this chemically induced liver injury model in Chapter 4. In this study, CCl_4-induced liver fibrosis was not altered by deficiency or overexpression of FGF15. We demonstrated that FGF15-mediated regulation of hepatic fibrosis occurs in a TBAP size-dependent manner. When considered together, the findings from Chapters 3 and 4 indicate that it is unlikely that FGF15 and FGF19 function as profibrotic mediators. Therefore, the safety concern raised by Chapter 2 that FGF15 and FGF19

may increase fibrosis in NASH patients is likely invalid. In agreement, clinical trials with the FGF19 analog protein and FXR agonists have demonstrated decreased severity of fibrosis in non-cirrhotic NASH patients after treatment.[169, 181] BAs and FXR signaling are proposed key mediators in mitigating the development of hepatic fibrosis and these findings in Chapter 5 provide more evidence supporting the use of FXR agonists to mitigate the development of hepatic fibrosis. However, we acknowledge that further studies of FGF15/19 in fibrosis need to be designed as liver injury-induced fibrosis by NASH and chemicals may have differential underlying mechanisms.

In animal models and human clinical trials, FGF19 decreased the severity of steatosis, inflammation, and metabolic syndrome. Overall, it is hypothesized that by strongly decreasing steatosis and inflammation, FGF19 mimetics will prevent or halt the progression fibrosis. Should pre-existing fibrosis levels be below the threshold of irreversibility, FGF19 analog therapy may allow for the reversal of fibrosis by removal of upstream injury and profibrotic mediator release. In fact, the ability of an FGF19 analog protein, NGM282, to reduce fibrosis in non-cirrhotic NASH patients has already been shown.[181] It is warranted to state that FGF19 therapy may not reduce fibrosis severity should pre-treatment fibrosis severity be beyond the threshold of irreversibility. In addition to effects on fibrosis, a secondary benefit of FGF19 analog therapy would be effects on concomitant conditions, as the majority of NASH patients are obese and have metabolic syndrome. In a Phase II study, NGM282 was shown to reduce body weights, BMI, and insulin resistance.[181]

As with FGF19 analog therapy, it can be hypothesized that FXR agonists will prevent and halt fibrosis progression in NASH patients by reducing steatosis and inflammation. However, unlike FGF19 analogs, FXR agonists may also reverse fibrosis severity even in patients past the threshold of otherwise irreversible fibrosis by activating FXR in HSCs. Directly pertaining to this matter, two Phase III trials investigating OCA

for the treatment of NASH are currently recruiting patients; one trial with non-cirrhotic NASH patients (REGENERATE trial) and one trial with cirrhotic NASH patients (REVERSE trial).[170, 171] The largest barriers facing the development of FXR agonists are potential cardiovascular and carcinogenetic risks. As described in section 1.5.3, the approval of FXR agonists for the treatment of NASH will likely be a risk-to-benefit decision. The risks of cardiovascular and carcinogenicity considered against efficacy in NASH and lack of any approved therapeutic agent to treat NASH. Lastly, NASH also predisposes patients to HCC, and therefore potential carcinogenicity of FXR agonists must also be weighed against HCC risk or additive effects in NASH.

5.2 STUDY LIMITATIONS AND POTENTIAL FUTURE DIRECTIONS

Several study design limitations were present in the research described in Chapters 2, 3, and 4. Based upon these limitations and gaps in the literature, there are several avenues for potential future studies to follow. These design limitations, data gaps, and potential future directions are described below.

We aimed to determine how FGF15 deficiency would affect the development of NASH. During study design, it was hypothesized that FGF15 deficiency would increase steatosis, inflammation, and metabolic syndrome. For this reason and the association of metabolic syndrome and NASH in patient populations, we used a mouse model that results in both NASH and metabolic syndrome. This being a long term HFD feeding model. A limitation of this model is that mice are naturally resistant against HFD induced fibrosis. During study design, we did not anticipate the strongest findings of our study to pertain to fibrosis and therefore proceeded to use the HFD model. As expected, the severity of fibrosis in our WT mice was low. Despite this limitation, we were still able to observe mitigated fibrosis in *Fgf15*$^{-/-}$ mice.

In Chapter 3, we investigated the direct effect of FGF19 treatment on HSC function and proliferation. As FGF15 and FGF19 share only 50% sequence homology, it

was of importance to match the species origin of the HSCs with the correct ortholog of FGF15 or FGF19. For greater human relevance, we selected the human HSC cell line LX-2 and FGF19 for our study. The first limitation of this study was that LX-2 cells are not quiescent, and they express both markers of a quiescent and activated HSC. LX-2 cells are a tool that allows for the determination if a particular treatment can alter the expression of particle genes, such as collagens, in HSCs. However, it is difficult to extrapolate if a certain treatment can induce a phenotypic switch as the cells were not quiescent to begin with. There is currently no HSC cell line that is quiescent. In order to best study phenotypic switch in HSCs one must use primary HSCs. Therefore, one future direction of research could be to repeat the study using primary isolated human HSCs. Unfortunately, primary HSCs transdifferentiate into an activated phenotype once removed from the body. Depending upon isolation technique and time since isolation, there can be variation in baseline activation of the primary cells. Therefore, there is currently no ideal model to study HSC phenotypic switch *in vitro*. To overcome limitations of *in vitro* HSC studies, future *in vivo* studies could be used to elucidate the effect of FGF19 on HSC phenotype via primary isolation of HSCs from FGF15 deficient or overexpressing mice without subsequent culture. Another limitation of our study design was that our focus was on how FGF19 affects only a portion of the known functions of HSCs. As cDNA and protein samples from treated LX-2 cells are already available, additional RT-qPCR or Western blot can be performed targeting genes and proteins involved in functions not yet studied, including but not limited to: vitamin A homeostasis, vasoregulation, and contractility. Microarray analysis could also be performed to broaden our investigation to many other functions. Instead of using LX-2 cells, the microarray could be performed on the previously proposed primary isolated HSCs from FGF15 deficient or overexpressing mice.

Another design limitation of our *in vitro* study was the use of TGFβ as a positive control for HSC activation. Though TGFβ activates HSC strongly, it does so through signaling pathways not shared with FGFR. Therefore, a factor that activates the same receptor may serve as a more relevant positive control. Unlike TGFβ, FGF2 activates the same receptors as FGF19, although with heparin sulfate as a co-factor rather than obligate co-receptor βKL. FGF2 has been previously reported to increase *Col1α1* and *αSma* expression in primary isolated rat HSCs and increase proliferation of LX-2 cells.[73, 77] Use of FGF2 as a positive control would therefore increase the confidence in our findings that FGF19 does not serve as a profibrotic mediator or mitogen to HSCs.

In Chapter 3, we demonstrated that FGF19 reduces NFκB signaling in LX-2 cells. The ability of FGF19 to reduce NFκB activation was also reported in the prostate cancer cell line DU-145.[151] It would be of great interest to observe if and how FGF19 alters the phenotype of macrophages. Macrophages are abundantly present in the liver, are shown to express FGFRs and βKL, and are an important cell type involved in liver inflammation and fibrosis.[210, 211] This could provide insight into the mechanisms by which FGF19 affects hepatic inflammation and fibrosis, and even inflammation in other organs.

In Chapter 4, we sought to determine the BA dependent and independent mechanisms by which FGF15 affects the development of hepatic fibrosis. In this study, a well-established CCl_4 hepatic fibrosis model was used. This model was selected as it was already published in the literature that FGF15 deficiency was protective against CCl_4 induced fibrosis.[72] A major limitation of the CCl_4 model of fibrosis is that it involves hepatocellular necrosis, inflammation, and fibrosis, thus the underlying mechanisms leading to liver fibrosis may be different from NASH-associated fibrosis. Additionally, FGF15 has been shown to regulate hepatocellular regeneration and inflammation.[149, 151, 183, 195, 196] Therefore, FGF15 can potentially affect the severity of each step in the critical

path of CCl_4 toxicity and thereby alter overall liver injury by many means. To overcome this challenge, we assessed the effects of genotype and diet on liver necrosis and inflammation. These effects were then considered when interpreting fibrosis severity.

An initially unforeseen limitation of our study design in Chapter 4 was that CA diet in combination with CCl_4 treatment induced cholestasis. A potential future study could be to repeat the study in FGF15 transgenic mice and replace the use of CA with a non-BA FXR agonist such as GW4064. The use of GW4064 instead of CA would increase FXR activity in transgenic mice while potentially avoiding cholestasis.

FGF19 signaling shifts BA synthesis away from the classical pathway towards the alternative pathway and thus changes the composition of the TBAP.[212] In mice, the alternative pathway leads to the production of the FXR antagonist MCA, whereas in humans the alternative pathway leads to the production of the FXR agonist CDCA.[213] Therefore, one must be careful when interpreting the human relevance of BA mediated effects in mouse models. In Chapter 4, we did not assess the composition of the TBAP, and therefore effects on fibrosis and inflammation were correlated to TBAP size and not to individual BA species. To aid in the cross species interpretation of BA mediated effects, profiling of the composition of the TBAP can be performed.

5.3 SUMMARY

In closing, our studies demonstrated that FGF15 deficiency is protective against hepatic fibrogenesis during the development of NASH. FGF15 and FGF19 do not appear to function as profibrotic mediators in the liver. Instead, FGF15 deficiency alters hepatic fibrogenesis via alterations to the TBAP and subsequently hepatic FXR activity. Our data therefore support the use of FGF19 mimetics and FXR agonists for the treatment of NASH. Furthermore, the findings from Chapters 3 and 4 alleviate the concern that these therapies may worsen fibrosis in NASH patients. To further elucidate how FGF15 and FGF19 affect HSC function, future studies with primary human HSCs or

HSCs isolated from FGF15 deficient or overexpressing mice can be performed. This would provide greater understanding of the clinical impact of FGF19 analogs and FXR agonists in the treatment of NASH and hepatic fibrosis.

REFERENCES

1. Chiang, J.Y. Bile acids: regulation of synthesis. *J Lipid Res* **50**, 1955-66 (2009).
2. Chiang, J.Y. Recent advances in understanding bile acid homeostasis. *F1000Res* **6**, 2029 (2017).
3. Makishima, M. et al. Identification of a nuclear receptor for bile acids. *Science* **284**, 1362-5 (1999).
4. Wang, H., Chen, J., Hollister, K., Sowers, L.C. & Forman, B.M. Endogenous bile acids are ligands for the nuclear receptor FXR/BAR. *Mol Cell* **3**, 543-53 (1999).
5. Parks, D.J. et al. Bile acids: natural ligands for an orphan nuclear receptor. *Science* **284**, 1365-8 (1999).
6. Inagaki, T. et al. Fibroblast growth factor 15 functions as an enterohepatic signal to regulate bile acid homeostasis. *Cell Metab* **2**, 217-25 (2005).
7. Nishimura, T., Utsunomiya, Y., Hoshikawa, M., Ohuchi, H. & Itoh, N. Structure and expression of a novel human FGF, FGF-19, expressed in the fetal brain. *Biochim Biophys Acta* **1444**, 148-51 (1999).
8. Xie, M.H. et al. FGF-19, a novel fibroblast growth factor with unique specificity for FGFR4. *Cytokine* **11**, 729-35 (1999).
9. Goetz, R. et al. Molecular insights into the klotho-dependent, endocrine mode of action of fibroblast growth factor 19 subfamily members. *Mol Cell Biol* **27**, 3417-28 (2007).
10. Song, K.H., Li, T., Owsley, E., Strom, S. & Chiang, J.Y. Bile acids activate fibroblast growth factor 19 signaling in human hepatocytes to inhibit cholesterol 7alpha-hydroxylase gene expression. *Hepatology* **49**, 297-305 (2009).
11. Kurosu, H. et al. Tissue-specific expression of betaKlotho and fibroblast growth factor (FGF) receptor isoforms determines metabolic activity of FGF19 and FGF21. *J Biol Chem* **282**, 26687-95 (2007).
12. Yu, C., Wang, F., Jin, C., Huang, X. & McKeehan, W.L. Independent repression of bile acid synthesis and activation of c-Jun N-terminal kinase (JNK) by activated hepatocyte fibroblast growth factor receptor 4 (FGFR4) and bile acids. *J Biol Chem* **280**, 17707-14 (2005).
13. Kong, B. et al. Mechanism of tissue-specific farnesoid X receptor in suppressing the expression of genes in bile-acid synthesis in mice. *Hepatology* **56**, 1034-43 (2012).
14. Fu, T. et al. FXR Primes the Liver for Intestinal FGF15 Signaling by Transient Induction of beta-Klotho. *Mol Endocrinol* **30**, 92-103 (2016).
15. Wunsch, E. et al. Expression of hepatic Fibroblast Growth Factor 19 is enhanced in Primary Biliary Cirrhosis and correlates with severity of the disease. *Sci Rep* **5**, 13462 (2015).
16. Schaap, F.G., van der Gaag, N.A., Gouma, D.J. & Jansen, P.L. High expression of the bile salt-homeostatic hormone fibroblast growth factor 19 in the liver of patients with extrahepatic cholestasis. *Hepatology* **49**, 1228-35 (2009).
17. Goodwin, B. et al. A regulatory cascade of the nuclear receptors FXR, SHP-1, and LRH-1 represses bile acid biosynthesis. *Mol Cell* **6**, 517-26 (2000).
18. Lu, T.T. et al. Molecular basis for feedback regulation of bile acid synthesis by nuclear receptors. *Mol Cell* **6**, 507-15 (2000).
19. Kim, I. et al. Differential regulation of bile acid homeostasis by the farnesoid X receptor in liver and intestine. *J Lipid Res* **48**, 2664-72 (2007).
20. Ornitz, D.M. & Itoh, N. The Fibroblast Growth Factor signaling pathway. *Wiley Interdiscip Rev Dev Biol* **4**, 215-66 (2015).

21. Ornitz, D.M. FGFs, heparan sulfate and FGFRs: complex interactions essential for development. *Bioessays* **22**, 108-12 (2000).
22. Potthoff, M.J., Kliewer, S.A. & Mangelsdorf, D.J. Endocrine fibroblast growth factors 15/19 and 21: from feast to famine. *Genes Dev* **26**, 312-24 (2012).
23. Olsen, S.K. et al. Insights into the molecular basis for fibroblast growth factor receptor autoinhibition and ligand-binding promiscuity. *Proc Natl Acad Sci U S A* **101**, 935-40 (2004).
24. Wang, F., Kan, M., Yan, G., Xu, J. & McKeehan, W.L. Alternately spliced NH2-terminal immunoglobulin-like Loop I in the ectodomain of the fibroblast growth factor (FGF) receptor 1 lowers affinity for both heparin and FGF-1. *J Biol Chem* **270**, 10231-5 (1995).
25. Miki, T. et al. Determination of ligand-binding specificity by alternative splicing: two distinct growth factor receptors encoded by a single gene. *Proc Natl Acad Sci U S A* **89**, 246-50 (1992).
26. Yeh, B.K. et al. Structural basis by which alternative splicing confers specificity in fibroblast growth factor receptors. *Proc Natl Acad Sci U S A* **100**, 2266-71 (2003).
27. Partanen, J. et al. FGFR-4, a novel acidic fibroblast growth factor receptor with a distinct expression pattern. *Embo j* **10**, 1347-54 (1991).
28. Barak, H. et al. FGF9 and FGF20 maintain the stemness of nephron progenitors in mice and man. *Dev Cell* **22**, 1191-207 (2012).
29. Min, H. et al. Fgf-10 is required for both limb and lung development and exhibits striking functional similarity to Drosophila branchless. *Genes Dev* **12**, 3156-61 (1998).
30. Ohuchi, H. et al. The mesenchymal factor, FGF10, initiates and maintains the outgrowth of the chick limb bud through interaction with FGF8, an apical ectodermal factor. *Development* **124**, 2235-44 (1997).
31. Benedict, M. & Zhang, X. Non-alcoholic fatty liver disease: An expanded review. *World J Hepatol* **9**, 715-732 (2017).
32. Hashimoto, E., Taniai, M. & Tokushige, K. Characteristics and diagnosis of NAFLD/NASH. *J Gastroenterol Hepatol* **28 Suppl 4**, 64-70 (2013).
33. Michelotti, G.A., Machado, M.V. & Diehl, A.M. NAFLD, NASH and liver cancer. *Nat Rev Gastroenterol Hepatol* **10**, 656-65 (2013).
34. Grundy, S.M. et al. Diagnosis and management of the metabolic syndrome: an American Heart Association/National Heart, Lung, and Blood Institute Scientific Statement. *Circulation* **112**, 2735-52 (2005).
35. Day, C.P. & James, O.F. Steatohepatitis: a tale of two "hits"? *Gastroenterology* **114**, 842-5 (1998).
36. Singh, S. et al. Fibrosis progression in nonalcoholic fatty liver vs nonalcoholic steatohepatitis: a systematic review and meta-analysis of paired-biopsy studies. *Clin Gastroenterol Hepatol* **13**, 643-54.e1-9; quiz e39-40 (2015).
37. Caldwell, S.H. et al. NASH and cryptogenic cirrhosis: a histological analysis. *Ann Hepatol* **8**, 346-52 (2009).
38. Mittal, S. et al. Hepatocellular Carcinoma in the Absence of Cirrhosis in United States Veterans is Associated With Nonalcoholic Fatty Liver Disease. *Clin Gastroenterol Hepatol* **14**, 124-31.e1 (2016).
39. Chalasani, N. et al. The diagnosis and management of nonalcoholic fatty liver disease: Practice guidance from the American Association for the Study of Liver Diseases. *Hepatology* **67**, 328-357 (2018).

40. Dongiovanni, P., Anstee, Q.M. & Valenti, L. Genetic predisposition in NAFLD and NASH: impact on severity of liver disease and response to treatment. *Curr Pharm Des* **19**, 5219-38 (2013).
41. Romeo, S. et al. Genetic variation in PNPLA3 confers susceptibility to nonalcoholic fatty liver disease. *Nat Genet* **40**, 1461-5 (2008).
42. Younossi, Z.M. et al. Global epidemiology of nonalcoholic fatty liver disease-Meta-analytic assessment of prevalence, incidence, and outcomes. *Hepatology* **64**, 73-84 (2016).
43. Younossi, Z. et al. Global burden of NAFLD and NASH: trends, predictions, risk factors and prevention. *Nat Rev Gastroenterol Hepatol* **15**, 11-20 (2018).
44. U.S. Census Bureau. QuickFacts. (2017).
45. Organ Procurement and Transplantation Network. National data - Waiting List Additions Listing Year by Diagnosis; January, 1995 - May 31, 2018.
46. Bedossa, P. Utility and appropriateness of the fatty liver inhibition of progression (FLIP) algorithm and steatosis, activity, and fibrosis (SAF) score in the evaluation of biopsies of nonalcoholic fatty liver disease. *Hepatology* **60**, 565-75 (2014).
47. Kleiner, D.E. et al. Design and validation of a histological scoring system for nonalcoholic fatty liver disease. *Hepatology* **41**, 1313-21 (2005).
48. Brunt, E.M., Janney, C.G., Di Bisceglie, A.M., Neuschwander-Tetri, B.A. & Bacon, B.R. Nonalcoholic steatohepatitis: a proposal for grading and staging the histological lesions. *Am J Gastroenterol* **94**, 2467-74 (1999).
49. Vilar-Gomez, E. & Chalasani, N. Non-invasive assessment of non-alcoholic fatty liver disease: Clinical prediction rules and blood-based biomarkers. *J Hepatol* **68**, 305-315 (2018).
50. Friedman, S.L. Hepatic Stellate Cells: Protean, Multifunctional, and Enigmatic Cells of the Liver. *Physiol Rev* **88**, 125-72 (2008).
51. Giampieri, M.P., Jezequel, A.M. & Orlandi, F. The lipocytes in normal human liver. A quantitative study. *Digestion* **22**, 165-9 (1981).
52. Jezequel, A., Novelli, G., Venturini, C. & Orlandi, F. Quantitative Analysis of the Perisinusoidal Cells in Human Liver: The Lipocytes. *Front Gastrointestinal Res* **8**, 85–90 (1983).
53. Wake, K. Cell-cell organization and functions of 'sinusoids' in liver microcirculation system. *J Electron Microsc (Tokyo)* **48**, 89-98 (1999).
54. Ueno, T. et al. Hepatic stellate cells and intralobular innervation in human liver cirrhosis. *Hum Pathol* **28**, 953-9 (1997).
55. Senoo, H., Kojima, N. & Sato, M. Vitamin A-storing cells (stellate cells). *Vitam Horm* **75**, 131-59 (2007).
56. Puche, J.E., Saiman, Y. & Friedman, S.L. Hepatic stellate cells and liver fibrosis. *Compr Physiol* **3**, 1473-92 (2013).
57. Troeger, J.S. et al. Deactivation of hepatic stellate cells during liver fibrosis resolution in mice. *Gastroenterology* **143**, 1073-83.e22 (2012).
58. Kisseleva, T. et al. Myofibroblasts revert to an inactive phenotype during regression of liver fibrosis. *Proc Natl Acad Sci U S A* **109**, 9448-53 (2012).
59. Fickert, P. et al. Farnesoid X receptor critically determines the fibrotic response in mice but is expressed to a low extent in human hepatic stellate cells and periductal myofibroblasts. *Am J Pathol* **175**, 2392-405 (2009).
60. Fiorucci, S. et al. A farnesoid x receptor-small heterodimer partner regulatory cascade modulates tissue metalloproteinase inhibitor-1 and matrix metalloprotease expression

in hepatic stellate cells and promotes resolution of liver fibrosis. *J Pharmacol Exp Ther* **314**, 584-95 (2005).
61. Fiorucci, S. et al. The nuclear receptor SHP mediates inhibition of hepatic stellate cells by FXR and protects against liver fibrosis. *Gastroenterology* **127**, 1497-512 (2004).
62. Carino, A. et al. Disruption of TFGbeta-SMAD3 pathway by the nuclear receptor SHP mediates the antifibrotic activities of BAR704, a novel highly selective FXR ligand. *Pharmacol Res* **131**, 17-31 (2018).
63. Fiorucci, S. et al. Cross-talk between farnesoid-X-receptor (FXR) and peroxisome proliferator-activated receptor gamma contributes to the antifibrotic activity of FXR ligands in rodent models of liver cirrhosis. *J Pharmacol Exp Ther* **315**, 58-68 (2005).
64. Renga, B. et al. SHP-dependent and -independent induction of peroxisome proliferator-activated receptor-gamma by the bile acid sensor farnesoid X receptor counter-regulates the pro-inflammatory phenotype of liver myofibroblasts. *Inflamm Res* **60**, 577-87 (2011).
65. Li, J. et al. Roles of microRNA-29a in the antifibrotic effect of farnesoid X receptor in hepatic stellate cells. *Mol Pharmacol* **80**, 191-200 (2011).
66. Verbeke, L. et al. Obeticholic acid, a farnesoid X receptor agonist, improves portal hypertension by two distinct pathways in cirrhotic rats. *Hepatology* **59**, 2286-98 (2014).
67. Vallance, P., Leone, A., Calver, A., Collier, J. & Moncada, S. Accumulation of an endogenous inhibitor of nitric oxide synthesis in chronic renal failure. *Lancet* **339**, 572-5 (1992).
68. Xu, W., Lu, C., Zhang, F., Shao, J. & Zheng, S. Dihydroartemisinin restricts hepatic stellate cell contraction via an FXR-S1PR2-dependent mechanism. *IUBMB Life* **68**, 376-87 (2016).
69. Li, J. et al. Inhibition of endothelin-1-mediated contraction of hepatic stellate cells by FXR ligand. *PLoS One* **5**, e13955 (2010).
70. Antoine, M. et al. Expression and function of fibroblast growth factor (FGF) 9 in hepatic stellate cells and its role in toxic liver injury. *Biochem Biophys Res Commun* **361**, 335-41 (2007).
71. Shi, Y.F. et al. Hypoxia induces the activation of human hepatic stellate cells LX-2 through TGF-beta signaling pathway. *FEBS Lett* **581**, 203-10 (2007).
72. Uriarte, I. et al. Ileal FGF15 contributes to fibrosis-associated hepatocellular carcinoma development. *Int J Cancer* **136**, 2469-75 (2015).
73. Lin, N. et al. NP603, a novel and potent inhibitor of FGFR1 tyrosine kinase, inhibits hepatic stellate cell proliferation and ameliorates hepatic fibrosis in rats. *Am J Physiol Cell Physiol* **301**, C469-77 (2011).
74. Chaudhary, N.I. et al. Inhibition of PDGF, VEGF and FGF signalling attenuates fibrosis. *Eur Respir J* **29**, 976-85 (2007).
75. Bowen, W.C. et al. Development of a chemically defined medium and discovery of new mitogenic growth factors for mouse hepatocytes: mitogenic effects of FGF1/2 and PDGF. *PLoS One* **9**, e95487 (2014).
76. Baruch, Y., Shoshany, G., Neufeld, G. & Enat, R. Basic fibroblast growth factor is hepatotropic for rat liver in regeneration. *J Hepatol* **23**, 328-32 (1995).
77. Nakamura, I. et al. Brivanib Attenuates Hepatic Fibrosis In Vivo and Stellate Cell Activation In Vitro by Inhibition of FGF, VEGF and PDGF Signaling. *PLoS One* **9** (2014).
78. Huynh, H. et al. Brivanib alaninate, a dual inhibitor of vascular endothelial growth factor receptor and fibroblast growth factor receptor tyrosine kinases, induces growth inhibition in mouse models of human hepatocellular carcinoma. *Clin Cancer Res* **14**, 6146-53 (2008).

79. Yu, C. et al. Role of Fibroblast Growth Factor Type 1 and 2 in Carbon Tetrachloride-Induced Hepatic Injury and Fibrogenesis. *Am J Pathol* **163**, 1653-62 (2003).
80. Rosenbaum, J. et al. Fibroblast growth factor 2 and transforming growth factor beta 1 interactions in human liver myofibroblasts. *Gastroenterology* **109**, 1986-96 (1995).
81. Aziz, K.A. et al. The role of autocrine FGF-2 in the distinctive bone marrow fibrosis of hairy-cell leukemia (HCL). *Blood* **102**, 1051-6 (2003).
82. Sturm, J.W. et al. Altered apoptotic response and different liver structure during liver regeneration in FGF-2-deficient mice. *Cell Physiol Biochem* **14**, 249-60 (2004).
83. Steiling, H. et al. Activated Hepatic Stellate Cells Express Keratinocyte Growth Factor in Chronic Liver Disease. *Am J Pathol* **165**, 1233-41 (2004).
84. Otte, J.M. et al. Differential regulated expression of keratinocyte growth factor and its receptor in experimental and human liver fibrosis. *Regul Pept* **144**, 82-90 (2007).
85. Tsai, S.M. & Wang, W.P. Expression and function of fibroblast growth factor (FGF) 7 during liver regeneration. *Cell Physiol Biochem* **27**, 641-52 (2011).
86. Mutanen, A., Lohi, J., Heikkila, P., Jalanko, H. & Pakarinen, M.P. Loss of ileum decreases serum fibroblast growth factor 19 in relation to liver inflammation and fibrosis in pediatric onset intestinal failure. *J Hepatol* **62**, 1391-7 (2015).
87. Pereira-Fantini, P.M. et al. Altered FXR signalling is associated with bile acid dysmetabolism in short bowel syndrome-associated liver disease. *J Hepatol* **61**, 1115-25 (2014).
88. Xu, P. et al. Fibroblast growth factor 21 attenuates hepatic fibrogenesis through TGF-beta/smad2/3 and NF-kappaB signaling pathways. *Toxicol Appl Pharmacol* **290**, 43-53 (2016).
89. Fisher, F.M. et al. Fibroblast growth factor 21 limits lipotoxicity by promoting hepatic fatty acid activation in mice on methionine and choline-deficient diets. *Gastroenterology* **147**, 1073-83.e6 (2014).
90. Mutanen, A. et al. Serum FGF21 increases with hepatic fat accumulation in pediatric onset intestinal failure. *J Hepatol* **60**, 183-90 (2014).
91. Li, H. et al. Fibroblast growth factor 21 levels are increased in nonalcoholic fatty liver disease patients and are correlated with hepatic triglyceride. *J Hepatol* **53**, 934-40 (2010).
92. Li, H. et al. High serum level of fibroblast growth factor 21 is an independent predictor of non-alcoholic fatty liver disease: a 3-year prospective study in China. *J Hepatol* **58**, 557-63 (2013).
93. Alisi, A. et al. Association between Serum Atypical Fibroblast Growth Factors 21 and 19 and Pediatric Nonalcoholic Fatty Liver Disease. *PLoS One* **8**, e67160 (2013).
94. Dushay, J. et al. Increased fibroblast growth factor 21 in obesity and nonalcoholic fatty liver disease. *Gastroenterology* **139**, 456-63 (2010).
95. Gai, Z. et al. The effects of farnesoid X receptor activation on arachidonic acid metabolism, NF-kB signaling and hepatic inflammation. *Molecular Pharmacology* (2018).
96. Ma, Y., Huang, Y., Yan, L., Gao, M. & Liu, D. Synthetic FXR agonist GW4064 prevents diet-induced hepatic steatosis and insulin resistance. *Pharm Res* **30**, 1447-57 (2013).
97. Evans, M.J. et al. A synthetic farnesoid X receptor (FXR) agonist promotes cholesterol lowering in models of dyslipidemia. *Am J Physiol Gastrointest Liver Physiol* **296**, G543-52 (2009).
98. Zhang, S., Wang, J., Liu, Q. & Harnish, D.C. Farnesoid X receptor agonist WAY-362450 attenuates liver inflammation and fibrosis in murine model of non-alcoholic steatohepatitis. *J Hepatol* **51**, 380-8 (2009).

99. Wu, W. et al. Bile acids override steatosis in farnesoid X receptor deficient mice in a model of non-alcoholic steatohepatitis. *Biochem Biophys Res Commun* **448**, 50-5 (2014).
100. Kong, B., Luyendyk, J.P., Tawfik, O. & Guo, G.L. Farnesoid X receptor deficiency induces nonalcoholic steatohepatitis in low-density lipoprotein receptor-knockout mice fed a high-fat diet. *J Pharmacol Exp Ther* **328**, 116-22 (2009).
101. Ma, K., Saha, P.K., Chan, L. & Moore, D.D. Farnesoid X receptor is essential for normal glucose homeostasis. *J Clin Invest* **116**, 1102-9 (2006).
102. Verbeke, L. et al. FXR agonist obeticholic acid reduces hepatic inflammation and fibrosis in a rat model of toxic cirrhosis. *Sci Rep* **6**, 33453 (2016).
103. Jung, D. et al. FXR-induced secretion of FGF15/19 inhibits CYP27 expression in cholangiocytes through p38 kinase pathway. *Pflugers Arch* **466**, 1011-9 (2014).
104. Schmitt, J. et al. Protective effects of farnesoid X receptor (FXR) on hepatic lipid accumulation are mediated by hepatic FXR and independent of intestinal FGF15 signal. *Liver Int* **35**, 1133-44 (2015).
105. Pineda Torra, I. et al. Bile acids induce the expression of the human peroxisome proliferator-activated receptor alpha gene via activation of the farnesoid X receptor. *Mol Endocrinol* **17**, 259-72 (2003).
106. Watanabe, M. et al. Bile acids lower triglyceride levels via a pathway involving FXR, SHP, and SREBP-1c. *J Clin Invest* **113**, 1408-18 (2004).
107. Lambert, G. et al. The farnesoid X-receptor is an essential regulator of cholesterol homeostasis. *J Biol Chem* **278**, 2563-70 (2003).
108. Zhang, Y. et al. Activation of the nuclear receptor FXR improves hyperglycemia and hyperlipidemia in diabetic mice. *Proc Natl Acad Sci U S A* **103**, 1006-11 (2006).
109. Plyte, S.E., Hughes, K., Nikolakaki, E., Pulverer, B.J. & Woodgett, J.R. Glycogen synthase kinase-3: functions in oncogenesis and development. *Biochim Biophys Acta* **1114**, 147-62 (1992).
110. Cariou, B. et al. Transient impairment of the adaptive response to fasting in FXR-deficient mice. *FEBS Lett* **579**, 4076-80 (2005).
111. Sun, W., Liu, Q., Leng, J., Zheng, Y. & Li, J. The role of Pyruvate Dehydrogenase Complex in cardiovascular diseases. *Life Sci* **121**, 97-103 (2015).
112. Savkur, R.S., Bramlett, K.S., Michael, L.F. & Burris, T.P. Regulation of pyruvate dehydrogenase kinase expression by the farnesoid X receptor. *Biochem Biophys Res Commun* **329**, 391-6 (2005).
113. Badman, M.K. et al. Hepatic fibroblast growth factor 21 is regulated by PPARalpha and is a key mediator of hepatic lipid metabolism in ketotic states. *Cell Metab* **5**, 426-37 (2007).
114. Cyphert, H.A. et al. Activation of the farnesoid X receptor induces hepatic expression and secretion of fibroblast growth factor 21. *J Biol Chem* **287**, 25123-38 (2012).
115. Zhang, F. et al. Minireview: Roles of Fibroblast Growth Factors 19 and 21 in Metabolic Regulation and Chronic Diseases. *Mol Endocrinol* **29**, 1400-13 (2015).
116. Staiger, H., Keuper, M., Berti, L., Hrabe de Angelis, M. & Haring, H.U. Fibroblast Growth Factor 21-Metabolic Role in Mice and Men. *Endocr Rev* **38**, 468-488 (2017).
117. Potthoff, M.J. FGF21 and metabolic disease in 2016: A new frontier in FGF21 biology. *Nat Rev Endocrinol* **13**, 74-76 (2017).
118. Markan, K.R. & Potthoff, M.J. Metabolic fibroblast growth factors (FGFs): Mediators of energy homeostasis. *Semin Cell Dev Biol* **53**, 85-93 (2016).
119. Guan, D., Zhao, L., Chen, D., Yu, B. & Yu, J. Regulation of fibroblast growth factor 15/19 and 21 on metabolism: in the fed or fasted state. *J Transl Med* **14**, 63 (2016).

120. Nies, V.J. et al. Fibroblast Growth Factor Signaling in Metabolic Regulation. *Front Endocrinol (Lausanne)* **6**, 193 (2015).
121. Lee, J.H. et al. An engineered FGF21 variant, LY2405319, can prevent non-alcoholic steatohepatitis by enhancing hepatic mitochondrial function. *Am J Transl Res* **8**, 4750-4763 (2016).
122. Liu, X. et al. Lack of fibroblast growth factor 21 accelerates metabolic liver injury characterized by steatohepatities in mice. *Am J Cancer Res* **6**, 1011-25 (2016).
123. Cray, C., Zaias, J. & Altman, N.H. Acute phase response in animals: a review. *Comp Med* **59**, 517-26 (2009).
124. Zhang, S., Liu, Q., Wang, J. & Harnish, D.C. Suppression of interleukin-6-induced C-reactive protein expression by FXR agonists. *Biochem Biophys Res Commun* **379**, 476-9 (2009).
125. Armstrong, L. et al. Effects of Acute-Phase Proteins in Mediating Hepatic FXR's Protection of Mice from NASH Development. *AASLD 2017 Liver Meeting Abstract 643* (2017).
126. Porez, G. et al. The hepatic orosomucoid/alpha1-acid glycoprotein gene cluster is regulated by the nuclear bile acid receptor FXR. *Endocrinology* **154**, 3690-701 (2013).
127. Mencarelli, A. et al. The bile acid sensor farnesoid X receptor is a modulator of liver immunity in a rodent model of acute hepatitis. *J Immunol* **183**, 6657-66 (2009).
128. Wang, K.X. & Denhardt, D.T. Osteopontin: role in immune regulation and stress responses. *Cytokine Growth Factor Rev* **19**, 333-45 (2008).
129. Deshmane, S.L., Kremlev, S., Amini, S. & Sawaya, B.E. Monocyte chemoattractant protein-1 (MCP-1): an overview. *J Interferon Cytokine Res* **29**, 313-26 (2009).
130. Li, L. et al. Activation of farnesoid X receptor downregulates monocyte chemoattractant protein-1 in murine macrophage. *Biochem Biophys Res Commun* **467**, 841-6 (2015).
131. Kim, D.H. et al. A dysregulated acetyl/SUMO switch of FXR promotes hepatic inflammation in obesity. *Embo j* **34**, 184-99 (2015).
132. Wang, Y.D. et al. Farnesoid X receptor antagonizes nuclear factor kappaB in hepatic inflammatory response. *Hepatology* **48**, 1632-43 (2008).
133. Gai, Z. et al. The effects of farnesoid X receptor activation on arachidonic acid metabolism, NF-kB signaling and hepatic inflammation. *Mol Pharmacol* (2018).
134. Dai, M. et al. Epoxyeicosatrienoic acids regulate macrophage polarization and prevent LPS-induced cardiac dysfunction. *J Cell Physiol* **230**, 2108-19 (2015).
135. Renga, B. et al. FXR mediates a chromatin looping in the GR promoter thus promoting the resolution of colitis in rodents. *Pharmacol Res* **77**, 1-10 (2013).
136. Renga, B. et al. Glucocorticoid receptor mediates the gluconeogenic activity of the farnesoid X receptor in the fasting condition. *Faseb j* **26**, 3021-31 (2012).
137. Jiang, C. et al. Intestinal farnesoid X receptor signaling promotes nonalcoholic fatty liver disease. *J Clin Invest* **125**, 386-402 (2015).
138. Jiang, C. et al. Intestine-selective farnesoid X receptor inhibition improves obesity-related metabolic dysfunction. *Nat Commun* **6**, 10166 (2015).
139. Xie, C. et al. An Intestinal Farnesoid X Receptor-Ceramide Signaling Axis Modulates Hepatic Gluconeogenesis in Mice. *Diabetes* **66**, 613-626 (2017).
140. Li, F. et al. Microbiome remodelling leads to inhibition of intestinal farnesoid X receptor signalling and decreased obesity. *Nat Commun* **4**, 2384 (2013).
141. Fang, S. et al. Intestinal FXR agonism promotes adipose tissue browning and reduces obesity and insulin resistance. *Nat Med* **21**, 159-65 (2015).

142. Pathak, P. et al. Intestine farnesoid X receptor agonist and the gut microbiota activate G-protein bile acid receptor-1 signaling to improve metabolism. *Hepatology* (2018).
143. Pathak, P. et al. Farnesoid X receptor induces Takeda G-protein receptor 5 cross-talk to regulate bile acid synthesis and hepatic metabolism. *J Biol Chem* **292**, 11055-11069 (2017).
144. Kawamata, Y. et al. A G protein-coupled receptor responsive to bile acids. *J Biol Chem* **278**, 9435-40 (2003).
145. Maruyama, T. et al. Identification of membrane-type receptor for bile acids (M-BAR). *Biochem Biophys Res Commun* **298**, 714-9 (2002).
146. Tomlinson, E. et al. Transgenic mice expressing human fibroblast growth factor-19 display increased metabolic rate and decreased adiposity. *Endocrinology* **143**, 1741-7 (2002).
147. Zhou, M. et al. Engineered FGF19 eliminates bile acid toxicity and lipotoxicity leading to resolution of steatohepatitis and fibrosis in mice. *Hepatol Commun* **1**, 1024-1042 (2017).
148. Alvarez-Sola, G. et al. Fibroblast growth factor 15/19 (FGF15/19) protects from diet-induced hepatic steatosis: development of an FGF19-based chimeric molecule to promote fatty liver regeneration. *Gut* **66**, 1818-1828 (2017).
149. Schumacher, J.D. et al. The effect of fibroblast growth factor 15 deficiency on the development of high fat diet induced non-alcoholic steatohepatitis. *Toxicol Appl Pharmacol* **330**, 1-8 (2017).
150. de Boer, J.F. et al. Intestinal Farnesoid X Receptor Controls Transintestinal Cholesterol Excretion in Mice. *Gastroenterology* **152**, 1126-1138.e6 (2017).
151. Drafahl, K.A., McAndrew, C.W., Meyer, A.N., Haas, M. & Donoghue, D.J. The receptor tyrosine kinase FGFR4 negatively regulates NF-kappaB signaling. *PLoS One* **5**, e14412 (2010).
152. Kir, S. et al. FGF19 as a postprandial, insulin-independent activator of hepatic protein and glycogen synthesis. *Science* **331**, 1621-4 (2011).
153. Potthoff, M.J. et al. FGF15/19 regulates hepatic glucose metabolism by inhibiting the CREB-PGC-1alpha pathway. *Cell Metab* **13**, 729-38 (2011).
154. Benoit, B. et al. Fibroblast growth factor 19 regulates skeletal muscle mass and ameliorates muscle wasting in mice. *Nat Med* **23**, 990-996 (2017).
155. Fu, L. et al. Fibroblast growth factor 19 increases metabolic rate and reverses dietary and leptin-deficient diabetes. *Endocrinology* **145**, 2594-603 (2004).
156. Hsuchou, H., Pan, W. & Kastin, A.J. Fibroblast growth factor 19 entry into brain. *Fluids Barriers CNS* **10**, 32 (2013).
157. Gimeno, L., Brulet, P. & Martinez, S. Study of Fgf15 gene expression in developing mouse brain. *Gene Expr Patterns* **3**, 473-81 (2003).
158. Fon Tacer, K. et al. Research resource: Comprehensive expression atlas of the fibroblast growth factor system in adult mouse. *Mol Endocrinol* **24**, 2050-64 (2010).
159. Faouzi, M. et al. Differential accessibility of circulating leptin to individual hypothalamic sites. *Endocrinology* **148**, 5414-23 (2007).
160. Liu, S. et al. A gut-brain axis regulating glucose metabolism mediated by bile acids and competitive fibroblast growth factor actions at the hypothalamus. *Mol Metab* **8**, 37-50 (2018).
161. Marcelin, G. et al. Central action of FGF19 reduces hypothalamic AGRP/NPY neuron activity and improves glucose metabolism. *Mol Metab* **3**, 19-28 (2014).
162. Bullitt, E. Expression of c-fos-like protein as a marker for neuronal activity following noxious stimulation in the rat. *J Comp Neurol* **296**, 517-30 (1990).

163. Ryan, K.K. et al. Fibroblast growth factor-19 action in the brain reduces food intake and body weight and improves glucose tolerance in male rats. *Endocrinology* **154**, 9-15 (2013).
164. Chen, M.Z. et al. FGF21 mimetic antibody stimulates UCP1-independent brown fat thermogenesis via FGFR1/betaKlotho complex in non-adipocytes. *Mol Metab* **6**, 1454-1467 (2017).
165. Kolumam, G. et al. Sustained Brown Fat Stimulation and Insulin Sensitization by a Humanized Bispecific Antibody Agonist for Fibroblast Growth Factor Receptor 1/betaKlotho Complex. *EBioMedicine* **2**, 730-43 (2015).
166. Ocaliva (obeticholic acid)[package insert]. Intercept Pharmaceuticals, Inc. , New York, NY. (2018).
167. FDA approval letter - Ocaliva; NDA 207999. . (2016).
168. Mudaliar, S. et al. Efficacy and safety of the farnesoid X receptor agonist obeticholic acid in patients with type 2 diabetes and nonalcoholic fatty liver disease. *Gastroenterology* **145**, 574-82.e1 (2013).
169. Neuschwander-Tetri, B.A. et al. Farnesoid X nuclear receptor ligand obeticholic acid for non-cirrhotic, non-alcoholic steatohepatitis (FLINT): a multicentre, randomised, placebo-controlled trial. *Lancet* **385**, 956-65 (2015).
170. Intercept Pharmaceuticals. Randomized Global Phase 3 Study to Evaluate the Impact on NASH With Fibrosis of Obeticholic Acid Treatment (REGENERATE). **ClinicalTrials.gov Identifier: NCT02548351** (Revised May 28, 2018).
171. Intercept Pharmaceuticals. Study Evaluating the Efficacy and Safety of Obeticholic Acid in Subjects With Compensated Cirrhosis Due to Nonalcoholic Steatohepatitis (REVERSE). **ClinicalTrials.gov Identifier: NCT03439254** (Revised May 24, 2018).
172. Pharmaceuticals, W. Study Evaluating the Safety of FXR-450 in Healthy Subjects. **ClinicalTrials.gov Identifier: NCT00499629** (Revised March 13, 2008).
173. Novartis Pharmaceuticals. Study of Safety and Efficacy of Tropifexor (LJN452) in Patients With Non-alcoholic Steatohepatitis (NASH) (FLIGHT-FXR). **ClinicalTrials.gov Identifier: NCT02855164** (Revised April 18, 2018).
174. Novartis Pharmaceuticals. Safety, Tolerability, and Efficacy of a Combination Treatment of Tropifexor (LJN452) and Cenicriviroc (CVC) in Adult Patients With Nonalcoholic Steatohepatitis (NASH) and Liver Fibrosis (TANDEM). **ClinicalTrials.gov Identifier: NCT03517540** (Revised May 17, 2018).
175. Novartis Pharmaceuticals. Safety, Tolerability, Pharmacokinetics and Efficacy of LMB763 in Patients With NASH. **ClinicalTrials.gov Identifier: NCT02913105** (Revised May 31, 2018).
176. Enanta Pharmaceuticals. A Study to Assess the Safety, Tolerability, Pharmacokinetics and Efficacy of EDP-305 in Subjects With Non-Alcoholic Steatohepatitis. **ClinicalTrials.gov Identifier: NCT03421431** (Revised March 29, 2018).
177. Gilead Sciences. Evaluating the Safety, Tolerability, and Efficacy of GS-9674 in Participants With Nonalcoholic Steatohepatitis (NASH). **ClinicalTrials.gov Identifier: NCT02854605** (Revised January 17, 2018).
178. Gilead Sciences. Safety, Tolerability, and Efficacy of Selonsertib, GS-0976, and GS-9674 in Adults With Nonalcoholic Steatohepatitis (NASH). **ClinicalTrials.gov Identifier: NCT02781584** (Revised February 8, 2018).
179. Gilead Sciences. Safety and Efficacy of Selonsertib, GS-0976, GS-9674, and Combinations in Participants With Bridging Fibrosis or Compensated Cirrhosis Due to Nonalcoholic

Steatohepatitis (NASH) (ATLAS). **ClinicalTrials.gov Identifier: NCT03449446** (Revised June 11, 2018).
180. Hambruch, E. et al. Synthetic farnesoid X receptor agonists induce high-density lipoprotein-mediated transhepatic cholesterol efflux in mice and monkeys and prevent atherosclerosis in cholesteryl ester transfer protein transgenic low-density lipoprotein receptor (-/-) mice. *J Pharmacol Exp Ther* **343**, 556-67 (2012).
181. Harrison, S.A. et al. NGM282 for treatment of non-alcoholic steatohepatitis: a multicentre, randomised, double-blind, placebo-controlled, phase 2 trial. *Lancet* **391**, 1174-1185 (2018).
182. NGM Biopharmaceuticals. Phase 1 SAD and MAD Study of NGM282 in Healthy Adult Participants. **ClinicalTrials.gov Identifier: NCT01776528** (Revised December 31, 2013).
183. Harrison, S. et al. NGM282 improves fibrosis and NASH-related histology in 12 weeks in patients with biopsy-confirmed NASH, which is preceded by significant decreases in hepatic steatosis, liver transaminases and fibrosis markers at 6 weeks. *Journal of Hepatology* **68**, S65-S66 (2018).
184. NGM Biopharmaceuticals. Phase 1 Study of NGM313 in Healthy Adult Participants. **ClinicalTrials.gov Identifier: NCT02708576** (Revised September 14, 2017).
185. NGM Biopharmaceuticals. Study of NGM313 in Obese Participants. **ClinicalTrials.gov Identifier: NCT03298464** (Revised December 7, 2017).
186. U.S. Food and Drug Administration. Drug Safety Communication: FDA Drug Safety Communication: FDA warns about serious liver injury with Ocaliva (obeticholic acid) for rare chronic liver disease. (9/21/2017).
187. Administration, U.S.F.a.D. Drug Safety Communication - Ocaliva (obeticholic acid): Drug Safety Communication - Boxed Warning Added To Highlight Correct Dosing. (2/1/2018).
188. Zhou, M. et al. Mouse species-specific control of hepatocarcinogenesis and metabolism by FGF19/FGF15. *J Hepatol* **66**, 1182-1192 (2017).
189. Wu, X. et al. FGF19-induced hepatocyte proliferation is mediated through FGFR4 activation. *J Biol Chem* **285**, 5165-70 (2010).
190. Zhou, M. et al. Separating Tumorigenicity from Bile Acid Regulatory Activity for Endocrine Hormone FGF19. *Cancer Res* **74**, 3306-16 (2014).
191. Luo, J. et al. A nontumorigenic variant of FGF19 treats cholestatic liver diseases. *Sci Transl Med* **6**, 247ra100 (2014).
192. Vernon, G., Baranova, A. & Younossi, Z.M. Systematic review: the epidemiology and natural history of non-alcoholic fatty liver disease and non-alcoholic steatohepatitis in adults. *Aliment Pharmacol Ther* **34**, 274-85 (2011).
193. Li, S. et al. Cytoplasmic Tyrosine Phosphatase Shp2 Coordinates Hepatic Regulation of Bile Acid and FGF15/19 Signaling to Repress Bile Acid Synthesis. *Cell Metab* **20**, 320-32 (2014).
194. Lin, B.C., Wang, M., Blackmore, C. & Desnoyers, L.R. Liver-specific activities of FGF19 require Klotho beta. *J Biol Chem* **282**, 27277-84 (2007).
195. Kong, B. et al. Fibroblast growth factor 15 deficiency impairs liver regeneration in mice. *Am J Physiol Gastrointest Liver Physiol* **306**, G893-902 (2014).
196. Uriarte, I. et al. Identification of fibroblast growth factor 15 as a novel mediator of liver regeneration and its application in the prevention of post-resection liver failure in mice. *Gut* **62**, 899-910 (2013).
197. Schneider, C.A., Rasband, W.S. & Eliceiri, K.W. NIH Image to ImageJ: 25 years of image analysis. *Nat Methods* **9**, 671-5 (2012).

198. Csanaky, I.L., Aleksunes, L.M., Tanaka, Y. & Klaassen, C.D. Role of hepatic transporters in prevention of bile acid toxicity after partial hepatectomy in mice. *Am J Physiol Gastrointest Liver Physiol* **297**, G419-33 (2009).
199. Calvo, D., Gomez-Coronado, D., Suarez, Y., Lasuncion, M.A. & Vega, M.A. Human CD36 is a high affinity receptor for the native lipoproteins HDL, LDL, and VLDL. *J Lipid Res* **39**, 777-88 (1998).
200. Baillie, A.G., Coburn, C.T. & Abumrad, N.A. Reversible binding of long-chain fatty acids to purified FAT, the adipose CD36 homolog. *J Membr Biol* **153**, 75-81 (1996).
201. Li, T., Jahan, A. & Chiang, J.Y.L. Bile acids and cytokines inhibit the human cholesterol 7α-hydroxylase gene via the JNK/c-Jun pathway. *Hepatology* **43**, 1202-10 (2006).
202. Bieghs, V., Rensen, P.C., Hofker, M.H. & Shiri-Sverdlov, R. NASH and atherosclerosis are two aspects of a shared disease: central role for macrophages. *Atherosclerosis* **220**, 287-93 (2012).
203. Schumacher, J.D. & Guo, G.L. Regulation of Hepatic Stellate Cells and Fibrogenesis by Fibroblast Growth Factors. *Biomed Res Int* **2016**, 8323747 (2016).
204. Kong, B. & Guo, G.L. Soluble expression of disulfide bond containing proteins FGF15 and FGF19 in the cytoplasm of Escherichia coli. *PLoS One* **9**, e85890 (2014).
205. Lin, N. et al. NP603, a novel and potent inhibitor of FGFR1 tyrosine kinase, inhibits hepatic stellate cell proliferation and ameliorates hepatic fibrosis in rats. *American Journal of Physiology - Cell Physiology* **301**, C469-C477 (2011).
206. Schumacher, J.D. & Guo, G.L. Mechanistic review of drug-induced steatohepatitis. *Toxicol Appl Pharmacol* (2015).
207. Cheng, K. et al. Diminished gallbladder filling, increased fecal bile acids, and promotion of colon epithelial cell proliferation and neoplasia in fibroblast growth factor 15-deficient mice. *Oncotarget* **9**, 25572-85.
208. Sinal, C.J. et al. Targeted disruption of the nuclear receptor FXR/BAR impairs bile acid and lipid homeostasis. *Cell* **102**, 731-44 (2000).
209. Scholten, D., Trebicka, J., Liedtke, C. & Weiskirchen, R. The carbon tetrachloride model in mice. *Lab Anim* **49**, 4-11 (2015).
210. Yu, Y. et al. Fibroblast growth factor 21 (FGF21) inhibits macrophage-mediated inflammation by activating Nrf2 and suppressing the NF-kappaB signaling pathway. *Int Immunopharmacol* **38**, 144-52 (2016).
211. Fitzpatrick, E.A., Han, X., Xiao, Z. & Quarles, L.D. Role of Fibroblast Growth Factor-23 in Innate Immune Responses. *Front Endocrinol (Lausanne)* **9** (2018).
212. Wu, A.L. et al. FGF19 regulates cell proliferation, glucose and bile acid metabolism via FGFR4-dependent and independent pathways. *PLoS One* **6**, e17868 (2011).
213. Takahashi, S. et al. Cyp2c70 is responsible for the species difference in bile acid metabolism between mice and humans. *J Lipid Res* **57**, 2130-2137 (2016).